NTNU – Trondheim
Norwegian University of
Science and Technology

Optimal and Stable Production of High Pressure Steam

Torstein T Kristoffersen

Master of Science in Engineering Cybernetics
Submission date: June 2013
Supervisor: Lars Imsland, ITK
Co-supervisor: Dagfinn Snarheim, Statoil ASA
Marius Støre Govatsmark, Statoil ASA

Norwegian University of Science and Technology
Department of Engineering Cybernetics

NTNU

Faculty of Information Technology, Mathematics and Electrical Engineering
Department of Engineering Cybernetics

PROJECT DESCRIPTION SHEET

Name of the candidate: Torstein Thode Kristoffersen

Thesis title (English): Optimal and stable production of high pressure steam

Background

Kårstø is a natural gas processing plant north of Stavanger that refines natural gas and condensate from the fields in the northern parts of the North Sea. The steam delivery network at the plant is built to cover the large energy requirement of the different processes. The steam delivery network is closed and the steam boilers produce high pressure steam that is distributed to the consumers over the network. The objective of this master study is to create an application that can minimize the fuel consumption for the boilers at Kårstø, while simultaneously ensures stability of the process. The study builds on the project work in the fall of 2012.

Work Description

1. Give a brief overview of the steam delivery network's challenges and how an MPC controller and optimization can be used in this regard. Give a short presentation of the steam delivery network and relevant process units and their control structure.
2. Expand the model predictive controller to apply for all boilers and implement real constraints on the loads and rate of change of these loads. Demonstrate the performance compared to the existing controllers.
3. Present relevant theory for an efficiency analysis and perform such an analysis on each boiler, based on real plant data. Present the data relevant for further studies, both graphically and mathematically.
4. Formulate an optimization problem that exploits the efficiencies to minimize the fuel consumption of the boilers. The solution should be flexible in the number of boilers in operation and should not start or stop any of the boilers.
5. Consider how the optimization of the fuel consumption affects the control of the control of the high pressure steam, especially during a boiler trip.
6. If time permits, the following tasks should be considered:
    a. Modify the MPC application so that the remaining degrees of freedom can be utilized to minimize the fuel consumption. The main task of the MPC controller should still be to ensure a stable pressure of the high pressure steam.
    b. Check whether the boilers in the dynamic simulator (D-SPICE) have similar characteristics in terms of efficiency and try to demonstrate the functionality of the MPC application.
7. Write a report.

Start date: January 14th 2013 **Due date:** June 23rd 2013

Supervisor: Lars Imsland
Co-advisor(s): Dagfinn Snarheim and Marius Govatsmark, Statoil

Trondheim, __17.06.2013_____

Lars Imsland
Supervisor

Address
Sem Sælandsvei 5
NO-7491 Trondheim

Org.no. 974 767 880
E-mail:
postmottak@itk.ntnu.no
http://www.itk.ntnu.no

Location
O.S. Bragstads plass 2D
NO-7034 Trondheim

Phone
+ 47 73 59 43 76
Fax
+ 47 73 59 45 99

Phone: + 47 47 23 19 49

Abstract

Steam delivery networks are large energy consuming processes and an important source of energy in many processing plants. These networks are often subject to large disturbances, which can lead to costly operating periods due to lack of steam. Thus, there is a potential for stabilization and reduction of the energy consumption. The objective of this thesis is to stabilize a steam delivery network using a model predictive controller, and further minimize the energy consumption by incorporating an overlying optimization problem, that is an optimizer, on top of the model predictive controller. The controller and the optimizer developed in this thesis are applied to a simulator of the steam delivery network at Statoil Kårstø, but the principles are applicable for any steam delivery network.

A study of the steam delivery networks including its main components and control structure is performed. The study is based on real plant data and a dynamic simulator model. The network consists of eight boilers, in which all deliver high pressure steam into a common header. Steam is continuously drawn from the common header by various steam consumers, before it is returned to the boilers as condensate. This behavior makes it easy to obtain step response models of the boilers by performing a step in their inputs, that is increase their combustion.

These models are incorporated into the controller which is implemented using the SEPTIC application developed by Statoil. This controller optimizes the future response by solving a quadratic optimization problem, consisting of various weights and constraints on the considered variables in combination with the models of the system, at each control sample. The ideal values of this controller is calculated by the optimizer, derived from the mass and energy balances of the steam delivery network. Two different optimizers are developed and considered, one which does not allow for a boiler shutdown, and the second which allows for a boiler shutdown. These are named conservative and strictly economical optimization, respectively.

Three different case studies, with increasingly degrees of disturbances, are carried out to study the performance of the model predictive controller compared to the currently used PI control structure. Five additional case studies are performed to illustrate the potential and issues occurring by incorporating an optimizer. The results show improved performance and stability by including a model predictive controller and indicate a significant potential for reduction in both fuel consumption and CO_2 emissions by incorporating an optimizer. However, only the conservative optimizer showed robustness against model errors and large disturbances.

Sammendrag

Dampnettverk er store energiforbrukende prosesser og en viktig energikilde i flere prosessanlegg. Disse nettverkene er ofte utsatt for store forstyrrelser, som kan føre til kostbare operasjonsperioder grunnet mangel på damp og tungt belastede kjeler. Det er derfor et potensiale for bedre stabilisering og redusert energiforbruk. Hovedmålet med denne oppgaven er å stabilisere et dampnettverk med en modellprediktiv kontroller og videre minimalisere energiforbruket ved å innlemme et optimaliseringsproblem, altså en optimerer, over den modellprediktive kontrolleren. Kontrolleren og optimereren er i denne oppgave benyttet på dampnettverket ved Statoil Kårstø, men prinsippene er anvendbare for et hvilket som helst dampnettverk.

Det er utført en studie av dampnettverket med særlig vekt på hovedkomponentene og kontrollstrukturen. Den videre studien er basert på virkelige anleggsdata og en simulator. Dampnettverket består av åtte kjeler som alle leverer høytrykksdamp til en stor horisontal tank, kalt common header. Dampen fra denne tanken er kontinuerlig transportert til ulike dampforbrukere før den returneres tilbake til kjelene som kondensat. Denne strukturen gjør det enkelt å finne sprangrespons modeller av kjelene. Dette gjøres ved å øke forbrenningen.

Disse modellene er innlemmet i den modellprediktive kontrolleren som er lagt i SEPTIC applikasjonen utviklet av Statoil. Denne kontrolleren løser et optimaliseringsproblem, bestående av ulike vekter og begrensninger på de interessante variablene, ved hvert samplingspunkt. Idealverdiene til denne kontrolleren er funnet av optimereren, som er utviklet fra masse- og energibalansene for common headeren. To ulike optimaliseringsstrategier er studert, den ene tillater ikke avstengning av en kjele, mens den andre tillater det. Disse er henholdsvis kalt konservative og streng økonomisk optimalisering.

Tre ulike senarioer, med økende forstyrrelser, er utført og studert for den modellprediktive kontrolleren sammenliknet med den nåværende benyttede PI kontrollstrukturen. I tillegg er fem senarioer utført for å studere besparelsespotensiale og problemene ved å innlemme en optimerer. Resultatene viste forbedret ytelse og stabilitet ved å benytte en modellprediktiv kontroller og antydet betydelig reduksjon i både drivstofforbruk og CO_2 utslipp ved å innlemme en optimerer. Det viste seg imidlertid at kun den konservative optimaliseringsstrategien var robust mot modellfeil og store forstyrrelser.

Preface

This thesis is submitted as the final part of the degree, Master of Science in Engineering Cybernetics at the Norwegian University of Science and Technology (NTNU). The work concludes the work carried out over the past half year and represent the most challenging and educational part of my study.

I would like to thank my supervisor, Professor Lars Imsland, at the department of Engineering Cybernetics for clarifying discussions and motivation during the semester. A special thanks to my two co-supervisors, Dagfinn Snarheim, PhD, and Marius Støre Govatsmark, PhD, at Statoil Kårstø, for all enlightening discussions and for providing me with great ideas throughout the semester.

Lastly, I would like to thank my fellow students at the office, Anders Mørk, Mikael Berg, Håvard Håkon Raaen, Henrik Emil Wold and Tone Ljones for good advices and joyful lunches throughout the semester. In closing, I would like to express my great gratitude towards my great love, Gry Jannike Gossmann, for her support and patience.

"The important thing is not to stop questioning.
Curiosity has its own reason for existing."
Albert Einstein

Trondheim, June 2013
Torstein Thode Kristoffersen

Contents

List of Figures

List of Tables

Chapter 1

Introduction

This chapter introduces the Kårstø gas processing plant and provides a brief presentation of the steam delivery network at the plant. Furthermore, the challenges and previous work within control of steam delivery networks are presented. Based on this, a motivation for the utilization of model predictive control and optimization are stated, followed by the scope and outline of this thesis.

1.1 Kårstø Gas Processing Plant

Kårstø was the first gas processing plant in Norway to receive natural gas (rich gas) from the Norwegian continental shelf in 1985. Today the plant receives natural gas from several fields through the subsea pipelines Statpipe and Åsgard Transport and condensate through the subsea pipeline Sleipner.

At the plant, rich gas is separated into dry gas and natural gas liquids (NGLs), a mixture of ethane, propane, hexane and heptane, while the condensate from Sleipner is stabilized by removing the lighter NGLs. The dry gas, which mainly consists of methane, is transported to Germany through subsea pipelines and NGLs are further fractionated into ethane, propane, normal butane, butane, isobutane and naphtha. These products are stored and later shipped from Kårstø. This makes Kårstø the world's third largest export port for LPGs (liquefied petroleum gases), which embraces propane and butane (Statoil, 2007; Regjeringen, 2003).

The separation processes of both natural gas and condensate require large amounts of heat in order to separate the light component from the heavier components. In addition, there are several other components, such as steam turbines and steam-powered pumps that require large amounts of steam. To meet this demand of heat and steam, there is a large steam delivery network at Kårstø, which consists of eight boilers. These boilers collaborate in delivering high pressure (HP) steam with a pressure of 60 $[barg]$ and a temperature of 430 $[^{\circ}C]$ to the plant. Three of these boilers are not connected to gas turbines, but have the ability to fire two different fuel gases, natural gas and craier gas (CO_2 rich gas). The remaining five boilers are connected to separate gas turbines and are able to utilize the turbine

Figure 1.1: Kårstø gas processing plant. Photo: Statoil.

exhaust in addition to direct gas firing. The HP steam is currently controlled with a swing boiler, meaning that all the boilers but the swing boiler produces a constant amount of steam.

1.2 Motivation and Earlier Work

Steam delivery networks are an important part in many processing plants used to generate and deliver steam to various industrial processes, such as steam turbines, steam-powered pumps and distillation columns. The main task of a steam delivery network is to quickly follow the changes in load demand. Typically, these networks are exposed to large and fast load changes due to trips and start-ups of both boilers and different steam consumers. As stated in Hogg and El-Rabaie (1991), there is little or no coordination of the boilers within todays steam delivery networks and each boiler is typically controlled by several single-loop PI controllers. Hence, such disturbances are beyond the capacity of this type of control structures and can result in serious consequences, such as damages and shutdowns of boilers. Therefore, Majanne (2005) emphasizes the need for load leveling and stabilization of the common header pressure to ensure stability regardless of the disturbance. Load leveling is ability of distributing the load over the active boilers. Furthermore, the increased cost of energy and the increased global competition in both product quality and pricing forces the process industry to optimize various processes in order

to reduce cost and remain competitive (Glandt, Kelin, and Edgar, 2001). According to Downs and Skogestad (2011), economical optimization is solely conducted for processes at steady-state by a separate overlying controller. This illustrates the possibility of minimize the energy consumption with respect to stable operation. These requirements for increased stability and economically optimal operation lead to a complex multivariable control structure consisting of overriding control loops constraining the control actions of the stabilizing controllers (Majanne, 2005).

The steam delivery network control problem has been given some interest, but this interest is mainly restricted to networks consisting of only a single boiler in which coordination is irrelevant. Tyssø (1981) and Åström and Bell (2000) have both devoted a great effort in modeling the boiler dynamics to deepen the understanding of a boiler. This knowledge has enabled Hogg and El-Rabaie (1991); Lu and Hogg (1997); Havlena and Findejs (2005) and Majanne (2005) to study the control of a steam delivery network, consisting of a single boiler, using advanced control methods.

The Model Predictive Control (MPC) algorithm is an advanced controller which has gained much attention due to its success in the chemical industries (Qin and Bagwell, 2003). This controller treats multivariable control problems naturally, while simultaneously accounting for actuator limitations and constraints on process variables. Accordingly, the controller allows operation closer to system constraints and thereby enables a more efficient operation. The economically optimal setpoints are supplied from an overlaying controller and to this author's knowledge; there exist no published results on optimal production of high pressure steam. Therefore, the focus of this thesis is utilize multiple boilers to achieve stable and efficient control of a steam delivery network using a model predictive controller, and further minimize the energy consumption during steady-state operation using methods of optimization.

1.3 Scope and Outline

The objective of this thesis is to achieve stable and efficient control of the steam delivery network, and further minimize the energy consumption during stable operation, that is constant steam consumption. Stable and efficient operation is investigated by developing and testing of an MPC controller. The energy costs are minimized by minimizing the fuel consumption. This is examined through development and incorporation of an optimizer[1] on top of the MPC controller. Extensively research and effort is required to develop these two algorithms and it is assumed that the simulator, used to investigate these algorithms, provides a fairly accurate description of the steam delivery network.

Chapter 2 starts with a presentation of the steam delivery network under study followed by a description of its main components and control structure. In the following chapter, the relevant theory for the design of the optimizer is presented, which includes thermodynamics and optimization theory. Model predictive control

[1] In this case, an optimizer is a real time optimization problem used to minimize the fuel consumption for constant steam consumption, and is explained in Section 2.4.3.

and the SEPTIC application[2] are discussed in Chapter 4. Chapter 5 begins with an introduction of the steam delivery network control problem and previous solutions to this problem. A typical model predictive controller for control of a single boiler is derived from these results, and further extended to incorporate the complete steam delivery network. The chapter ends after a presentation of the tuning and models employed by the model predictive controller. In Chapter 6, a thermal efficiency analysis is derived and performed on the steam delivery network followed by the derivation of the real time optimization problem solved by the optimizer. In Chapter 7, different case studies are carried out. In the first part, the performance of the steam delivery network with and without model predictive control is compared for various disturbances. The second part investigates the potential reduction in fuel consumption and illustrates the issues when using two different real time optimization problems. The results are further discussed in Chapter 8 and the main conclusion and suggested further work are presented in Chapter 9. Additional plots and additional tables are attached in Appendix A and B, respectively. A proposal to a conference article is enclosed in Appendix C. This article provides a brief presentation of the results and findings of this thesis.

In this thesis, all vectors and matrices are typed as bold characters and all vectors are defined as column vectors. Furthermore, this thesis is constructed in such a way that all associated results are presented in succession and discussed together following the presentations.

This thesis is a continuation of the project report presented in Kristoffersen (2012). To make this report as extensively as possible, some of the sections in this thesis is based on the work performed in Kristoffersen (2012). Therefore, sections 2.1, 2.2, 2.5, 4.1 and 4.2 are copied with only minor changes, and the sections 2.4, 5.1, 5.2 and 5.3 are based on the material from the project report in addition to other sources.

[2]The SEPTIC application is the model predictive controller developed and utilized by Statoil.

Chapter 2

Process Description

This chapter begins with a presentation of the steam delivery network and its different operating modes. Furthermore, the main components of the steam delivery network are described in detail with emphasis on the issues regarding safe operation. In closing, the control hierarchy and various control structures for the different units in a boiler are explained in detail.

2.1 The Steam Delivery Network

The primary objective of the steam delivery network is to produce and deliver high pressure (HP) steam to different consumers at the plant. The steam delivery network is shown in Figure 2.1 and is equipped with eight parallel operating boilers feeding HP steam into the common header. The boilers cooperate in producing HP steam at a gage pressure of 60 $[bar]$ and a temperature of 430 $[°C]$ to maintain a stable common header pressure of 60 $[barg]$.

The steam delivery network is divided into three different pressure headers; HP, intermediate pressure (IP) and low pressure (LP) common header. These headers are displayed in Figure 2.1 as a red, pink and green line, respectively. The HP and IP common headers are connected through steam turbines, which drive compressors used to cool propane and ethane. The IP and LP common headers are connected through steam-powered pumps and compressors used to transport and cool gas. Lastly, the steam from the LP common header is returned to the boilers after transferring the remaining heat potential through various heat exchangers. The heat transferred through these heat exchangers is used in distillation columns to separate the light component form the heavier components. In order to achieve safe and efficient operation, these three common headers have to be stabilized. This means that the pressure falls, as a consequence of steam consumption, from a higher header to a lower header must happen without large fluctuations.

The HP common header is controlled by the steam generation in the boilers. The IP header and LP header are controlled by the turbine and pump utilization, respectively. Compared to the boilers, both the turbines and pumps have much

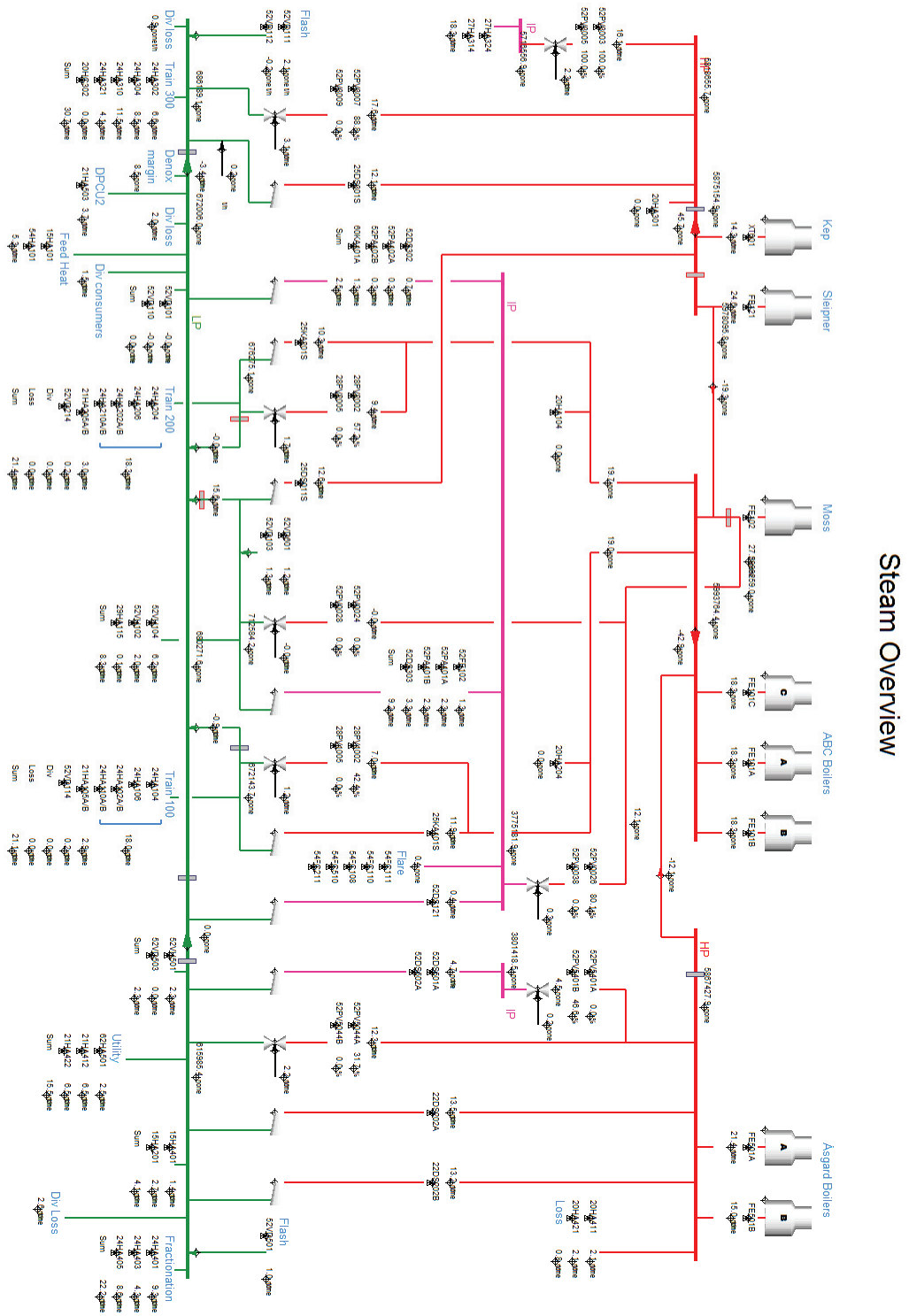

Figure 2.1: The steam delivery network. Photo: D-SPICE

wider control range and much faster control response. In practice, this means that the turbines and pumps have to be constrained in order to prevent disturbances in the IP and LP headers to propagate into the HP header. This is accomplished by overriding parallel controllers actuating the turbine and pump controllers. These controllers are assumed to provide fast and robust stabilization of the IP and LP headers and will not be further studied in this thesis. This thesis will focus on the control of the HP header and the interested reader is referred to Majanne (2005), where this is described.

Five of the boilers, the Åsgard boilers and the Foster Wheeler boilers[1], are connected to separate gas turbines, enabling utilization of gas turbine exhaust (TEG) in addition to ambient air (AA). Furthermore, all the boilers use natural gas as their main fuel source, while two of the boilers, Sleipner and Kristin (KEP), have the additional possibility of utilizing craier gas. Craier gas is the top product from the CO_2 strippers at the plant, where the impure ethane product is separated from the craier gas, which consists of ethane and carbon dioxide. Ethane is purified to meet sales specifications. In order to exploit the energy stored in the craier gas, that is the ethane, one of the boilers must burn the complete amount of craier gas. The Kristin boiler is commonly used for this purpose and since it is not possible to control the craier flow, the steam production for this boiler is uncontrollable. Hence, for the reminder of this thesis, the Kristin boiler is assumed to utilize all the craier gas and therefore not further considered.

2.2 Steam Boilers

Traditional steam boilers are well described in Balchen and Mumme (1988) and consist of a horizontal cylinder called drum and a combustion chamber containing several burners, as shown in Figure 2.2. In the combustion chamber, air and fuel are mixed and burned to produce a warm flue gas that passes around several vertical tubes called risers, carrying a mixture of water and steam. The drum is kept half full of water and the remaining half of steam. Due to gravity, water is driven down several tubes called downcomers to a smaller drum where mud is separated from the water. From here, the water is sent to the risers where evaporation occurs and steam rises to the drum.

The feedwater is commonly preheated in order to reduce the pressure fall in the drum. Moreover, steam delivery networks are commonly closed systems and the steam produced by a boiler is often returned as condensate to the drum, after delivering heat and energy to various steam consumers in the plant. In theory, steam delivery networks are without leakages and no water needs to be added. However, there are commonly leakages of steam, e.g. blowout valves, so it is often necessary to add additional feedwater to the drum.

The steam flow from the drum depends on the pressure difference between the drum and the common header. Before the steam leaves the drum, it needs to pass several superheaters separated by attemperators. The superheaters are

[1]The Foster Wheeler boiler are known as the ABC boilers in Figure 2.1.

heat exchangers where the warm flue gas from the combustion chamber transfers heat to the steam. The attemperators are valves that allow small fractions of the feedwater to be sprayed into the steam in the form of a fine mist. The purpose of the primary heat exchanger is to increase the temperature of the steam higher than that obtained in saturated state, i.e. increase the steam enthalpy. The objective of the following attemperator is to reduce the temperature of the steam to prevent a boiler meltdown, should the steam temperature become to high. Lastly, the steam passes the second superheater that ensures that the steam is without moisture to avoid rusting of turbine blades.

The required heat is generated in the combustion chamber through combustion of fuel and AA or TEG, which produce the warm flue gas. This flue gas is used to evaporate the water into steam by heat transfer through the heat exchangers surrounding the risers and superheaters. The combustion process poses some serious issues regarding safety and efficiency related to the air/exhaust to fuel ratio. The safety issue is related to the possibility of unburned fuel in the furnace due to lack of air/exhaust in the combustion process. This amount of unburned fuel can explode if it comes in contact with a hot spot. Furthermore, an excess of air/exhaust in the combustion process will lower the efficiency, as there will not be enough energy to heat the flue gas to the required temperature. It is obvious from these issues that there is a great need for control of the combustion process in order to ensure safe and efficient operation. This is a task for the regulatory layer and is studied in Section 2.4.1. The combustion process is discussed in Section 3.1.4.

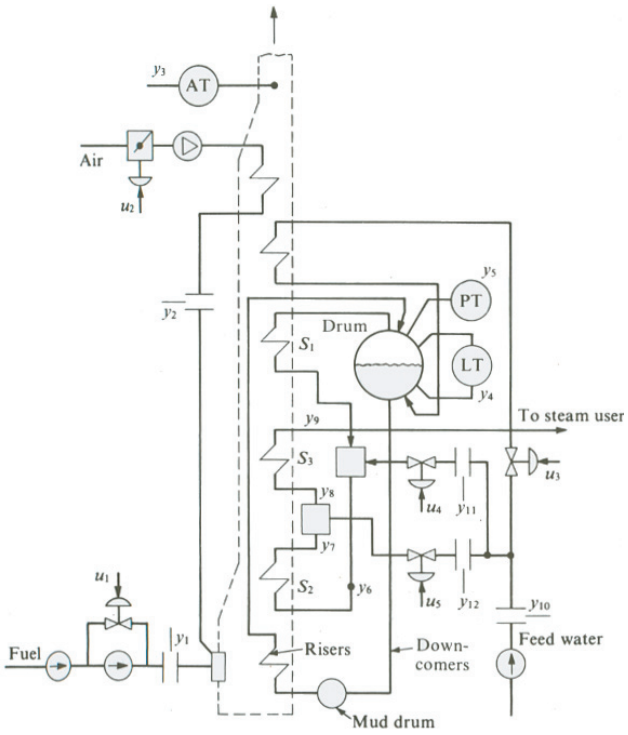

Figure 2.2: A steam boiler (Balchen and Mumme, 1988).

There has been made great effort by many researchers to describe the dynamics of steam boilers by nonlinear differential equations. Much of this research has been useful in explaining the inner phenomena occurring in a boiler and in turn, for the design and later control of boilers by feedback and state space estimation. One of these important phenomena occurs when the steam demand from the plant increases, which causes the steam flow from the drum to increase. This will result in a drum pressure drop, which in turn causes the steam bubbles in the riser and under the water level to increase in size. This is called the *swell effect* as the bubbles increase in size, which results in an increase of water level. This effect will disappear and the level will sink when the steam flow is kept constant. The opposite effect, when steam demand is reduced, causes an increase in drum pressure and in turn the bubbles to shrink in size. This effect is called the *shrink effect* as the level will drop. Again, the effect will disappear and the water level will rise when the steam flow is kept constant. From this, the researchers have shown that the control must be slow enough to avoid dealing with these phenomena. Both Tyssø (1981) and Åström and Bell (2000) provide a good mathematical description of the boiler dynamics. The interested reader is referred to these, as this thesis will use step response models of the different processes at the plant obtained by SEPTIC.

2.3 Gas Turbines

A gas turbine is a type of internal combustion engine commonly used to drive compressors and pumps. They are favored for their power-output-to-weight-ratio and reliability. Gas turbines are briefly described in Moran and Shapiro (2010) and consist of a compressor combined with a turbine connected through a combustion chamber, as shown in Figure 2.3.

Air at atmospheric pressure is continuously drawn into the compressor, where it is brought to higher pressure. After passing through the compressor, the air enters the combustion chamber where it is mixed with fuel and combustion occurs. The combustion process causes the exhaust gases to leave the chamber at significantly higher temperature than that of the air. Furthermore, the exhaust gases expand through the turbine and are subsequently used as the source of oxygen in the connected boiler's combustion process. Hence, if the gas turbine is not operational, the boiler must utilize AA rather than TEG at sig-

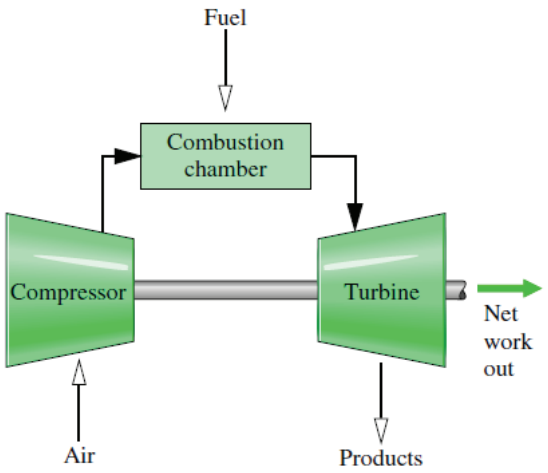

Figure 2.3: A gas turbine. (Moran and Shapiro, 2010)

nificantly lower temperature. The work developed due to the gas expansion is partly used to drive a compressor, while the remaining work is available for other purposes, e.g. to drive other types of compressors, pumps or electric generators.

2.4 Control Structure

In large chemical plants, the control system is divided into several layers separated by their computational timescale. They are:

- scheduling (weeks),
- site-wide optimization (days),
- local optimization (hours),
- supervisory control (minutes),
- regulatory control (seconds).

The layers are shown in Figure 2.4 and are linked by controlled variables, where the setpoint for a lower layer controlled variable is determined by an upper layer manipulated variable. The two lower layers, called base layers, operate continuously to ensure safe and optimal control of the plant, where as the other layers computes setpoints once the engineers get new information about different prices relevant for economic operation of the plant (Skogestad, 2004).

2.4.1 Regulatory control layer

The general purpose of the regulatory control layer is to locally stabilize the process, that is mathematically stabilizing unstable modes and prevent drifting away from nominal operating point. This is done with single-input-single-output (SISO) PI control loops. In the theory provided in Skogestad (2004), it is outlined how to choose good control variables for stabilization and disturbance rejection, so that the supervisory control layer can handle the effect of disturbances by determining the setpoint.

The control of the water level is a very important task for the regulatory control layer. Consider a sudden decrease in steam consumption for a boiler. This will cause a rise in water level and the water will eventually be mixed with the steam. Hence, liquid water will be transported with the steam to different steam consumers and cause corrosion of the equipment. However, a sudden increase in steam consumption for a boiler will cause a drop in water level. This will result in meltdown of the boiler if the water level becomes too low. These reasons, combined with the swell and shrink effect, clearly show the importance of level control to ensure safe and efficient operation. Since the level process is an integrating process, the simplest approach is to use the *single-element control* scheme. This control scheme consists of a single PI controller, which uses the drum level as measurement and the feedwater valve as actuator. This control scheme relies entirely on the drum level measurement and during transients; this measurement fails to capture the

complete dynamics. Therefore, modern boilers include an additional feedback part and a feedforward part. The idea is that there is a mass balance, that is, the steam leaving the boiler should equal the feedwater entering the boiler. Hence, the steam flow and the feedwater flow are measured. The steam flow provides feedback for output flows, while the drum level provides feedback compensation for unmeasured flows. These measurements are combined to form a cascade controller, in which the feedwater measurement provides the feedforward part. This control scheme is called *Three-element control* and is shown in Figure 2.5a (Smith and Corripio, 2006).

Another important task for the regulatory control layer is the control of the combustion process, as previously explained. There exist several control schemes for this task, but there are only three different control schemes employed at the plant. These will be presented after a short discussion about the principle of combustion control. The objective of the combustion control scheme is to ensure that there always is an excess of oxygen in the combustion process to prevent explosions. However, the excess should be as small as possible to increase the efficiency of the combustion process.

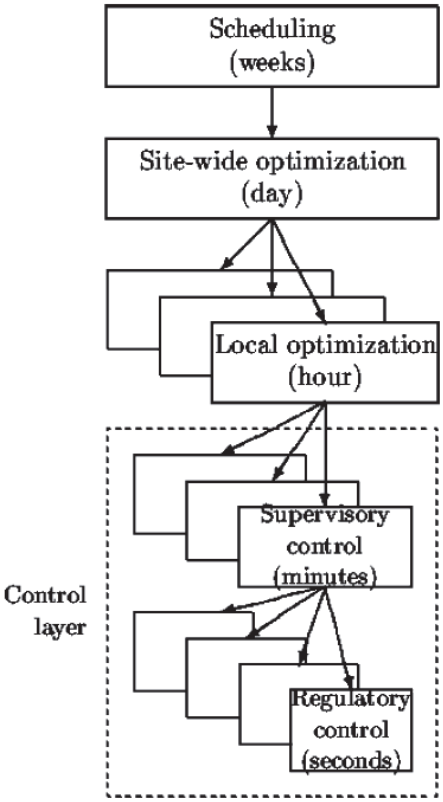

Figure 2.4: A typical control layer hierarchy (Skogestad, 2004).

The simplest combustion control scheme at the plant, used by each of the Foster Wheeler boilers, is the *ratio control* scheme, shown in Figure 2.5b. This control scheme, explained by Smith and Corripio (2006), consists of two flow measurements and two flow controllers. The fuel flow controller (FC16) receives its setpoint from an external source, e.g. an operator or an MPC controller. The setpoint for the oxygen flow controller (FC17) is the fuel flow measurement multiplied by the desired ratio, R. Another, more advanced controller can be derived from this control scheme by replacing the flow controllers with energy controllers and multiply both the flow measurements by the higher heating value for the fuel that is used. This type of control scheme is utilized by both the Åsgard boilers. For these types of control schemes the desired fuel flow rate is the degree of freedom. These control schemes are utilized by the boilers with a separate connection to a gas turbine because the TEG flow is uncontrollable, meaning that all the available TEG must either be

utilized by the combustion process or released through a blowout valve. Thus, the desired ratio, R, is fixed by the gas turbine when the boiler utilizes TEG. The reason for this implementation is it is costly not to utilize the energy which has already been supplied to the TEG flow.

Due to the reasons discussed above, it is desirable to always have an excess of oxygen. However, too great an excess of oxygen leads to an energy loss. Therefore, tight ratio control is desired. This implies that in the case of increased combustion, the source of oxygen must be increased before the fuel flow. However, in the opposite case, that is, in the case of reduced combustion, the fuel flow must be reduced before the source of oxygen. This complexity is not achieved with the two control schemes previously presented. Hence, they do not offer tight control and both require a bias to ensure that there always is an excess of oxygen.

The *cross-limiting control* scheme applied by the Moss and Sleipner boiler ensures tight control of the fuel to oxygen ratio. The control scheme is shown in Figure 2.5c and consist of one header pressure controller (PC22) and two flow controllers (FC23 and FC24), each with its own measurement. The setpoint to the pressure controller is set by an external source, while the setpoints to the flow controllers are calculated from the header pressure controller. The control scheme utilizes a high and a low selector to keep the fuel to oxygen ratio above a critical value, which ensures that the mixture is never rich in fuel. In the case of a drop in header pressure, due to an increase in steam demand, the pressure controller will demand more fuel. The cross-limiting control structure of selectors will ensure that the source of oxygen increases before the fuel. When the header pressure rises, due to a decrease in steam demand, the pressure controller will require less fuel. The cross-limiting control structure of selectors will ensure that the fuel decreases before the source of oxygen. Additionally, working outside cross-limiting control scheme, there is an oxygen trim, which slowly adjust the ratio on the basis of oxygen quality in the flue gas. For this type of control scheme, the desired header pressure is the degree of freedom (Smith and Corripio, 2006).

2.4.2 Supervisory control layer

The purpose of the supervisory control layer is to keep the controlled variables at optimal setpoints using the setpoints for the regulatory control layer as the manipulated variables. In order to achieve this, Skogestad (2004) proposes two different multivariable control strategies; decentralized and multivariable control. The first strategy is preferred for non-interacting processes and in cases where the active constraints remain constant, while the second strategy is preferred for interacting processes and in cases where the active constraints changes. Further discussion and comparison between these two strategies are conducted in Skogestad (2004).

A boiler is a multiple-input-multiple-output (MIMO) system, i.e. one input affects more than one output. A step applied to the combustion process might change several variables, such as the amount of produced steam, the steam temperature and the combustion pressure. All these variables can under different conditions meet their high limits and therefore become active constraints. Furthermore, the

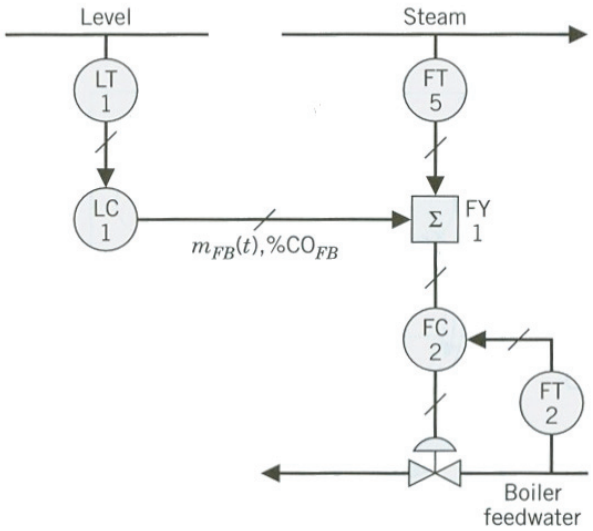

(a) The three element control scheme.

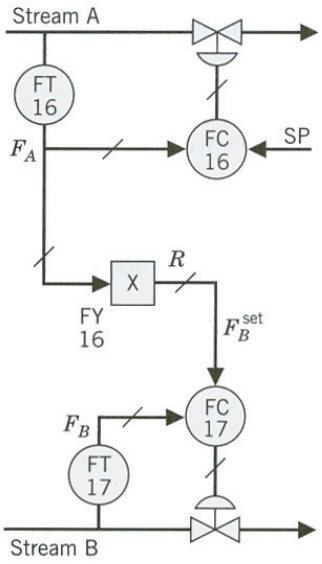

(b) A simple ratio control scheme.

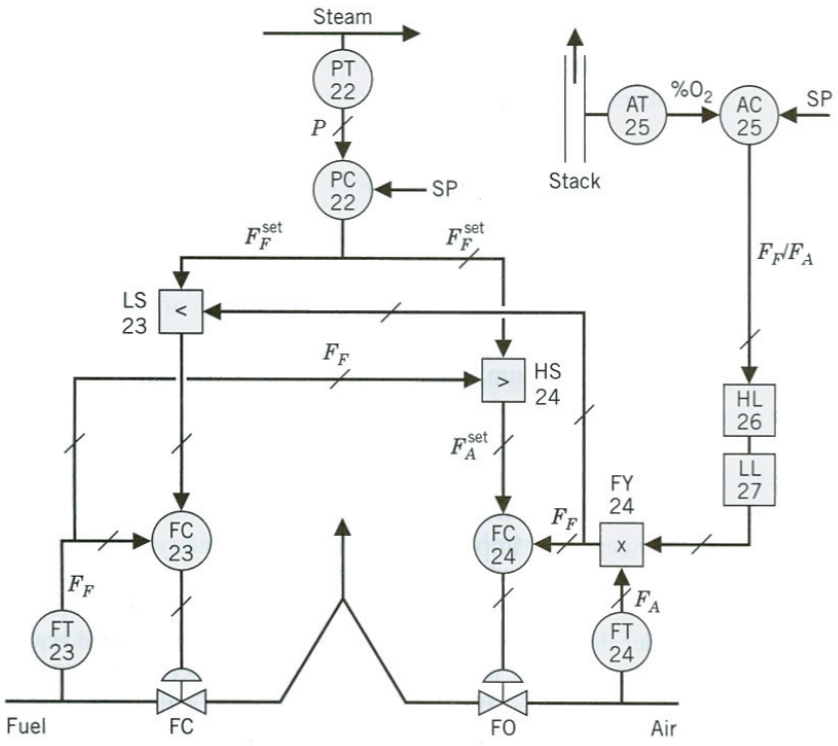

(c) The cross-limiting control scheme with O_2 trim.

Figure 2.5: A collection of various control schemes (Smith and Corripio, 2006).

steam demand is highly varying, which causes small and large fluctuations around the desired common header pressure. The regulatory control layer operate well under steady-state operations, as it manages to maintain a constant common header pressure for small disturbances, such as set-point changes. However, when large disturbances occur, e.g. a boiler trip[2], the regulatory layer tends to be inadequate. Hence, the single-input-single-output (SISO) control provided by the regulatory layer is not able to capture the complete dynamic and therefore has limited control over the steam delivery network.

These observations clearly show that there is a need for a MIMO controller to achieve good control of a boiler and consequently, of the steam delivery network. Hence, a multivariable controller is the obvious choice due to the highly interacting system and changes in active constraints. Therefore, an MPC controller is designed for the steam delivery network as this is a well-proven multivariable controller which fits the process behavior (Qin and Bagwell, 2003). The MPC controller is further discussed in Chapter 4 and designed for the steam delivery network in Chapter 5.

2.4.3 Optimization layer

There are two optimization layers, divided into local and site-wide optimization. Local optimization is conducted for a limited part of the plant, e.g. the steam delivery network, while site-wide optimization is performed for the whole plant. In this thesis, the focus will be on the local optimization layer, henceforth called the optimization layer.

Once the equipment and the controllers are installed, plant engineers strive to enhance the various processes in order to minimize cost, increase product quality and so on. Typically, this is achieved by formulation of an economically optimization problem, which is minimized on an hourly or daily basis, depending on the time scale and economical intensives. This optimization problem consists of an economical optimization problem which involves the cost of the process, for example the cost of raw materials and the value of products. The constraints typically include operating conditions and product impurities. The optimization problem is either solved off-line or on-line. Off-line optimization is preferred when the active constraints remain constant and we are able to find good self-optimizing controlled variables, this is thoroughly discussed in Skogestad (2004). However, when the active constraints do change, on-line optimization is the preferred strategy. Finally, the solution from the optimization strategy is passed down as setpoints or ideal values to the respective variables in the MPC controller (Glandt, Kelin, and Edgar, 2001).

As previously explained, the steam delivery network is expected to experience large disturbances, such as boiler trips. Disturbances like this will change the set of active boilers and thus the active constraints. This knowledge clearly indicates that an on-line optimization is the preferred strategy. On-line optimization is commonly conducted by a Real Time Optimization (RTO) optimizer, which is discussed in

[2]A boiler trip occurs when one or multiple operating parameters cross its maximum or minimum values, forcing the operators to shut down the boiler.

Section 3.2. In Chapter 6 an optimizer for the steam delivery network is derived.

2.5 The D-SPICE Simulator

D-SPICE (Dynamic Simulator for Process Instrumentation and Control Engineering) is a dynamic process simulator developed by Fantoft, now a part of Kongsberg Oil and Gas. D-SPICE allows for both development and operation of different oil and gas installations. The simulator provides a large library of common oil and gas operation units, such that models can easily be built by connecting various units and set parameters and initial conditions. Then numerical methods are used to solve mass-, energy- and component balances during simulations (Fan).

The advantages of D-SPICE simulator are the ability to divide large plants into several modules, that can be run separately or together using a so-called master model. This makes it easy to get an overview and test interesting sub-processes. Furthermore, separate programs, such as SEPTIC, can communicate with D-SPICE over TCP/IP by employing the standardized OPC protocol. In this way, SEPTIC can receive measurements and set setpoints to different controllers in D-SPICE.

A complete simulator model of the Kårstø gas processing plant has been created for the D-SPICE simulator and is used in this master thesis. Furthermore, an OPC server for communication between D-SPICE and SEPTIC was configured created using the XPress OPC server.

Chapter 3

Theory

This chapter provides a brief introduction to some of the relevant theory for this thesis. The first section presents the thermodynamics used in this thesis, while the second section presents optimization and its main elements. The section on thermodynamics is based on Moran and Shapiro (2010) and Young and Freedman (2008), while the subsequent section is based on Nocedal and Wright (2003) and Glandt, Kelin, and Edgar (2001).

3.1 Thermodynamics

Thermodynamics is a part of engineering science concerned with heat and its relation to energy and work. Basic for thermodynamics is the concept of the system and its surroundings separated by a specified boundary. The system is what we want to study and it is described by macroscopic variables[1], in which a subset of these variables specifies the state of the system. The state of the system changes when the system undergoes a thermodynamic process, which is a transformation from one state to another state. However, if the state of the system remains unchanged over time, the system is at steady-state, as none of the variables changes with time.

The system might be all from a simple heat exchanger to a complete boiler, and everything external to the system is considered as the surroundings. The system is separated from the surroundings by a specified boundary. A closed system always contains the same matter and there is no transfer of mass across the boundary. In addition, when there is no interaction with the surroundings, the system is called an isolated system. However, a control volume is a fixed region with open system boundaries, in which both mass and energy may flow through.

Energy is a fundamental concept of thermodynamics. The basic idea of energy is that it can be stored within a system in various forms, converted from one form to

[1] Macroscopic variables are variables that characterize the materials and radiation such as temperature (T), pressure (p), volume (V), mass (m) to which numerical values can be assigned without knowledge of the previous history of the system.

another form and transferred between systems. The total energy is conserved in all transfers and conversions. Furthermore, the conservation of energy principle states that the total energy for an isolated system remains constant and as a consequence, energy cannot be created or destroyed. The total energy of a system is made up by kinetic energy, potential energy and internal energy, in which the latter includes all the other forms of energy. The change in total energy is given by

$$\Delta E = \Delta KE + \Delta PE + \Delta U, \tag{1}$$

where KE, PE and U represent kinetic, potential and internal energy, respectively.

3.1.1 The laws of thermodynamics

Thermodynamics is based on four laws which deal with the properties of energy and the behavior of systems and processes. These laws can briefly be presented as follows:

- Zeroth law of thermodynamics: *If two bodies are in thermal equilibrium with a third body, they are also in thermal equilibrium with one another.*
- First law of thermodynamics: *Energy can neither be created or destroyed, only change from one form to another form.*
- Second law of thermodynamics: *Heat is always transferred in the direction from high to low temperature, never the opposite.*
- Third law of thermodynamics: *As the system approaches absolute zero, all thermodynamic processes stops.*

In this thesis, only the first law of thermodynamics is of interest and therefore this is only law further discussed.

The first law of thermodynamics

The *first law of thermodynamics* is a generalization of the principle of conservation of energy to include energy transfers as heat and mechanical work. The law states that energy is always conserved and can neither be created nor destroyed, only change from one form to another form. Hence, the first law of thermodynamics is expressed as

$$\Delta E = Q - W, \tag{2}$$

where Q and W represent the heat and work transfer across the system boundaries, respectively. This energy balance requires that the increase or decrease in energy of a closed system is equal to the net amount of energy transferred across the system boundaries. Often, there is a continuous flow of energy across the system boundaries and for those systems the energy balance becomes

$$\frac{dE}{dt} = \dot{Q} - \dot{W}. \tag{3}$$

These two equations apply for closed systems and they are energy balances for finite and continuous energy transfers, respectively. However, for control volumes the mass flows brings energy in and out of the system across the system boundaries. Therefore, it is necessary to extend these equations to account for the mass flows in and out of the system and the energy balance becomes

$$\frac{dE_{cv}}{dt} = \dot{Q} - \dot{W} + \sum_i \dot{m}_i \left(h_i + \frac{V_i^2}{2} + gz_i \right) - \sum_e \dot{m}_e \left(h_e + \frac{V_e^2}{2} + gz_e \right), \quad (4)$$

where the subscripts i and e denote inlets and exits, respectively. The variables V, g and z denote velocity, specific gravity and horizontal position, respectively.

Thermodynamic work

In thermodynamics, the work performed by the system is the energy required to create the necessary space for the system. Hence, the work is obtained from the expression

$$W = \int_{V_1}^{V_2} p \, dV, \quad (5)$$

where V and p denote volume and pressure, respectively.

3.1.2 The ideal gas law

The ideal gas law is a model of a hypothetical ideal gas and is given by the equation

$$pV = n\bar{R}T, \quad (6)$$

where V is the volume, n is the number of moles, T is the temperature and $\bar{R}$ is the universal gas constant equal to 8.314 [kJ/kmol K]. The relationship between the number of moles and the mass is $n = \frac{m}{M}$, and inserting this expression into the equation above yields

$$pV = \frac{m\bar{R}T}{M}, \quad (7)$$

where M is the molar weight of the gas. The model is fairly accurate for small pressures relative to the critical pressure and/or for large temperatures relative to the critical temperature[2].

The ideal gas law can be used to determine the mass or volume flow to the respective volume or mass flow measured at either normal[3] or standard[4] conditions.

[2]The critical pressure of a substance is the pressure required to liquefy a gas at its critical temperature. The critical temperature of a substance is the temperature at the point in which vapor of the substance cannot be liquefied, no matter how much pressure is applied.

[3]Normal variables are mass or volume flows measured at 15 [$^\circ C$] and 1 [atm].

[4]Standard variables are mass or volume flows measured at 0 [$^\circ C$] and 1 [atm].

3.1.3 Enthalpy and specific heat

Enthalpy is a measure of the total energy of a thermodynamic system. It is defined as the sum of the internal energy required to create the system, and the volume and pressure required to make room for the system. Hence, the enthalpy is given by

$$h = u + pv, \tag{8}$$

where u and v are the specific internal energy and specific volume per unit mass, respectively.

Given the pressure or temperature, thermodynamic tables can be used to provide values for specific enthalpy. In the case of vapor, the specific enthalpy can be read directly thermodynamic tables given the temperature and the pressure. However, for a liquid-vapor mixture there are two values of enthalpy available in the thermodynamic tables, saturated liquid h_f and saturated vapor h_g. Therefore, the specific enthalpy is found in terms of the quality, that is the ratio of the mass of vapor present to the total mass of the mixture given as

$$x = \frac{m_{vapor}}{m_{liquid} + m_{vapor}}, \tag{9}$$

where x, m_{vapor} and m_{liquid} are the quality, the amount of vapor and the amount of liquid. Hence, the specific enthalpy is given as

$$h = h_f + x(h_g - h_f). \tag{10}$$

Several properties related to internal energy are important in thermodynamics and one of these is the specific heat. Specific heat is the amount of heat required to raise a unit mass of a substance by one degree in temperature. The heat supplied to a unit mass of a substance can be expressed as

$$dQ = c \cdot dT, \tag{11}$$

where c is the specific heat of the substance. This expression can be rearranged to express the specific heat for the given substance

$$c = \frac{dQ}{dT}. \tag{12}$$

Then, the expressions for the specific heat at constant volume and pressure can be derived by inserting for the first law and calculate the work at constant volume and pressure, respectively. Hence, the expressions become

$$c_V = \frac{du}{dT}, \qquad \wedge \qquad c_p = \frac{dh}{dT}, \tag{13}$$

where c_V is the specific heat at constant volume and c_p is the specific heat at constant pressure.

3.1.4 Combustion

In a combustion reaction, the combustible elements of the fuel are oxidized resulting in a release of energy through the increased temperature of the combustion products. The fuel and oxidant are generally referred to as *reactants* and combustion products are generally referred to as *products*.

A fuel is a combustible substance. It can consist of various combinations of the three major combustible substances, namely carbon (C), hydrogen (H) and sulfur (S). In this thesis, the combustible parts of the fuel is assumed to consists of various forms of hydrocarbons (C_aH_b), this because natural gas is the fuel used at the plant.

Oxygen is required in every chemical reaction and the most common source of oxygen is air. However, air is not pure oxygen, but consists mainly of oxygen and nitrogen. Air is usually considered to be 21 [%] oxygen (O_2) and 79 [%] nitrogen (N_2) on a molar basis. With this model of the air, the ratio of nitrogen to oxygen becomes 3.76[5]. Furthermore, nitrogen is considered as an inert. This means that nitrogen is present in the combustion process, but that it does not react in the chemical reaction.

The combustion is *complete* when all the carbon present in the fuel is burned to carbon dioxide (CO_2), all the hydrogen is burned to water (H_2O), all sulfur is burned to sulfur dioxide (SO_2) and all other combustible elements are fully oxidized. The combustion is *incomplete* when there is not enough oxygen to completely produce CO_2 and H_2O, and the carbon only partly reacts and produces carbon monoxide (CO). Thus, to achieve complete combustion there must be enough oxygen to fully oxidize the reactants.

For this thesis, the general chemical reaction equation for a complete combustion reaction is on the form

$$C_aH_b + \left(a + \frac{b}{4}\right)(O_2 + 3.76N_2) \rightarrow aCO_2 + \frac{b}{2}H_2O + \left(a + \frac{b}{4}\right)3.76N_2, \qquad (14)$$

where a and b represent the numbers of moles of the respective substances.

Energy Balances for Reacting Systems

In thermodynamics, the energy released through combustion can be calculated using an energy balance for combustion reactions. This reaction can easily be explained by a generalized system in which all gases are regarded as ideal gas mixtures, as shown in Figure 3.1. The fuel and air enters the system separately, while the combustion products leave the system as one flow. Then, given the chemical reaction equation, the steady-state energy balance for systems involving combustion are given by

$$\dot{Q}_{cv} - \dot{W}_{cv} = \dot{n}_F \left[\sum_P \dot{n}_e \bar{h}(T,p)_e - \sum_R \dot{n}_i \bar{h}(T,p)_i\right], \qquad (15)$$

[5] $0.79/0.21 = 3.76$

where the subscripts i and e denote the inlet and exit flows, respectively. The count variables P and R represent the products and reactants, respectively, while the $\dot{n}_F$ is the mole rate of fuel. The specific enthalpy of a substance $\bar{h}(T,p)$ is evaluated using the following equation

$$\bar{h}(T,p) = \bar{h}_f^\circ + [\bar{h}(T,p) - \bar{h}(T_{ref}, p_{ref})] = \bar{h}_f^\circ + \Delta\bar{h}, \tag{16}$$

where $\bar{h}_f^\circ$ is the enthalpy of formation and $\bar{h}$ is the enthalpy of a substance per mole.

The enthalpy of combustion $\bar{h}_{RP}$ is the energy released when complete combustion occurs and is defined as the difference between the enthalpy of the products and the enthalpy of the reactants. That is

$$\bar{h}_{RP} = \sum_P n_e \bar{h}_e - \sum_R n_i \bar{h}_i, \tag{17}$$

which is the same expression as inside the square brackets in Equation (15). The *heating value* of a fuel is a positive number equal to the magnitude of the enthalpy of combustion. There are two different heating values, which are related to the phase of the water formed by combustion. The *higher heating value* (HHV) is used when the water formed by combustion is a liquid and the *lower heating value* (LHV) is used when the water formed by combustion is a vapor.

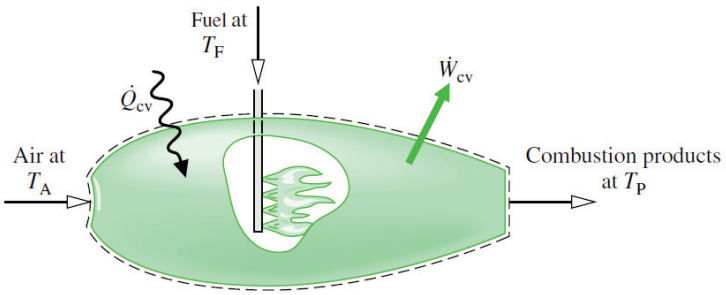

Figure 3.1: A generalized system involving a combustion process (Moran and Shapiro, 2010).

3.2 Optimization

Optimization is the use of specific methods to determine the most cost-effective solution to a process problem within given constraints. This technique has evolved to become an essential tool in most engineering activities, among others, in optimization of process operations. The optimization problem contains two essential elements:

- an *objective function* that provides a quantitative measure of the process,
- a model that describes the behavior of the process and which can be transferred into one or more *equality* and/or *inequality constraints*.

The objective function represents the cost of the problem and is to be minimized without exceeding the constraints. An optimal solution of the problem satisfies the constraints and provides an optimal value of the objective function. There may be none, one or several optimal solutions depending on the formulation of the problem. The interested reader is referred to Nocedal and Wright (2003) and Glandt, Kelin, and Edgar (2001), which this section is based on, for a thorough discussion of the existence of optimal solutions.

Optimization problems can be classified in several categories according to whether the objective function and the constraints are linear and whether the variables are continuous and/or discrete. Optimization problems with discrete variables are called *integer programming* problems and those with both discrete and continuous variables are called *mixed integer programming* problems. When both the objective function and the constraints are linear, the optimization problem is a *linear programming* problem. However, when at least one of the constraints or the objective function is non-linear functions, the optimization problem is a *Non-Linear Programming* (NLP) problem.

In this thesis, the optimization problem of interest is a NLP problem. These problems are mathematically formulated as

$$\begin{aligned} \underset{x\in\mathbb{R}^n}{\text{minimize}} \quad & f(\mathbf{x}), && \text{(18a)} \\ \text{subject to} \quad & \mathbf{h}(\mathbf{x}) = \mathbf{0}, && \text{(18b)} \\ & \mathbf{g}(\mathbf{x}) \leq \mathbf{0}, && \text{(18c)} \end{aligned}$$

where $\mathbf{x}$ is a vector of n variables, $\mathbf{h}(\mathbf{x})$ is a vector of equality constraints, $\mathbf{g}(\mathbf{x})$ is a vector of inequality constraints and $f(\mathbf{x})$ is the scalar objective function.

In this thesis, the *Active Set Method for Convex QPs* was selected as the algorithm to solve the NLP problem. This method is selected for its ability to take large steps and handle non-smooth constraints. It is not the purpose of this thesis to give a deepening understanding of optimization solvers. Therefore, only a short presentation of the active set method is included and the interested reader is referred to Nocedal and Wright (2003) for a deeper understanding of optimization solvers. Generally, the active set method for convex QPs tries to solve an

optimization problem on the form

$$\min_{x} \quad \frac{1}{2}x^T Gx + x^T c, \tag{19a}$$

$$\text{s.t} \quad a_i^T x = b_i \qquad i \in \mathcal{E}, \tag{19b}$$

$$a_i^T x \leq b_i \qquad i \in \mathcal{I}, \tag{19c}$$

to find the optimal solution x^*, where $\mathcal{E}$ and $\mathcal{I}$ are the set of equality and inequality constraints, respectively. Initially, the method starts by guessing an initial working set $\mathcal{W}$ of active constraints, where all included inequality constraints are set as equality constraints. Then, an equality constrained QP on the form

$$\min_{p} \quad \frac{1}{2}p^T Gp + g_k^T p, \tag{20a}$$

$$\text{s.t} \quad a_i^T p = 0 \qquad i \in \mathcal{W}_k, \tag{20b}$$

is solved to find the step p towards the optimal solution. This is repeated until the optimal active set is found and the Karush-Kuhn-Tucker (KKT) conditions, presented in Nocedal and Wright (2003), are satisfied. The step p is shortened by a factor α should it be too long and violate any of the constraints.

The optimization problem is implemented into a RTO optimizer used to optimize specified plant operations. A RTO optimizer is an algorithm incorporated on top of the MPC controller and utilizes optimization theory to solve the optimization problem. These algorithms typically operate in closed-loop, meaning that they utilize process measurements at the start of each iteration. The frequency of the iterations depends on the time scale of the process and is chosen long enough for the process to reach steady-state. In the first part of the iterations, the current operating point of the process is used to update the model and as initial point for the optimization. Following this, the optimization is performed using the updated model and the economic requirements to find the new optimal operating point. This new optimal operating point is a set of optimal operating variables which is passed to the controlled variables for the MPC controller either as setpoints or as ideal values, the latter is used in this thesis.

Chapter 4

Model Predictive Control

This chapter provides a presentation of the model predictive control principle and the SEPTIC application used in this thesis. The chapter begins by introducing the process models employed by the SEPTIC application, followed by a detailed presentation of the model predictive control principle. The last section presents the SEPTIC application and its main features.

4.1 Process Models

In the academic literature most chemical processes are described by state space models and there are several system identification methods available for finding these models. However, this approach of modeling chemical plants can be complex and since most chemical processes can easily be described by step or impulse responses this is the common approach in the industry and for this project.

The step response is discussed in Maciejowski (2002) and Proakis and Manolakis (2007). The idea is that one can apply a step at each input and record the open-loop response at each output variable until it settles at a constant value. Then, by assuming linearity of the process, the response of any other input signal can be deduced by knowing the step responses of the process.

There are some drawbacks associated with the step response model, e.g. it can only be applied on asymptotically stable plants. Steps on input can be too disruptive and step response models are ineffective for large multivariable systems as it require large storage capacity.

A step response model for a single input variable is described mathematically by assuming that the process is at steady-state, with all input and output initially at 0. Then, by applying a unit step on input j, that is

$$\{u_j(t) = 1 | t \geq 0\}, \tag{21}$$

the recorded step response on output i becomes

$$y_i(t) = \sum_{k=0}^{t} h_{ij}(t-k)u_j(k), \tag{22}$$

$$y_i(t) = \sum_{k=0}^{t} h_{ij}(t-k), \tag{23}$$

where $h_{ij}(t-k)$ is the output response of output i to a step on input j at time t. This equation can be simplified by knowing that

$$\sum_{k=0}^{t} h_{ij}(t-k) = \sum_{k=0}^{N} h_{ij}(k), \tag{24}$$

and inserting this into Equation (23) yields

$$y_i(t) = \sum_{k=0}^{t} h_{ij}(k). \tag{25}$$

The sequence of output responses $(h_{ij}(0), h_{ij}(1), \ldots)$ can be used as a model of the input-output relationship if N is sufficiently large, i.e. $h_{ij}(N+1) \approx h_{ij}(N)$, and such a case is shown in Figure 4.1.

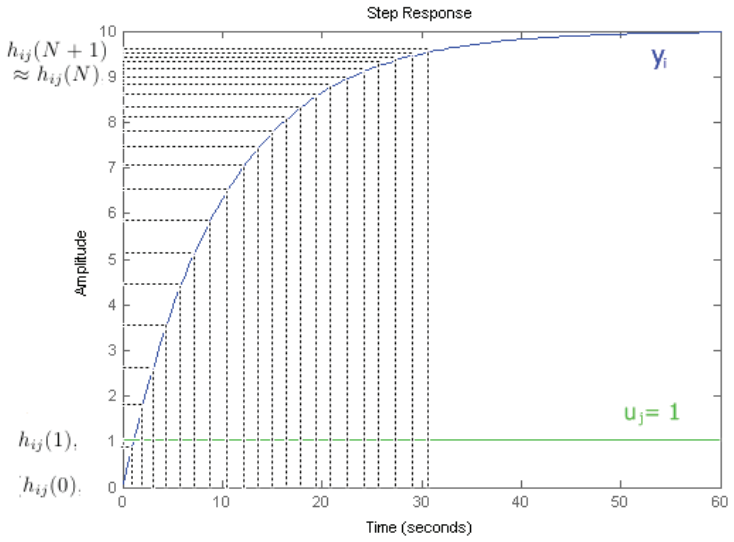

Figure 4.1: The step response idea.

Now, the idea can be extended to obtain a complete model of the plant. First, all the response coefficients for a step at time t needs to be combined into a single vector for every input. Hence, the response coefficient vector for input j is given as

$$\mathbf{h}_j(t) = \begin{bmatrix} h_{1j}(t) & h_{2j}(t) & \ldots & h_{pj}(t) \end{bmatrix}^T. \tag{26}$$

Next, a matrix is constructed by combining all the inputs respective response coefficient vectors

$$\mathbf{H}(t) = \begin{bmatrix} h_{11}(t) & h_{12}(t) & ... & h_{1m}(t) \\ h_{21}(t) & h_{22}(t) & ... & h_{2m}(t) \\ \vdots & \vdots & \ddots & \vdots \\ h_{p1}(t) & h_{p2}(t) & ... & h_{pm}(t) \end{bmatrix}, \tag{27}$$

where p is the number of outputs and m is the number of inputs. Now, the response $y(t)$ to an arbitrary input signal vector $u(t)$, because of assumed linearity, is given by

$$y(t) = \sum_{k=0}^{t} \mathbf{H}(t-k)u(k). \tag{28}$$

In the standard MPC formulation the input change $\Delta u(t) = u(t) - u(t-1)$ is used rather than the input itself. Therefore, the response is rewritten to depend on the change in input. To achieve this, the step response matrix is defined as

$$\mathbf{S}(t) = \sum_{k=0}^{N} \mathbf{H}(k). \tag{29}$$

This matrix or sequence is often called the *Dynamic Matrix* and can be used as a model of the plant if N is sufficiently large, i.e. $\mathbf{S}(N+1) \approx \mathbf{S}(N)$. Now, Equation (28) is rewritten to depend on the input change rather than the input itself

$$y(t) = \sum_{k=0}^{t} \mathbf{H}(t-k) \sum_{i=0}^{k} \Delta u(i). \tag{30}$$

Further, by assuming that $u(0) = 0$ and inserting for the step response matrix, the sequence becomes

$$y(t) = \sum_{k=0}^{t} \mathbf{H}(k)\Delta u(0) + \sum_{k=0}^{t-1} \mathbf{H}(k)\Delta u(1) + \ldots + \mathbf{H}(0)\Delta u(t), \tag{31}$$

$$y(t) = \sum_{k=0}^{t} \mathbf{S}(t-k)\Delta u(k), \tag{32}$$

$$y(t) = \sum_{k=0}^{t} \mathbf{S}(k)\Delta u(t-k). \tag{33}$$

This last equation is used by the MPC controller to model the plant.

4.2 Model Predictive Control

Model predictive control (MPC) is an advanced computer controller, as previously explained commonly implemented in the supervisory control layer. A short introduction to MPC is provided by Imsland (2002) and for a more thorough description the reader is referred to Morari and Lee (1998) and Maciejowski (2002).

Maciejowski (2002) states that the advantages and main reasons for the success of MPC applications are that:

- it handles multivariable control problems naturally.
- it can take actuator limitations into account.
- it allows for operation closer to constraints, which frequently leads to more profitable operation.
- the control update for these applications is slow enough for a solution to be found.

The MPC principle is that the controller uses a multivariable process model to predict future behavior of the process. At each time sample, the controller solves a dynamic optimization problem to obtain an optimal input sequence with respect to weights on setpoint deviations and on constraints for both inputs and controlled variables. Only the first element in the optimal input sequence is applied to the process, and the procedure is repeated at the next time sample. This is because the models employed are imperfect and that the available measurements are affected by noise.

To better illustrate how the MPC controller works, the MPC principle is extended with a feedback connection and discussed in more detail. The process is assumed to be a single-input-single-output (SISO) process and described by an estimated step response model described by

$$y(t+1) = \sum_{k=0}^{N} h(t-k)u(k-1). \tag{34}$$

This model predicts the future response one time step ahead. Since this model most likely is not perfect, there will be a deviation d from the actual response given as

$$d(t+1) = y(t+1) - \hat{y}(t+1). \tag{35}$$

Feedback connection is achieved by combining equations (34) and (35), and sloving for $\hat{y}$

$$\hat{y}(t+1) = \sum_{k=0}^{N} h(t-k)u(k-1) - d(t+1). \tag{36}$$

Next, prediction is extended from one to j time samples ahead and the disturbance is assumed constant during the whole prediction, i.e. $d(t+1) = d(t)$. Hence, the model becomes

$$\hat{y}(t+j) = \sum_{k=0}^{N} h(t-k)u(k+j-1) - d(t). \tag{37}$$

The dynamic optimization problem, solved by the MPC controller to obtain the optimal input sequence, takes the form of a quadric problem (QP)

$$\min \sum_{i=0}^{N} q(\hat{y}(t+1+i) - y^d(t+1+i))^2 + r(u(t+i) - u^d(t+i))^2, \tag{38}$$

$$\text{subject to: } \underline{y} \leq y(t+1+i) \leq \overline{y}, \tag{39}$$

$$\underline{u} \leq u(t+i) \leq \overline{u}, \tag{40}$$

where d signifies desired value, that is the reference. This problem is solved at each time sample to obtain the optimal future performance over the prediction horizon N. Equations (39) and (40) are constraints for the outputs and inputs, respectively. The variables with an under and over bar are the high and low limits, respectively. The scalars q and r are weights for punishing deviation from desired value for the outputs and inputs, respectively. Both the weights and the prediction horizon are tuning parameters.

The optimization problem is illustrated in Figure 4.2 and the MPC principle is at each time sample to repeat the process:

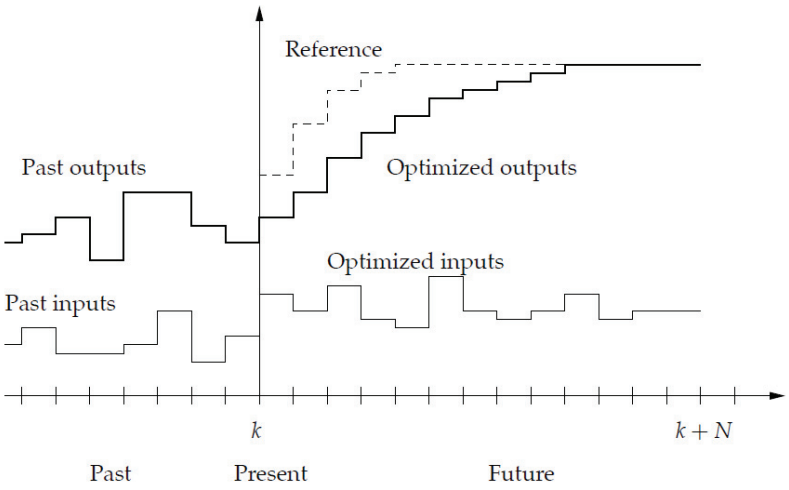

Figure 4.2: The MPC principle. The emphasized words in the text are the trajectories in the figure. (Imsland, 2002).

1. measure the actual plant response $y(t)$.
2. estimate the bias $d(t)$ as the difference between the actual and the estimated output.
3. predict future ouput $\hat{y}(t+j)$ over the prediction horizon using the estimate bias.
4. use the prediction of future output to solve the QP to obtain an optimal, feasible input sequence.
5. apply only the first input of the input sequnce to the process.

6. set $t = t + 1$ and go to step 1.

The models employed by the MPC controller can be linear or nonlinear and hence, the names linear and nonlinear MPC is commonly used.

4.3 SEPTIC

SEPTIC (Statoil Estimation and Prediction Tool for Identification and Control) is an in-house model predictive controller developed by Statoil R&D. The controller has the ability to use both linear and nonlinear first principle models, but only linear experimental models are utilized in Statoil's implemented MPC applications due to reports of good performance. All the material on SEPTIC MPC is based on the paper by Strand and Sagli (2003).

The SEPTIC MPC optimization problem is formulated as a Quadratic Problem (QP) on the form

$$\min_{\Delta u} \quad \mathbf{y}_{dev}^T \mathbf{Q}_y \mathbf{y}_{dev} + \mathbf{u}_{dev}^T \mathbf{Q}_u \mathbf{u}_{dev} + \Delta \mathbf{u}^T \mathbf{P} \Delta \mathbf{u}, \tag{41a}$$

$$\text{subject to} \quad \mathbf{u}_{min} < \mathbf{u} < \mathbf{u}_{max}, \tag{41b}$$

$$\Delta \mathbf{u}_{min} < \Delta \mathbf{u} < \Delta \mathbf{u}_{max}, \tag{41c}$$

$$\mathbf{y}_{min} < \mathbf{y} < \mathbf{y}_{max}, \tag{41d}$$

$$\mathbf{y} = \mathbf{M}(\mathbf{y}, \mathbf{u}, \mathbf{d}, \mathbf{v}), \tag{41e}$$

and is solved at each control sample to obtain the optimal input sequence. The quadratic function in Equation (41a) penalizes deviations from setpoints ($\mathbf{y}_{dev}$), deviations from ideal values ($\mathbf{u}_{dev}$) and input usage ($\Delta \mathbf{u}$) using the diagonal weight matrices $\mathbf{Q}_y$, $\mathbf{Q}_u$ and $\mathbf{P}$, respectively. The following equations are the constraints for the optimization problem. The first equation is the high and low limits of the manipulated variables (MV), the second equation is MV rate of change limits and the third equation is the high and low limits for the controlled variables (CV). The last equation is the dynamic process models which predict the CV responses. The MVs are the variables that affect the process, the CVs are the variables that need to be controlled and the DVs are the variables that can disturb the process. The setpoints and ideal-values are desired settle points for the CVs and MVs, respectively.

In the quadratic problem above, the time horizon is implicitly stated as the dimension of the vectors $\mathbf{y}_{dev}$ and $\mathbf{u}_{dev}$ as the prediction horizon and control horizon, respectively. The time horizon is more easily observed with an element formulation as in Section 4.2, where the control horizon is equal to the prediction horizon. In this thesis, the control horizon is set equal to the prediction horizon for simplicity and an element formulation is given as

$$\sum_{i=1}^{N_{pred}} q_i(y(t+i) - y^d(t+i))^2 + r_i(u(t+i) - u^d(t+i))^2 + p_i \Delta u(t+i)^2, \tag{42}$$

where $\Delta u(t+i) = u(t+i) - u(t-1+i)$ and N_{pred} is the prediction horizon. The prediction horizon is a tuning parameter and should be chosen long enough for the slowest CV to reach steady-state. A too long prediction horizon results in less aggressive control.

The weight matrices $\mathbf{Q}_y$ and $\mathbf{Q}_u$ are used to penalize deviations from setpoints and deviations from ideal-values, respectively. In general, these matrices are used to treat steady-state errors and large elements improve the corresponding elements at the expense of the other elements. The $\mathbf{P}$ matrix penalizes the input usage and large elements reduces the magnitude of the corresponding inputs, which results in larger deviations and longer settling times for the respective outputs.

The dynamic process models are required by MPC controller in order to predict the future behavior and describe the effect of a change in a MV on the respective CVs. Such models can be found experimentally with the SEPTIC SISO identification algorithm described in Section 4.1.

A serious problem which can arise is that the MPC controller can arrive at an infeasible solution. This can happen for several reasons, e.g. large disturbances, large differences in the behavior between the real process and the predicted process or generally when the degrees of freedom are too low. The degrees of freedom are the number of variables that determine the state of the system and are defined as

$$n_{DOF} = n_{MV} - n_{CV}, \tag{43}$$

where n_{DOF}, n_{MV}, n_{CV} are the degrees of freedom, the number of active MVs and the number of actively controlled CVs, respectively. There exist several techniques available to help the MPC controller reach a feasible solution, but when these do not succeed, the previous input will be used. This is in SEPTIC resolved by using a priority level hierarchy and solving several steady-state quadratic optimization problems. The variables in the priority level hierarchy are given their priority depending on the severity of a constraint violation, where the highest priority is given the variable which a constraint violation is most severe. The priority level hierarchy in decreasing order is given as

I MV rate of change limits.

II MV high and low limits.

III CV hard constraints.

IV CV set-point, CV high and low limits and MV ideal values with priority level 1.

V CV set-point, CV high and low limits and MV ideal values with priority level n.

VI CV set-point, CV high and low limits and MV ideal values with priority level 99.

The MVs rate of change is always respected, as it has the highest priority. At each of the following stages, a quadratic steady-state optimization problem is solved with respect to the remaining specifications. The solution at each stage respects the results from the previous stages and gives the smallest possible deviation from the original specifications. Should there be more CVs to control than there are MVs, n_{DOF} will become negative and the MPC controller will successively drop the least important priority levels until a solution can be obtained. At stages

where several variables have the same priority, the weights will be the deciding factor. This technique performs indirectly another well-known method used to overcome the infeasibility problem, namely softening of the least important hard CV constraints.

The ability for optimal constraint handling is an important feature of the MPC controller. In SEPTIC, the constraints can be defined as either soft or hard. Hard constraints are not allowed to be broken, while soft constraints are allowed to be broken occasionally, but only if necessary. Soft constraints are derived by softening hard constraints, meaning that the hard constraint is changed to a breakable limit and then, defining the maximum allowable breaking distance, which is the distance this limit are allowed to be broken. Then, the sum of the soft limit and the maximum allowable breaking distance is the hard limit for the soft constraint. Hence, the constraints are defined as follows

- soft upper constraint: $High$,
- soft lower constraint: $Lower$,
- hard upper constraint: $High + HighLimit$,
- hard lower constraint: $Low + LowLimit$,

where $HighLimit$ and $LowLimit$ are the upper and lower maximum allowable breaking limits, respectively. Generally, the MVs are restricted by physical properties, such as valve openings, and are therefore only restricted by hard constraints.

Normally, the complete MPC application is running, meaning that all the MPC variables are active. Often one or several CVs depend only on one MV. In the case of a bad measurement of one of the CVs or a deactivation of the MV, the correct action might be to deactivate the dependent variables to avoid undesirable events. Sub-groups are another feature offered by SEPTIC to deal with this type of situations. Every defined MPC variables in SEPTIC must be placed in one or more groups either as a member or as a critical member, where the group is only active when the critical member is active. Hence, should the critical member become deactivated, the complete group will subsequently become deactivated.

Chapter 5

Model Predictive Controller Design

This chapter begins with the introduction of the steam delivery network control problem and a brief overview over some of the previous solutions to this problem. Based on this, a typical MPC controller for control of a single boiler is derived and further extended to make up the MPC controller for the steam delivery network. In closing, the step response models employed by the MPC controller is presented followed by a description of the tuning performed.

5.1 The Steam Delivery Network Control Problem

According to Majanne (2005), the steam delivery network control problem is to design an overall controller that ensures stable and efficient operation of the steam delivery network. Stable operation is guaranteed by tight control of the common header pressure, while efficient control can be achieved through load leveling, that is by distributing the required load change over the active boilers. Furthermore, in this thesis, it is desirable to investigate the possibility of including optimization into the steam delivery network control problem to achieve economically optimal production of HP steam. The latter is investigated in the next chapter, while the MPC controller developed in the chapter can be used to achieve stable and efficient operation.

An individual MPC controller is constructed for each of the boilers within the steam delivery network and then, these are combined into a single MPC controller for the steam delivery network. The MPC controller for a single boiler is based on the work by Hogg and El-Rabaie (1991), Lu and Hogg (1997), Havlena and Findejs (2005) and Majanne (2005).

Stable and safe control of a boiler is achieved through tight control of the boiler header pressure, while ensuring that critical variables are kept within prescribed

Table 5.1: A Typical MPC controller for stable and safe boiler control.

Variable	Description	Type of control	Constraints
CV	combustion pressure		hard constraints
CV	temperature after second superheater		hard constraints
CV	attemperator valve opening		soft constraints
CV	header pressure	setpoint	soft constraints
MV	combustion controller	ideal value	hard constraints

limits. A typical MPC controller for stable and safe boiler control is listed in Table 5.1. The primary objective of the MPC controller is to guarantee safe operation, which is achieved by guaranteeing that explosions and meltdowns are prevented. This is guaranteed by security mechanisms in the regulatory layer, but the MPC controller must also guarantee this so that it does not control the boiler towards instability. In earlier works, the researchers have identified good measurements of critical processes within the boiler, which needs to be controlled and kept within specific limits in order to prevent undesirable events. The combustion pressure provides a good measurement of the combustion process and is proposed to be kept within specific limits to prevent explosions. Hence, the combustion pressure is selected as one of the primary CVs to help ensure safe operation. Stabilization of the drum water level is another critical process within the boiler, as both the steam production and steam temperature depends heavily on this level. However, as explained in Section 2.4.1, the drum water level is not a good measurement and the focus is shifted towards the HP steam temperature. The HP steam temperature is controlled by the regulatory layer to maintain a constant HP steam temperature in order to ensure a common steam quality and prevent boiler meltdown. Therefore, the HP steam temperature is selected as another primary CV and kept within prescribed limits to prevent meltdown. Furthermore, the MPC controller needs to be aware of the boilers cooling capacity to control the HP steam temperature. Therefore, the attemperator valve opening is chosen as the final primary CV. The secondary objective of the MPC controller is to ensure stable operation though tight control of the boiler header pressure. This can only be accomplished given that safe operation is guaranteed. Therefore, the header pressure is selected as the only secondary CV controlled by setpoint. Furthermore, the steam production is determined by the amount of energy supplied to the boiler and is therefore controlled by the combustion process. Hence, the MV is the combustion controller. However, as explained in Section 2.4.1, the combustion control scheme is different for each type of boiler and thus, the MV will differ for each type of boiler. This problem and other boiler specific problem are addressed in the following individual boiler analysis, while efficient operation and control of the common header pressure are addressed in the Section 5.2.

5.1.1 Åsgard boilers control analysis

The two Åsgard boilers are both connected to a separate gas turbine, enabling utilization of TEG in addition to AA. Furthermore, the boilers are only able to utilize natural gas as fuel in the combustion process. In these boilers, the water level is controlled by a single feedforward PI level controller and the combustion process by a single PI energy controller, both control schemes are explained in Section 2.4.1. The setpoint to this energy controller is the only degree of freedom of each for the boilers and is therefore selected as the MV for each of the boilers.

The combustion process depends on the source of oxygen. Therefore, both the step response models and the constraints for the combustion processes are different for AA and TEG mode. This implies that two sets of constraints and models are required, one for AA mode and one for TEG mode.

The two Åsgard boilers are each able to deliver a maximum amount of HP steam equal to 100,000 $[kg/h]$. The maximum change in steam production for these boilers are 10 $[\%/min]$ and this restriction is implemented by the engineers at Kårstø to reduce the damage on the boilers and to expand their lifespan. Given these two values and the nominal operating point in Table B.1 in Appendix B on page 113[1], the maximum rate of change in actuation per time sample can be calculated for both boilers. Since the boilers are equal, the limitation is only calculated for Åsgard boiler A and applied on both boilers. The maximum change in steam production for Åsgard boiler A is

$$100,000 \left[\frac{kg}{h}\right] \cdot 0.1 \left[\frac{max\ change}{min}\right] = 10,000 \left[\frac{kg \cdot max\ change}{min \cdot h}\right]. \tag{44}$$

The MPC controller is allowed 1 change per sample, equivalent to 60 changes per minute. Thus, the maximum change in steam production per sample is

$$\frac{10,000 \left[\frac{kg \cdot max\ change}{min \cdot h}\right]}{60 \left[\frac{change}{min}\right]} = 166,67 \left[\frac{max kg}{h}\right]. \tag{45}$$

Then, using the steady-state nominal operating point in Table B.1 in Appendix B on page 113, the ratio between the applied energy and the steam production for Åsgard boiler A can be found as

$$138.67 \left[\frac{GJ}{h}\right] x = 84,332.50 \left[\frac{kg}{h}\right], \tag{46}$$

$$x = 608.15 \left[\frac{kg}{GJ}\right], \tag{47}$$

where x is the increase in steam production for a unit change in the energy controller. Given this ratio, the maximum rate of change in actuation for the energy

[1]The nominal operating point is taken from the simulator.

controller per time sample is

$$y \cdot 608.15 \left[\frac{kg}{GJ}\right] = 166,67 \left[\frac{max kg}{h}\right], \tag{48}$$

$$y = 0.27 \left[\frac{max\ GJ}{h}\right], \tag{49}$$

$$y \approx 0.25 \left[\frac{max\ GJ}{h}\right]. \tag{50}$$

This limit is then implemented as the maximum rate of change per time sample in actuation for each of the Åsgard boilers[2]. Furthermore, these boiler are placed in groups 1 and 2, respectively.

5.1.2 Moss boiler control analysis

The Moss boiler is strictly natural gas fired without connection to a separate gas turbine. In this boiler, the water level is controlled by a single feedforward PI level controller and the combustion process by the PI header pressure controller, both control structures are explained in Section 2.4.1. The output value of this header pressure controller directly manipulates both the fuel and air flow and is the only degree of freedom for this type of boiler. Hence, the output value of this controller is selected as the MV for the Moss boiler.

The Moss boiler is able to produce a maximum amount of steam equal to 120,000 $[kg/h]$. The engineers at the plant have implemented a maximum change in steam production equal to 15 $[\%/min]$ for this boiler to reduce the damage on the boiler and expand its lifetime. With these values and the nominal operating point in Table B.1 in Appendix B on page 113, the maximum rate of change in actuation is calculated in the same manner as above and found to be approximately 0.20 $[\frac{max\ bar}{h}]$. Furthermore, the Moss boiler is placed in group 3.

5.1.3 Sleipner boiler control analysis

The Sleipner boiler is able to utilize both natural gas and craier gas, but is without connection to a separate gas turbine. The Sleipner boiler is very similar to the Moss boiler as its water level is controlled with a single feedforward PI controller and the combustion process is controlled by a PI header pressure controller, both these control schemes are discussed in Section 2.4.1. As for the Moss boiler, the output value of this header pressure controller directly adjusts both the fuel and air flow and is the only degree of freedom for this type of boiler. Thus, the output value of this controller is selected as the MV for the Sleipner boiler.

The Sleipner boiler is able to produce a maximum amount of steam equal to 145,000 $[kg/h]$. The steam production is not allowed to change more than 10 $[\%/min]$ to reduce damages on the boiler and expand its lifespan. Given these

[2]In SEPTIC, these values are set as $MaxUp$ and $MaxDn$ for the maximum rate of change in actuation in the upwards and downwards direction, respectively.

values and the nominal operating point in Table B.1 in Appendix B on page 113, the maximum rate of change in actuation is calculated in the same manner as above and found to be approximately 0.10 $[\frac{max\ bar}{h}]$. Furthermore, the Sleipner boiler is placed in group 4.

5.1.4 Foster Wheeler boiler control analysis

The three Foster Wheeler boilers are strictly natural gas fired and are each connected to a separate gas turbine, enabling utilization of TEG in addition to AA. In these boilers, the water level is controlled by a single feedforward PI level controller and the combustion process is controlled with a ratio control scheme, both explained in Section 2.4.1. The setpoint to the fuel flow controller in this ratio control scheme is the only degree of freedom for each of the boilers and is therefore chosen as the MV for each of the boilers.

The boilers ability to utilize two different sources of oxygen implies the need for two sets of constraints for the combustion process and step response models depending on the operating mode.

The three Foster Wheeler boilers are each able to deliver a maximum steam production of 70,000 $[kg/h]$. In order to reduce the damages on the boilers and extend their lifespan, these boilers are only allowed to change their steam production by 10 [%]. From these values and the nominal operating point in Table B.1 in Appendix B on page 113, the maximum rate of change in actuation are calculated in the same ways as above and found to be approximately 7.85 $[\frac{max\ kg}{h}]$. Moreover, the Foster Wheeler boilers are placed in group 6, 7 and 8, respectively.

5.2 The Steam Delivery Network Model Predictive Controller

Considering the entire steam delivery network, the MPC controller for this network is created by combining all the MPC controllers into a single MPC controller. The only necessary adjustment is to merge all the header pressures into a single header pressure, the common header pressure. The MPC controller for the steam delivery network achieves the desired ability of efficient operation, as all the boilers are able to cooperate and contribute in the production of HP steam sent to the common header, that is load leveling. Now, an increase in steam consumption can quickly be covered by increasing the steam production of all the active boilers, and for the opposite case, by reducing the steam production of all the active boilers. This MPC controller is presented in Table 5.2[3,4] and is programmed into SEPTIC. In this code, all the variables are defined along with other temporary variables. The temporary variables are used in intermediate calculations to identify the operating modes and to calculate the active set of constraints and models. The operating modes are recognized by tracking the valve opening of the TEGs and from this

[3] ABD: allowable breaking distance.
[4] x°: critical member.

opening, the MPC can adjust the set of active step response models and constraints. Furthermore, the output of the header pressure controller for the Kristin boiler is implemented as a DV. Then, this variable works as a feedforward for the Kristin boiler and provides information about changes in this boiler's steam production prior to the changes observed in the common header.

Furthermore, the primary CVs for all the boilers are the same as those presented in the typical MPC controller. These are the combustion pressure, the HP steam temperature and the attemperator valve opening, which are all controlled to remain within their specific limits. The combustion pressure and the HP steam temperature are both given a lower and higher hard constraint, as the severity of a constraint violation might result in an explosion or boiler meltdown, respectively. However, the attemperator valve opening and the header pressure are both given a lower and higher soft constraint and an allowable breaking distance, because breaking these constraints are unavoidable and does not lead to any undesirable events. The constraint limits are found from data sheet and are listed in Table 5.2. The attemperator valve opening is for all boilers limited by physical properties to a lower and upper opening of 0 and 100 [%], respectively. However, in order to preserve cooling capacity, the variable is given a higher soft constraint of 95 [%] and hence, an allowable breaking distance of 5 [%]. The header pressure is given a lower and upper soft constraint of 57 and 63 [$barg$], respectively and an allowable breaking distance of 2 [$barg$]. Moreover, the header pressures and the MVs are the only critical group members in each MPC controller.

Safe operation is a prerequisite for maintaining a constant common header pressure. Therefore, the combustion pressure and the HP steam temperature for all the boilers are given priority 1, while the common header pressure is given priority 2. The attemperator valve opening for all the boiler is given priority level 3, as this variable are not used to prevent any undesirable events.

At steady-state, only one boiler is necessary to control the common header pressure, while the other boilers produce a constant amount of steam, i.e. constant load. This leads to a surplus of unused available degrees of freedom depending on the number of active boilers. A boiler's degree of freedom is only available if the primary CVs for this boiler does not require any control, i.e. the primary CVs are not pushing on any of its limits. Thus, the available degrees of freedom can be used to achieve economical optimal production of HP steam by adjusting the fuel flow for each of the boilers producing a constant amount of steam. This possibility is discussed in the next chapter.

Table 5.2: The MPC controller for steam delivery network. The abbreviations are explained in the nomenclature and the ∘ symbolizes a critical variable.

MPC type	Description	High priority	SP/IV priority	Low priority	AA mode			TEG mode			ABD	Group
					High limit	SP/ IV	Low limit	High limit	SP/ IV	Low limit		
CV	CHP	2	2	2	63	60	57	63	60	57	2	1°, 2°, 3°, 4°, 5°, 6°, 7°
					Åsgard boiler A							
CV	CP	1	-	1	0.44	-	0	0.15	-	0	-	1
CV	HPST	1	-	1	395	-	0	395	-	0	-	1
CV	AVO	3	-	3	95	-	0	95	-	0	5	1
MV	EC	-	4	-	315	-	0	180	-	0	-	1°
					Åsgard boiler B							
CV	CP	1	-	1	0.44	-	0	0.15	-	0	-	2
CV	HPST	1	-	1	395	-	0	395	-	0	-	2
CV	AVO	3	-	3	95	-	0	95	-	0	5	2
MV	EC	-	4	-	315	-	0	180	-	0	-	2°
					Moss boiler							
CV	CP	1	-	1	1.90	-	0	-	-	-	-	3
CV	HPST	1	-	1	440	-	0	-	-	-	-	3
CV	AVO	3	-	3	95	-	0	-	-	-	5	3
MV	HPC	-	4	-	92	-	0	-	-	-	-	3°
					Sleipner boiler							
CV	CP	1	-	1	1.90	-	0	-	-	-	-	4
CV	HPST	1	-	1	440	-	0	-	-	-	-	4
CV	AVO	3	-	3	95	-	0	-	-	-	5	4
MV	HPC	-	4	-	60	-	0	-	-	-	-	4°
					Foster Wheeler boiler A							
CV	CP	1	-	1	0.15	-	0	0.44	-	0	-	5
CV	HPST	1	-	1	395	-	0	395	-	0	-	5
CV	AVO	3	-	3	95	-	0	95	-	0	5	5
MV	FFC	-	4	-	4550	-	0	4175	-	0	-	5°
					Foster Wheeler boiler B							
CV	CP	1	-	1	0.15	-	0	0.44	-	0	-	6
CV	HPST	1	-	1	395	-	0	395	-	0	-	6
CV	AVO	3	-	3	95	-	0	95	-	0	5	6
MV	FFC	-	4	-	4550	-	0	4175	-	0	-	6°
					Foster Wheeler boiler C							
CV	CP	1	-	1	0.44	-	0	0.15	-	0	-	7
CV	HPST	1	-	1	395	-	0	395	-	0	-	7
CV	AVO	3	-	3	95	-	0	95	-	0	5	7
MV	FFC	-	4	-	4550	-	0	4175	-	0	-	7°
					Kristin boiler							
DV	HPC	-	-	-	-	-	-	-	-	-	-	8

5.3 Step Response Models

Identification of accurate process models is the single most important part of the MPC design procedure, because good predictions have a great impact on the performance of the closed loop system (Majanne, 2005). In the development of this MPC controller, the plant is assumed to be linear and time invariant. From these assumptions, linearized models can be obtained by applying steps on the plant inputs and record the plant outputs. Following this, linearized models can be derived from techniques of *system identification*, which covers a large range of methods. SEPTIC offers several system identification methods including the step response method, which is applied for obtaining the required models. Step response models are *black-box* models, i.e. they only represent the input-output behavior of the plant.

Before any step response modeling can begin, it is a prerequisite to know the processes responses and how to model these responses. Generally, the response of a process either settles within reasonable time or changes constantly. In process engineering, the first type of response is modeled as either a first or second order model depending on the transient dynamics, while the latter type of response is modeled as an integrating process.

The common header can be viewed as a large horizontal tank for storage of HP steam, with one input for every boiler and several outputs. Hence, the mass rate balance for the common header becomes

$$\frac{dm_{ch}}{dt} = \dot{m}_{in} - \dot{m}_{out}, \tag{51}$$

where first term denotes the time rate of change of steam within the common header, while $\dot{m}_{in}$ and $\dot{m}_{out}$ are the rate of steam produced and consumed, respectively. Because steam is continuously supplied and varyingly drawn from the common header, the first term cannot be removed. Furthermore, the steam flows in and out of the common header are assumed to be independent of pressure. The ideal gas law can be used to express the amount of steam within the common header at any specified time instant as a function of among others common header pressure. Hence, the steam within the common header at a specified time instant is given as

$$m_{ch} = \frac{pVM}{\bar{R}T}, \tag{52}$$

where T, p and M are the temperature, pressure and molar mass of the HP steam, respectively. The common header volume is denoted by V and $\bar{R}$ is the ideal gas constant. In order to find the response of the common header pressure, the ideal gas law is inserted into the mass rate balance

$$\frac{d}{dt}\left(\frac{pVM}{\bar{R}T}\right) = \dot{m}_{in} - \dot{m}_{out}. \tag{53}$$

The molar mass, ideal gas constant and common header volume are all assumed to be constant and the HP steam temperature is kept at a constant value by the

regulatory layer. Hence, the mass rate balance becomes

$$\frac{VM}{\bar{R}T} \cdot \frac{dp}{dt} = \dot{m}_{in} - \dot{m}_{out}, \tag{54}$$

$$\frac{dp}{dt} = \frac{\bar{R}T}{VM} \left(\dot{m}_{in} - \dot{m}_{out} \right). \tag{55}$$

Solving this equation yields

$$p = p_0 + \frac{\bar{R}T}{VM} \int_{t_0}^{t} \left(\dot{m}_{in} - \dot{m}_{out} \right) d\tau, \tag{56}$$

where the constant term has been combined into the constant p_0. Assuming that both the steam produced and consumed are constant, this equation reveals that the common header will constantly increase when $\dot{m}_{in} > \dot{m}_{out}$ and constantly decrease when $\dot{m}_{in} < \dot{m}_{out}$. Hence, the common header pressure is an integrating process. However, the common header pressure is stable when $\dot{m}_{in} = \dot{m}_{out}$ and thus, the steam delivery network is a marginally stable system. This is what we want to achieve with a closed loop controller. A similar analysis was performed for the other CVs and revealed that all the other processes can be modeled as first order responses.

In SEPTIC, the responses can be either modeled as first or second order models with or without time delay,

$$g(s) = \frac{k}{\tau_1 s + 1} e^{-\theta s}, \qquad g(s) = \frac{k}{(\tau_1 s + 1)(\tau_2 s + 1)} e^{-\theta s}, \tag{57}$$

where k, τ_1, τ_2 and θ are the steady-state gain, the dominant time lag constant, the second order lag time constant and the time delay, respectively. Typically, the derivative of an integrating process changes fast in the beginning before settling. Hence, integrating processes are in SEPTIC modeled from their derivatives as either first or second order models. The limited complexity achieved from the models offered by SEPTIC might not be sufficient to capture all the transient dynamics. Therefore, the step responses must be simplified to fit into the applicable models, which might result in a loss of the higher order dynamics. When performing this *model reduction*, it is important to capture the dominant dynamics (Balchen, Andresen, and Foss, 1999). The interested reader is referred to Skogestad (2002) for a thorough discussion about these process models and how to approximate step response models.

Starting at a steady-state nominal operating point, all the step response models related to one MV are derived by injecting it a step and record the response on all the affected CVs. Furthermore, the recorded data is used by SEPTIC to generate SISO step response models from the MV to each of the affected CVs. This procedure is sequentially conducted for all the MVs to obtain all the required step response models, so that the entire future behavior can be predicted.

In this thesis, the step response models depend on the source of oxygen and therefore, two sets of step response models are required for these boilers. Furthermore, provided the applied oxygen source, the MPC controller must be able

to switch between the two sets of models. This is achieved using *model scheduling*. Hence, two nominal operating points are necessary to cover all the operating modes for the boilers. These nominal operating points are given in tables B.1 and B.2 in Appendix B on page 113. The injected step is equivalent to an increase of 1,000 $[kg/h]$ in steam production. However, the step varies for each type of control structure and possible operating modes, as shown in Table 5.3.

Table 5.3: Required step change for an increase of 1,000 $[kg/h]$ in steam production.

Boiler	Step change	
	AA mode	TEG mode
Åsgard A	3.3 $[GJ/h]$	3.1 $[GJ/h]$
Åsgard B	3.3 $[GJ/h]$	3.1 $[GJ/h]$
Moss	0.85 $[barg]$	-
Sleipner	0.5 $[barg]$	-
Forster Wheeler A	65 $[kg/h]$	50 $[kg/h]$
Forster Wheeler B	65 $[kg/h]$	50 $[kg/h]$
Forster Wheeler C	65 $[kg/h]$	50 $[kg/h]$

The derived step response models show the result of a unit step in the respective MV, but since the range of actuation varies for each of the control structures, the models are not comparable. Therefore, the models are scaled so that they have an equal range of actuation from 0 to 100.

The step response models of the common header pressure for both AA and TEG mode are shown in figures 5.1 and 5.2, respectively. In these figures, the red lines are the calculated pressure gradients, while the blue lines are the estimated pressure gradients. These step response model are as expected, the pressure gradient increases sharply in the beginning due to the applied step before it settles at the constant pressure gradient corresponding to the constant increase caused by the integral effect. The model approximations fits the calculated pressure gradients perfectly except of the Moss boiler, which fails to capture some of the higher order dynamics. However, the approximation is satisfactory, as it manages to capture much of the dominant dynamics without much deviation. The time delay indicates the time elapsed before the applied fuel affects the common header and depends on the boiler structure, operating mode and the distance between the boiler and the common header pressure measurement. The steady-state gain indicates the increase rate in common header pressure for a unit change in actuation, i.e. 1 $[kg/h]$ fuel gas. This increase should be equal for all the boilers, but this is not the case for the Foster Wheeler boilers. A reason for this might be that Foster Wheeler boilers are located far away from the common header pressure measurement and steam is passed to various consumers before it reaches the measurement.

The step response models of the primary CVs for all the boilers are shown in figures A.3 and A.4 Appendix A on page 109 for AA and TEG mode, respectively.

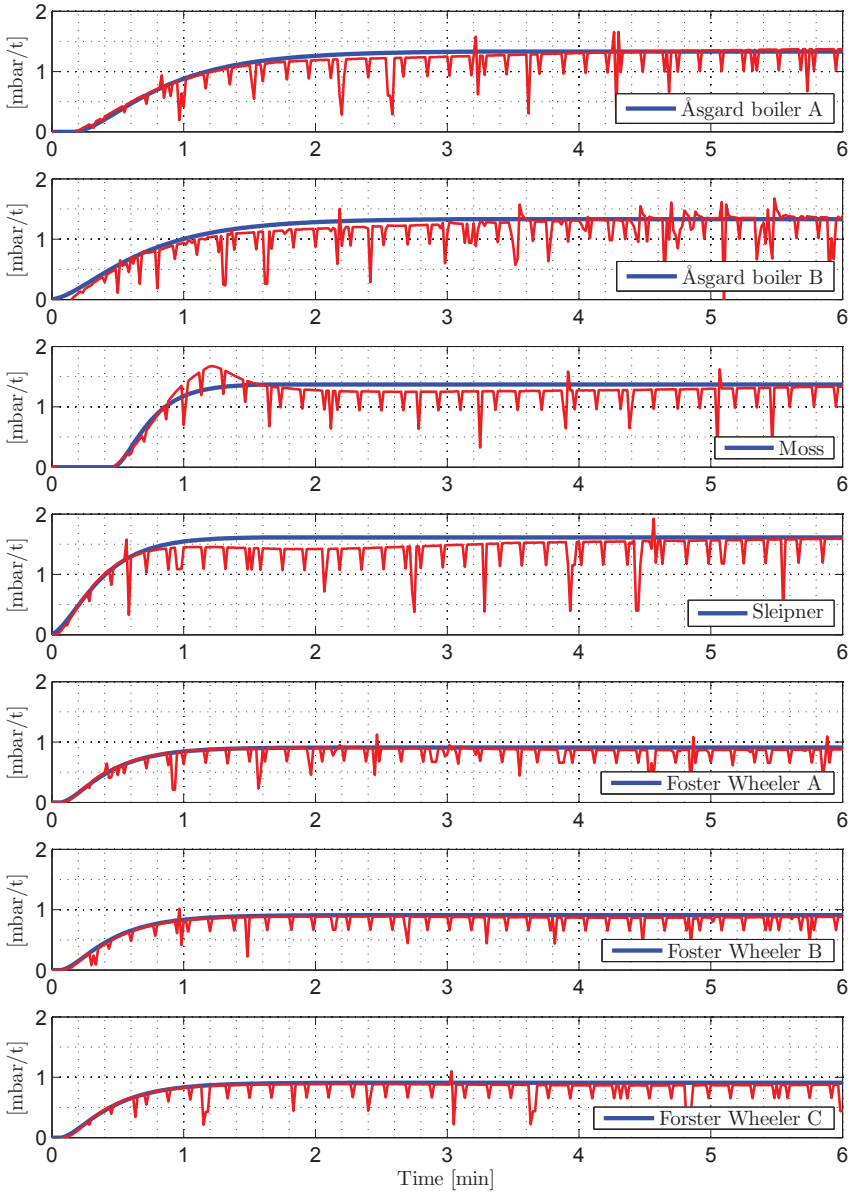

Figure 5.1: Step response models for all the respective boilers input to the common header pressure gradient in AA mode.

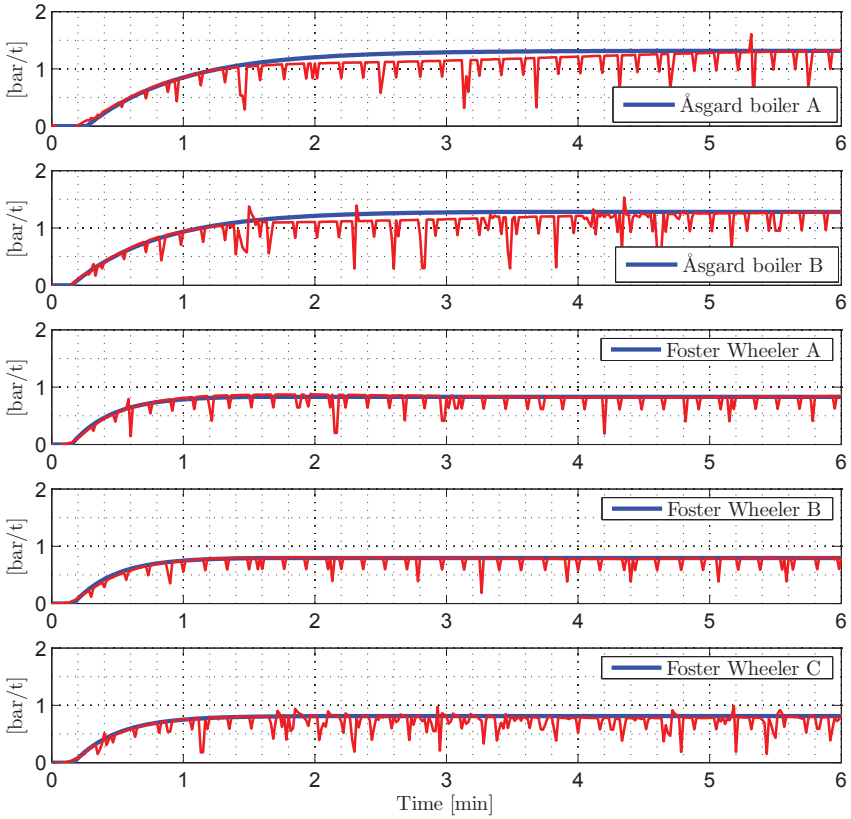

Figure 5.2: Step response models for all the respective boilers input to the common header pressure gradient in TEG mode.

5.4 Tuning

Tuning is a technique in which various parameters are adjusted to guarantee closed-loop performance and improve overall performance. There are several tuning parameters in an MPC controller, both the standard formulation parameters and the additional software specific parameters. In this thesis, only the adjusted tuning variables relevant for the SEPTIC application are discussed. The theory from this section is based on the work by Strand and Sagli (2003); Hauger (2012) and Maciejowski (2002).

The sampling frequency is the time between each control update and normally, more frequent sampling results in better control. Thus, the sampling frequency is set at $1[Hz]$, which corresponds to a sample at each second. The prediction horizon should be chosen long enough for the slowest CV to reach steady-state. Hence, by examination of figures 5.1 and 5.2, the longest settling time is approximately 6 minutes, i.e. 360 seconds, and therefore, the prediction horizon is set as 360.

In SEPTIC, the diagonal elements within the weight matrices, introduced in Section 4.3, are defined as

$$q_{y,i} = \left(\frac{Fulf}{Span}\right)^2 \qquad q_{u,i} = \left(\frac{Fulf}{Span}\right)^2 \qquad p_i = \left(\frac{MovePnlty}{Span}\right)^2, \tag{58}$$

where $Span$ is a unique scaling parameter for each of the MPC variables and is usually set as the acceptable range of variation for the respective variable. Hence, if the attemperator valve opening has an operating range of 0-100% and is expected to vary within 10% of this range, the $Span$ is set to 10. The $Fulf$ variables represent the penalty of deviation from setpoint and ideal value for the CVs and MVs, respectively, and increased weighting of one variable improves the steady-state error at the expense of others. The input usage is punished with the $MovePnlty$ variable. More specific, this variable penalizes the change of input from one sample to the next and is increased for frequently changing variables. In this thesis, the acceptable variation of a variable is chosen to be 10%, but since the common header pressure is of particular interest, the acceptable variation of this variable is only 1%. The $Fulf$ and $MovePnlty$ variables are initially set to 1 and further adjusted in order to improve performance.

Input blocking is a unique tuning parameter for each of the MVs and is an important variable for reducing the computational time needed to solve the MPC optimization problem. This technique reduces the number of optimization points and divides the optimal input sequence into time intervals with constant value. Commonly, these time intervals are of increasing length. Furthermore, the input blocking is defined as a row vector covering the entire prediction horizon. The first element specifies the number of blocking elements, which often is in the range of 4-8 blocking elements, as this provides a good balance between computational time and performance. The first blocking element specifies the length of the first constant input intervals, and the second blocking element, beginning directly after the first constant input interval, specifies the length of the second constant input interval, and so on. The last constant input interval, beginning directly after the last specified constant input interval, has a length equal to the remaining prediction horizon. In this way, the sum of all the specified lengths would indicate the control horizon, as the input is constant after the last blocking element.

In this thesis, the blocking is chosen to consist of eight elements and is derived from the CV with the longest settling time, that is, the Åsgard boilers common header pressure response. Hence, the common header pressure experiences a setpoint change equal to 0.1 $[bar]$ with only the Åsgard boiler B active and the applied input is observed, as shown in Figure 5.3. The applied input, observed as the energy controller output, settles approximately after 4 minutes, that is, 240 seconds. Hence, considering the sampling frequency of 1 $[Hz]$ and the prediction horizon of 360 seconds, the control horizon should be equal to 240 seconds. Moreover, the blocking elements should be selected such that the initial prediction of optimal input sequence resembles the applied input. Hence, the input blocking is selected to be

$$Blocking = \begin{bmatrix} 8 & 3 & 5 & 10 & 16 & 22 & 35 & 40 & 49 \end{bmatrix}. \tag{59}$$

The selected input blocking resembles the applied input, as shown by the dashed green line in Figure 5.3. Finally, the input blocking was verified by observing that the initial predicted optimal input sequence resembled the applied input for another simulated step change equal to the prediction horizon.

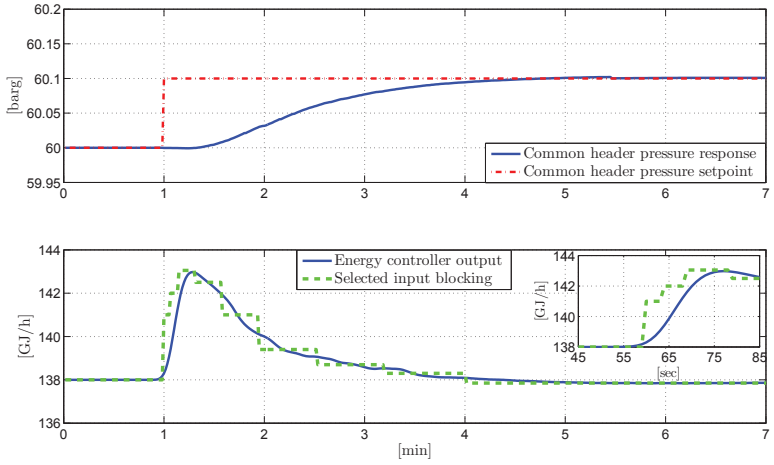

Figure 5.3: Derivation of the input blocking. The figure shows the common header pressure response to a setpoint change of 0.1 [*bar*] with only the Åsgard boiler B active.

The MPC optimization problem is further simplified by evaluating the MPC optimization problem at specified evaluation points. The MPC optimization problem is automatically evaluated at the end of each constant input interval in addition to a number of equally distributed evaluation points. The additional equally distributed evaluation points are specified by the engineers, and are commonly chosen within the range of 5-20. In this thesis, five additional evaluation points are chosen. Furthermore, it is desirable to avoid evaluation of the MPC optimization problem during dead-time[5] and inverse responses[6], because the MPC controller would increase or reduce its actuation to counteract these events, which in worst case could result in instability. Therefore, the variable *EvalDT* is used decide the number of samples to ignore in the beginning of the prediction horizon for each of the CVs.

In closing, each CV is given a priority according to the priority level hierarchy introduced in Section 4.3. Since safe operation is a prerequisite for stable control, all the combustion pressures and HP steam temperatures are given priority 1. The common header pressure is given priority 2, because stable operation is the second most important objective of the MPC controller. The last CVs, the attemperator valve openings, are given priority 3, as these variables are only included so that the MPC controller can be aware of its cooling capacity. Finally, all the IVs are given priority level 4, so that the remaining degrees of freedom can be used to achieve optimal production of HP steam.

[5]Dead-time is the time after an event where no response is observed on the CVs.

[6]Inverse responses are responses where the initial change is in the opposite direction of the final direction.

Chapter 6

Optimizer Design

This chapter begins with the derivation of the thermal efficiency analysis, which subsequently is performed for all the boilers. The results are further presented and discussed followed by the derivation of the RTO optimizer for the steam delivery network. The derivation of the thermal efficiency analysis is based on theory presented in Chapter 3.2 and on Moran and Shapiro (2010).

6.1 Thermal Efficiency Analysis

In order to analyze the thermal efficiency of a boiler we need to define a control volume and identify the mass and heat that flows through this control volume. Since the thermal efficiency is determined by the energy in and out of the boiler, the control volume must include the flows that bring the energy in and out of the boiler. Therefore, the entire boiler is a natural choice as the control volume. The control volume with its inlet and outlet flows is shown in Figure 6.1. This choice allows us to calculate the energy entering the system from the fuel[1] and the oxygen flows, where the latter can be either AA or TEG. The energy leaving the system is found from the enthalpy difference between the steam and the feedwater. The feedwater is condensed steam which returns to the boiler, and the term condensate is used for the remainder of this thesis. The temperature difference between the steam and the combustion gases indicates the heat loss which arises from steam production.

Some assumptions are necessary before any calculations can begin and these are listed below.

- The system is at steady-state, i.e. none of the properties changes with time.
- The condensate has a constant temperature of $125°C$.
- The composition of molecules in the fuel is assumed to be constant over time and equal for every boiler. The fuel composition and the LHV values are

[1] The fuel can be both natural gas or craier gas, but boilers utilizing craier gas are not controllable and therefore not analyzed, as explained in Section 2.1 on page 5.

stated in Table 6.1.

- The heat loss indicated by the combustion gases are negligible.
- Heat and work transfers are negligible and the change in potential and kinetic energy from input to output can be ignored.
- The combustion is complete.

All these assumptions are made to simplify the calculations without causing too large errors in the calculations. The steady-state assumption holds as the regulatory control layer ensures that the water level in the drum remains constant. Then, since no mass is accumulated in the drum, the condensate entering the boiler equals the steam leaving the boiler. Furthermore, the condensate temperature only slightly varies around $125°C$, resulting in only minor changes in the condensate enthalpy. The fuel composition varies widely with the processing of the oil and gas coming in from the Norwegian continental shelf, as the refined gas is used as fuel for the boilers. Thus, this assumption introduces a significant calculation error. Lastly, complete combustion is expected to be a correct assumption, as combustible gases at the plant pose a great explosion hazard, and would result in shutdown of the boiler.

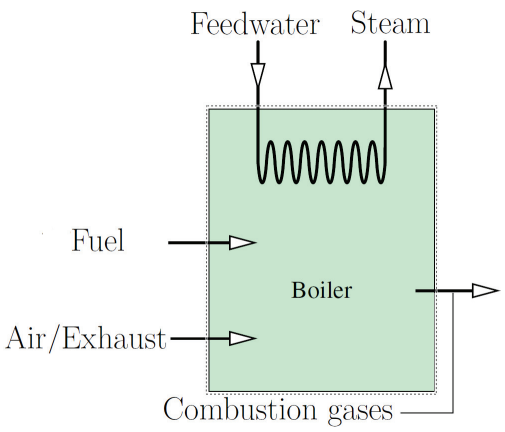

Figure 6.1: Boiler control volume. (Moran and Shapiro, 2010)

Mole fractions	Fuel
y_{CH_4}	0.914
$y_{C_2H_6}$	0.049
$y_{C_3H_8}$	0.006
y_{CO_2}	0.025
y_{N_2}	0.006
Molecules	LHV [kJ/kg]
CH_4	50,020
C_2H6	47,480
C_3H_8	46,360
CO_2	0
N_2	0

Table 6.1: Composition and LHV for fuel.

The energy entering the boiler can be found by calculating the enthalpy of combustion, which implies finding the enthalpy difference between the reactants and the products. A simpler approach, without introducing any significant computational errors, is to calculate the fuel and the exhaust contribution separately in terms of heating values and specific heat capacity, respectively. Thus, the general expression for the energy entering the system is given by

$$\dot{E}_{in} = \dot{E}_{fuel} + \dot{E}_{exhaust}, \tag{60}$$

where $\dot{E}_{fuel}$ and $\dot{E}_{exhaust}$ are the energy contribution from the fuel and exhaust, respectively.

The energy released through complete combustion between the fuel and air is calculated using heating values. In this thesis, the energy entering the boiler is

stated on the basis of the lower heating value, as the water product is in vapor phase after the combustion. Therefore, the fuel contribution is on the form

$$\dot{E}_{fuel} = \dot{m}_{fuel} \cdot LHV_{fuel}, \tag{61}$$

where $\dot{m}_{fuel}$ and LHV_{fuel} are the mass flow of fuel and the lower heating value of fuel, respectively.

The energy contribution from air is included in the calculations of the fuel contributions when using LHVs. Therefore, ambient air is defined to add no additional energy to the combustion. The energy contribution provided by an additionally warmer energy source, in this thesis the exhaust, is derived using the definition of specific heat at constant pressure. Starting with the definition on the form

$$c_p(T) = \frac{dh}{dT}, \tag{62}$$

and by further assuming that the exhaust behaves like an ideal gas and that the specific heat is constant, the energy contribution per unit exhaust is given as

$$\Delta h_{exhaust} = c_p \int_{t_0}^{t} T \, dT. \tag{63}$$

Since the energy contribution brought with the exhaust must be given relative to the energy in air, due to the utilization of LHVs, the expression becomes

$$\Delta h_{exhaust} = c_p \cdot (T_{exhaust} - T_{air}), \tag{64}$$

where $T_{exhaust}$ and T_{air} are the temperature of the TEG and AA, respectively. Now, the exhaust contribution is found by multiplying this equation with the mass flow of exhaust

$$\dot{E}_{exhaust} = \dot{m}_{exhaust} \cdot c_p \cdot (T_{exhaust} - T_{air}), \tag{65}$$

where $\dot{m}_{exhaust}$ is the mass flow of exhaust, that is the TEG.

Finally, these two energy contributions are inserted into Equation (60) to obtain a general expression for the energy entering the system. Hence, the general equation is expressed as

$$\dot{E}_{in} = \dot{m}_{fuel} \cdot LHV_{fuel} + \dot{m}_{exhaust} \cdot c_p \cdot (T_{exhaust} - T_{air}). \tag{66}$$

This equation shows the energy contribution ratio between the fuel and exhaust. It is worth noting that utilization of exhaust reduces the need for fuel, because the exhaust contributes with "free" energy[2] to the evaporation of the condensate.

A necessary assumption at this point is to assume that air and exhaust, i.e. AA and TEG, have the equal properties. Nitrogen is the main component in both air and exhaust, which takes about 79 [%] of the available space. In air, the remaining space is filled by oxygen, and in exhaust, some of the oxygen has been displaced

[2]By this, it is meant that the energy already has been paid for by another process.

by the combustion products (H_2O and CO_2). Hence, the oxygen concentration varies from a few percent up to 17 [%] in exhaust, compared to 21 [%] in air. Therefore, according to Poling, Prausnitz, and O'Connell (2001), this assumption only introduces a calculation error of magnitude less than 2 [%].

The energy out of the boiler can be derived from the energy balance and the assumption that the system is at steady-state. Starting with the latter assumption, the mass rate balance becomes

$$\frac{dm_{water}}{dt}^{0} = \dot{m}_c - \dot{m}_s, \tag{67}$$

$$\dot{m}_s = \dot{m}_c, \tag{68}$$

where $\dot{m}_s$ and $\dot{m}_c$ are the mass flow of steam and condensate, respectively. Then, the energy rate balance can be applied to find the heat used to evaporate the condensate, i.e. the energy supplied to the condensate. Hence, the energy rate balance becomes

$$\frac{\dot{E}_{out}}{dt}^{0} = \dot{Q} - \cancel{\dot{W}} + \dot{m}_c(h_c + \frac{V_c^2}{2} + \cancel{gz_c}) - \dot{m}_s(h_s + \frac{V_s^2}{2} + \cancel{gz_s}), \tag{69}$$

$$\dot{Q} = \dot{m}_s(h_s - h_c), \tag{70}$$

where $\dot{Q}$ is the heat transfered to the condensate and the variables h_s and h_c are the enthalpy of the steam and condensate, respectively. The value of these variables are found from data tables provided by Moran and Shapiro (2010).

The thermal efficiency indicates how effectively the heat exchangers are able to transfer the heat from the combustion products to the condensate inside the boiler. Therefore, the thermal efficiency is given as the ratio between the heat used to evaporate the condensate and the energy applied to the boiler. Thus, the thermal efficiency is given as

$$\eta = \frac{\dot{Q}}{\dot{E}_{in}}, \tag{71}$$

where η is the thermal efficiency.

6.2 Modeling the Thermal Efficiency

There are in total eight boilers at the plant, in which seven of these are controllable, as explained in Section 2.1 on page 5. The Åsgard boilers and Foster Wheeler boilers are connected to separate gas turbines enabling utilization of TEG in addition to AA. This ability means that these boilers have two different operating modes and the thermal efficiency varies for these operating modes. Therefore, the thermal efficiency analysis, performed on all the boilers, must also be conducted for each of their different operating modes.

The thermal efficiency analysis was performed for all the boilers, both for the real plant and for the simulator. Data points, covering the entire operating range of the boilers, are required to perform the thermal efficiency analysis. In order to obtain real plant data, the relevant TAG-names and the time intervals for the various operating modes had to be identified. The TAG-names were found by studying the P&IDs[3] for the steam delivery network, while the time intervals for the various operating modes were identified using Aspen Process Explorer. Then, the real plant data was imported to Microsoft Excel using the relevant TAG-names and the time intervals as input variables and further exported to MATLAB. The simulator data was obtained by recording the relevant boiler data, for various steam production through simulations ranging from minimum to maximum steam production, for each of the boilers. Then, this data was extracted to MATLAB.

Because the thermal efficiency analysis only applies for steady-state data, the simulator data was only recorded when the boilers reached steady-state. However, real plant data are often very contaminated by noise, partly because of measurement errors, trips and varying steam consumption. Therefore, the real plant data was obtained by taking the average value over the sampling interval of four hours. This filtering, known as *moving average*, reduces the effect of noise as a function of the sampling frequency. The sampling frequency was chosen long enough for the steam delivery network to reach steady-state within the sampling interval. Furthermore, there are no available measurements of the mass flow of TEG, so these flows were found from data sheets as a function of measured TEG temperatures. Lastly, the thermal efficiency analysis requires calculations of the enthalpy of both condensate and steam at various temperatures and pressures. This was resolved by creating a MATLAB script which could calculate the enthalpy of water in both liquid and vapor phase.

Given the filtered real plant data and the simulator data, the thermal efficiency analysis was implemented and performed for each of the boilers and their different operating modes. A graphical representation of the results are shown in figures 6.2, 6.3, 6.4, 6.5, 6.6 and 6.7 for the Åsgard boilers in AA mode, the Åsgard boilers in TEG mode, the Moss boiler in AA mode, the Sleipner boiler in AA mode, the Foster Wheeler boilers in AA mode and the Foster Wheeler boilers in TEG mode, respectively. In these graphs, the thermal efficiency is plotted as a function of applied fuel. However, these graphs are not very useful and must

[3] Piping and Instrumentation Diagram is a schematic illustration of the piping, instrumentation and equipments for a system.

be expressed mathematically for utilization by the RTO optimizer. Generally, the graphical representations show that the dynamics are well captured by an empirical quadratic equation on the form

$$y = \beta_0 + \beta_1 x + \beta_2 x^2, \tag{72}$$

where the βs are the estimated coefficients, y is the calculated thermal efficiency and x is the applied fuel. Furthermore, because the model is linear in coefficients, *linear regression*, was used to estimate the coefficients. The estimated functions are shown in their associated graph, and the estimated coefficients for the various operating conditions are listed in tables B.3 and B.4 in Appendix B on page 113 for the plant and simulator, respectively.

Generally, the thermal efficiency curve for a boiler has approximately the same form in the plant as that in the simulator. However, the curve is typically shifted towards left for the boilers in the simulator, which leads to a larger operating range for the boilers in the simulator. This is probably due to imperfect modeling of the steam delivery network and/or measurement errors.

Furthermore, the maximum thermal efficiency is approximately equal for each of the boilers in the simulator, regardless of operating mode. The only difference is that the maximum thermal efficiency is reached at lower fuel consumption in TEG mode, than in AA mode. This is expected since the exhaust provides additional energy, so compared with air, less fuel is required to produce an equivalent amount of heat used to evaporate the condensate. However, for the real plant, the maximum thermal efficiency is observed to be somewhat smaller in TEG mode, than in AA mode. Since the heat exchangers are the same for both operating modes, this is probably not an accurate description of the thermal efficiency for these boilers. The lack of a flow measurement of the exhaust introduces a substantial uncertainty in the calculation of the thermal efficiency in TEG mode. Therefore, with a flow measurement of the exhaust, the maximum thermal efficiency in TEG mode should be approximately equal to the maximum thermal efficiency in AA mode.

The thermal efficiency for the Moss and Sleipner boilers are almost constant compared to the other boilers. According to Glandt, Kelin, and Edgar (2001), the thermal efficiency depends substantially on the air to fuel ratio, and decreases with increasing air to fuel ratio. In the Moss boiler and the Sleipner boiler, the combustion process is controlled by the cross-limiting control structure, explained in Section 2.4.1, which stabilizes the air to fuel ratio. Therefore, the variations in thermal efficiency for these boilers are small and almost constant over the entire range of fuel consumption. However, in the Åsgard boilers and the Foster Wheeler boilers, the combustion process is controlled by an energy controller and a simple flow ratio controller, respectively, both explained in Section 2.4.1. These control strategies does not stabilize the air to fuel ratio, but mainly ensures that there always is an excess of air in the combustion process. Hence, the air to fuel ratio decreases as the fuel consumption increases, which leads to higher thermal efficiency for higher fuel consumption.

The decrease in thermal efficiency observed for all the boilers can partly be explained by basic knowledge of heat exchangers, provided by Skogestad (2009).

The heat transfer through a heat exchanger are mathematically described by the equation

$$Q = U \cdot A \cdot (T_{combustion\,gases} - T_{steam}), \tag{73}$$

where U, A, $T_{combustion\,gases}$ and T_{steam} are the thermal conductivity for the heat exchanger, the cross section area of the heat exchanger, the temperature of the combustion gases and the temperature of the steam, respectively. The energy used to evaporate the condensate is transferred by the combustion gases, and the temperature of the combustion gases increase with increased fuel consumption. Since, the steam temperature is controlled to maintain a constant temperature, the driving forces, that is the temperature difference, becomes smaller with increased combustion. As a result of this, the heat transfer across the heat exchanger stabilizes and the combustion gases leave the boiler with higher temperature. Hence, the efficiency decreases, as less of the applied energy is used to heat the condensate.

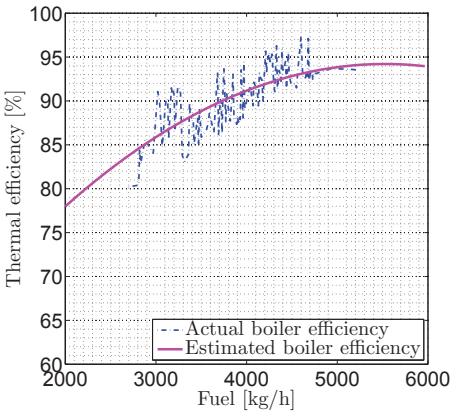

(a) Thermal efficiency for the Åsgard boilers in AA mode for the plant.

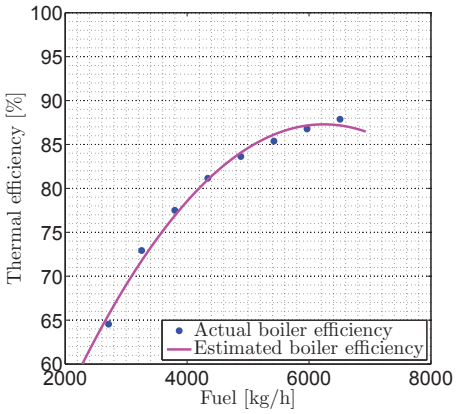

(b) Thermal efficiency for the Åsgard boilers in AA mode for the simulator.

Figure 6.2: Thermal efficiency versus applied fuel for the Åsgard boilers in AA mode.

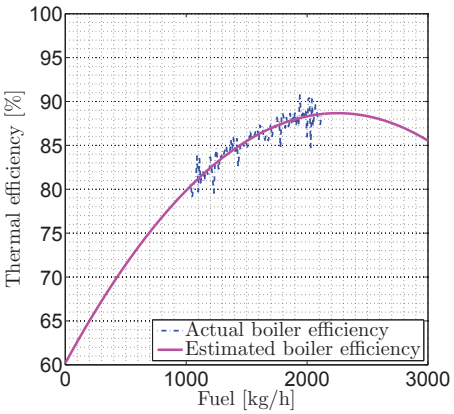

(a) Thermal efficiency for the Åsgard boilers in TEG mode for the plant.

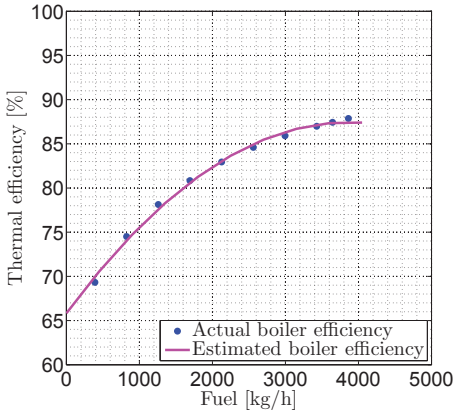

(b) Thermal efficiency for the Åsgard boilers in TEG mode for the simulator.

Figure 6.3: Thermal efficiency versus applied fuel for the Åsgard boilers in TEG mode.

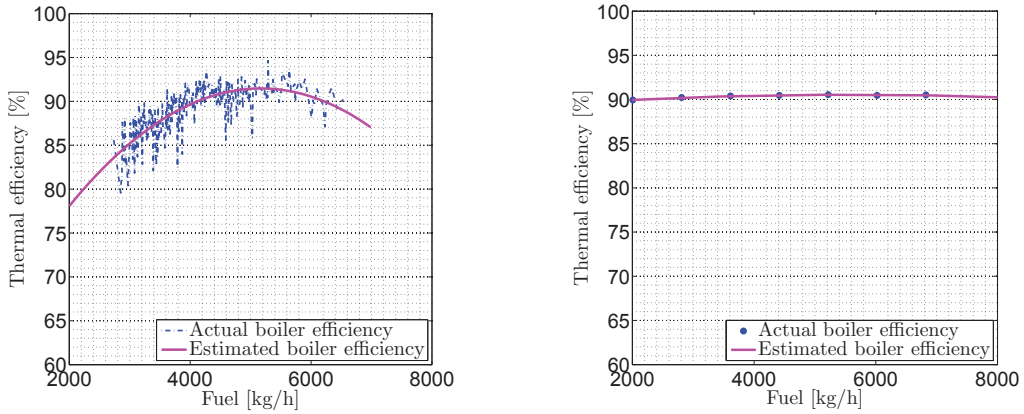

(a) Thermal efficiency for the Moss boiler in AA mode for the plant.

(b) Thermal efficiency for the Moss boiler in AA mode for the simulator.

Figure 6.4: Thermal efficiency versus applied fuel for the Moss boiler in AA mode.

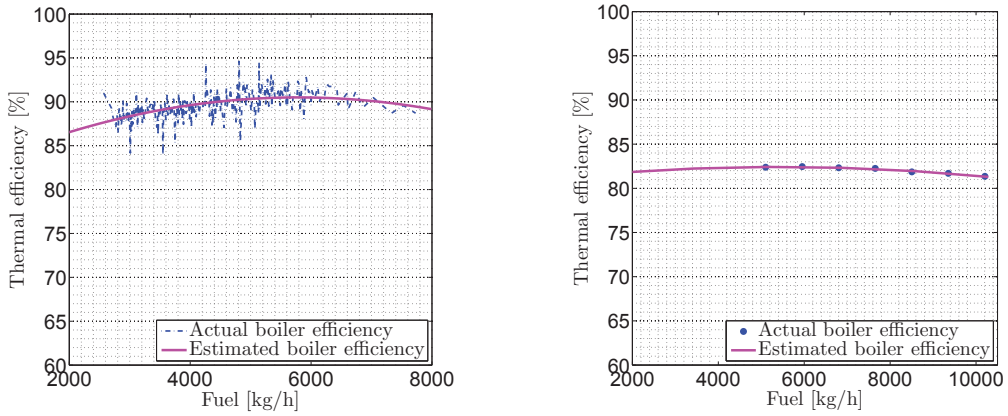

(a) Thermal efficiency for the Sleipner boilers in AA mode for the plant.

(b) Thermal efficiency for the Sleipner boilers in AA mode for the simulator.

Figure 6.5: Thermal efficiency versus applied fuel for the Sleipner boiler in AA mode.

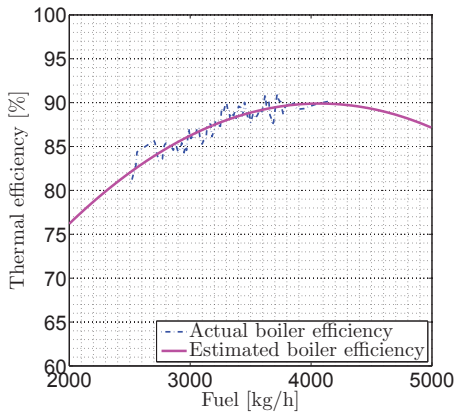

(a) Thermal efficiency for the Foster Wheeler boilers in AA mode for the plant.

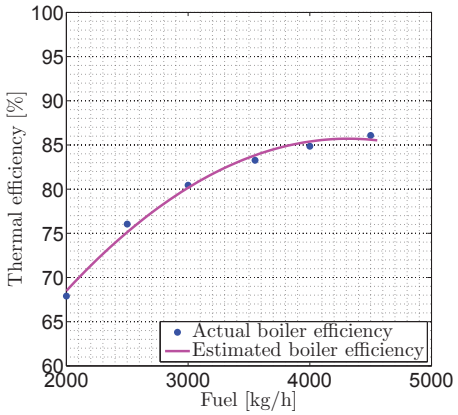

(b) Thermal efficiency for the Foster Wheeler boilers in AA mode for the simulator.

Figure 6.6: Thermal efficiency versus applied fuel for the Foster Wheeler boilers in AA mode.

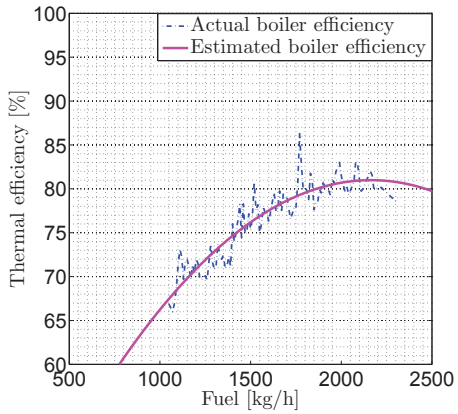

(a) Thermal efficiency for the Foster Wheeler boilers in TEG mode for the plant.

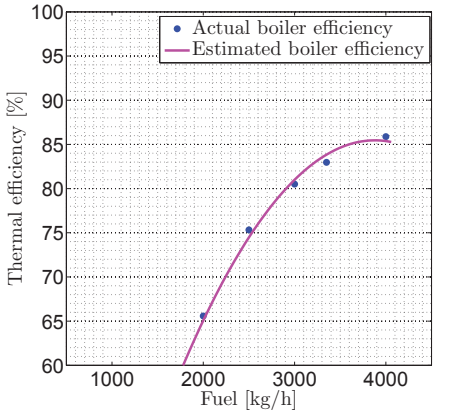

(b) Thermal efficiency for the Foster Wheeler boilers in TEG mode for the simulator.

Figure 6.7: Thermal efficiency versus applied fuel for the Foster Wheeler boilers in TEG mode.

6.3 The Optimization Problem

The MPC controller, derived in the previous chapter stabilizes the common header pressure, while ensuring safe operation. At steady-state, the steam delivery network is marginally stable, as explained in Section 5.3, and only one degree of freedom is necessary to keep the steam delivery network stable. Thus, there is an excess of available degrees of freedom, which can be used for other purposes. Therefore, in this section, a RTO optimizer and its optimization problem are derived to economically optimize the steam production, so that the available degrees of freedom can be used to achieve optimal steam production and reduce the energy consumption.

The RTO optimizer is derived from the optimization problem presented in Section 3.2. Since the steam delivery network is a closed system, no raw materials are added[4] and no products are extracted. Therefore, the objective function only consist of the cost of energy, which is the fuel consumed by the boilers. Thus, the objective function is given as

$$f = \sum_{i}^{n} u_i, \tag{74}$$

where n and u_i are the number of active boilers and the applied fuel for boiler i.

Furthermore, the optimization only applies when the steam delivery network is at steady-state, which is when the common header pressure is stable and the steam consumption is constant. Therefore, the optimization problem must include an operational constraint that accounts for a stable common header pressure, and such a constraint can be derived from the mass rate balance for the common header. Assuming that the steam delivery network is at steady-state, the steam into the common header equals the steam out of the common header, i.e. the steam produced by the boilers is equal to the steam utilized by the steam consumers. Hence, the mass rate balance for the common header becomes

$$0 = \dot{m}_{in} - \dot{m}_{out}, \tag{75}$$

where $\dot{m}_{in}$ and $\dot{m}_{out}$ are the steam in and out of the header, respectively.

The steam produced by a boiler can be derived from the thermal efficiency function for that boiler. The thermal efficiency is defined as the energy used to evaporate the condensate divided by the energy applied to the boiler. By multiplying this expression with the energy applied to the boiler, that is the lower heating value times the applied fuel, we are left with the energy used to evaporate the condensate. Then, the produced amount of steam is found by dividing this expression with the enthalpy of evaporation. Finally, by combining the thermal efficiency and the applied fuel for all the boilers in two separate vectors, the steam produced by all the boilers are given as the scalar product of these two vectors times the lower heating value divided by the enthalpy of evaporation. Thus, the steam produced by the boilers are given by

$$\dot{m}_{in} = \frac{k}{\Delta h}(\boldsymbol{\eta}^T \mathbf{u}), \tag{76}$$

[4]The small amount of water that is added, due to losses is in the network, are neglectable and represent no cost.

where k, Δh, $\boldsymbol{\eta}$ are $\mathbf{u}$ are the lower heating value, the enthalpy of evaporation, the thermal efficiency and the applied fuel, respectively.

The steam out of the common header is difficult to measure exact, as the steam is drawn out by several consumers at different output locations, some without any flow measurements. However, the steam consumption can be found using the steady-state assumption, which states that the steam into the common header must be equal to the steam out of the common header. Ergo, prior to the optimization, the steam out of the common header equals the steam into common header. Hence, the steam consumption can be found in the same manner as above by using the initial applied fuel consumption. Thus, the steam consumption is given by

$$\dot{m}_{out} = \frac{k}{\Delta h}(\boldsymbol{\eta}^T \mathbf{u}_0), \tag{77}$$

where $\mathbf{u}_0$ is the initially applied fuel consumption.

Moreover, the thermal efficiency, in the previous equation, is found for two different operating modes. In order to insert these thermal efficiencies into the equations above, it is necessary with a variable that represent the current mode for each boiler. Therefore, a vector, $\mathbf{H}$, of binary elements are introduced, in which 0 and 1 represent AA and TEG mode, respectively. Then, using this variable and the Hadamard product[5], the two equations above can be extended to apply for AA and TEG modes. Now, the steam produced by the boilers is given as

$$\dot{m}_{in} = \frac{k}{\Delta h}\Big(((\mathbf{1}-\mathbf{H}) \circ \boldsymbol{\eta}_{AA})^T \mathbf{u} + (\mathbf{H} \circ \boldsymbol{\eta}_{TEG})^T \mathbf{u}\Big), \tag{78}$$

where $\mathbf{1}$ is vector consisting only of ones. The rows in the vectors $\boldsymbol{\eta}_{AA}$ and $\boldsymbol{\eta}_{TEG}$ are the thermal efficiencies in AA and TEG mode for each boiler, respectively. In a similar manner, the steam consumption is given by

$$\dot{m}_{out} = \frac{k}{\Delta h}\Big(((\mathbf{1}-\mathbf{H}) \circ \boldsymbol{\eta}_{AA})^T \mathbf{u}_0 + (\mathbf{H} \circ \boldsymbol{\eta}_{TEG})^T \mathbf{u}_0\Big). \tag{79}$$

Inserting these two equations into the mass balance and performing some simple restructuring, the mass rate balance yields

$$\frac{k}{\Delta h}\Big(((\mathbf{1}-\mathbf{H}) \circ \boldsymbol{\eta}_{AA})^T \cdot (\mathbf{u}-\mathbf{u}_0) + (\mathbf{H} \circ \boldsymbol{\eta}_{TEG})^T \cdot (\mathbf{u}-\mathbf{u}_0)\Big) = 0. \tag{80}$$

Another operational constraint is necessary to account for the boilers range of actuation. The boilers can either be out of operation or operate within the range of minimum and maximum fuel consumption, specific for each type of boilers. The range of actuation for the Åsgard boilers is shown in Figure 6.8, where the light blue line and the dark blue points are the allowable operating areas. The figure shows that the range of actuation for one of these boilers can be expressed as a convex quadratic function on the form

$$-u^2 + bu \leq 0, \tag{81}$$

[5]The Hadamard product is an element-wise multiplication of two matrices, symbolized by $\circ$.

where b is the minimum fuel consumption for this boiler. The operational constraint can be derived from this equation by replacing the variables with vectors, where each vector element represents a specific boiler. Hence, the operational constraint becomes

$$-\mathbf{u} \circ \mathbf{u} + \mathbf{B}\mathbf{u} \leq 0, \tag{82}$$

where B is the minimum fuel consumption for each of the boilers. The operational constraint is further extended to include the two operating modes

$$-\mathbf{u} \circ \mathbf{u} + \Big((\mathbf{1} - \mathbf{H}) \circ \mathbf{B}_{AA} + \mathbf{H} \circ \mathbf{B}_{TEG}\Big) \circ \mathbf{u} \leq 0, \tag{83}$$

where $\mathbf{B}_{AA}$ and $\mathbf{B}_{TEG}$ are the minimum fuel consumption for each of the boilers in AA and TEG mode, respectively.

Now, the optimization problem for the RTO can be summarized as follows

$$\min_{u} \quad \sum_{i}^{n} u_i, \tag{84a}$$

$$\text{s.t} \quad \frac{k}{\Delta h}\Big(((\mathbf{1} - \mathbf{H}) \circ \boldsymbol{\eta}_{AA})^T \cdot (\mathbf{u} - \mathbf{u}_0) + (\mathbf{H} \circ \boldsymbol{\eta}_{TEG})^T \cdot (\mathbf{u} - \mathbf{u}_0)\Big) = 0, \tag{84b}$$

$$-\mathbf{u} \circ \mathbf{u} + \Big((\mathbf{1} - \mathbf{H}) \circ \mathbf{B}_{AA} + \mathbf{H} \circ \mathbf{B}_{TEG}\Big) \circ \mathbf{u} \leq 0. \tag{84c}$$

This optimization problem minimizes the total fuel consumption by utilizing the thermal efficiency functions to find the optimal operating point. At the optimal operating point, the optimal steam production equals the initial steam production, as the steam consumption remains constant during the optimization. The optimal fuel consumption is set as the ideal values for the respective boiler.

Two optimization strategies are examined in this thesis. The first optimization strategy, called conservative optimization, does not allow for a boiler shutdown, while the second optimization strategy, named strictly economical optimization, allows for a boiler shutdown.

For the conservative optimization strategy, the additional operating points of no fuel consumption are of no interest. Thus, the feasible region is convex, shown as the light blue area in Figure 6.8, and the optimization problem is a NLP problem. Therefore, the optimization problem was implemented in the MATLAB function *fmincon* and solved using the active set method for convex QPs, explained in Section 3.2. However, for the strictly economical optimization strategy, the additional operating points of no fuel consumption are of interest. Thus, the feasible

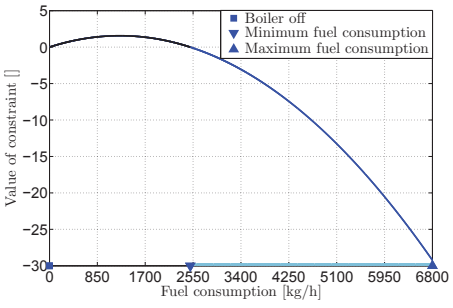

Figure 6.8: Range of actuation for the Åsgard boilers.

region is non-convex, and the optimization problem is naturally formulated as a *Mixed Integer Non-Linear Programming* (MINLP) problem. In order to consider these additional points, the strictly economical optimization strategy solves a sequence of NLPs for all relevant combinations of active and disabled boilers, and selects the best of these solutions. These NLPs were implemented in the MATLAB function *fmincon* and solved in the same way as above. There exists easier methods for solving MINLP, but because the number of integer values is small, these methods have not been investigated.

Since the combustion control structure varies for each type of boiler, the optimal fuel consumption must be converted to the boilers respective actuation. This was achieved by using the equation

$$\mathbf{z} = \mathbf{T}^T \mathbf{u}, \tag{85}$$

where $\mathbf{z}$ and $\mathbf{T}$ are the actuation for each of the boilers and the transformation matrix, respectively. This equation assumes that the process is linear, which is not completely correct. However, the limited testing performed revealed that this was a fairly good approximation. The transformation matrix is found by observing the change in fuel flow when performing a step, and equals

$$\mathbf{T} = \begin{bmatrix} 21.6 & 21.6 & 80.2 & 170.1 & 1 & 1 & 1 \end{bmatrix}^T. \tag{86}$$

Chapter 7

Results

In this chapter, several test cases are carried out to study the performance and stability of the steam delivery network and the possible reduction in fuel consumption by incorporating a RTO optimizer on top of the MPC controller. Therefore, the chapter is divided into two parts, the MPC performance group and the optimization performance group. The first part compares two simulations with and without MPC control with respect to performance and stabilization for various disturbances. The second part compares two different RTO optimization strategies regarding the possible reduction in fuel consumption and the issues arising by using these two optimization strategies.

7.1 MPC Performance

The overall objective of this group is to show improved performance and stability of the steam delivery network when using an MPC controller. This is demonstrated by comparing the performance of the steam delivery network for three different cases. In each of the cases, the steam delivery network is exposed to a disturbance which occurs five minutes into the simulation and the severity of the disturbance increases for each case.

In case I, the handling of a setpoint change for the common header pressure is presented. In the following two cases, the handling of a loss in steam demand and a boiler trip is presented sequentially.

In all the cases, the design of the regulatory layer enables only the Åsgard boiler A energy controller to adjust its setpoint. Hence, this is the only boiler with the ability to adjust its steam production and thus, change the common header pressure. In practice, operators would supervise the steam delivery network and adjust the steam production on other boilers, should a large disturbance occur. In this analysis, the operators have been removed, as the two control strategies are to be compared. However, the MPC controller is able to adjust the steam production on every boiler. Because of the repeating behavior for both control strategies, the observed behavior is explained following the presentation of the three cases.

7.1.1 Case I: Handling a setpoint change

In this case the steam delivery network was exposed to a setpoint change equal to 1 [*bar*] in the common header pressure. The simulations were carried out from the nominal operating point 1 with initial common header pressure at 60 [*barg*], stated in Table B.1 in Appendix B on page 113.

The common header pressure responses for the simulations with and without MPC control are presented in figures 7.1a and 7.1b, respectively. The steam production and applied fuel for each boiler for the simulations with and without MPC control are shown in figures 7.2 and 7.3, respectively. Furthermore, all the primary CVs remained within their respective limits and are therefore not presented.

The simulations were carried out for a time span equivalent to two hours for both control strategies, and common header pressure experienced an overshoot of approximately 0.15 [*bar*] and 0.25 [*bar*] and settles after approximately 20 and 120 minutes for the case with and without MPC control, respectively. Steam production data for all the boilers for both control strategies are listed in Table 7.1.

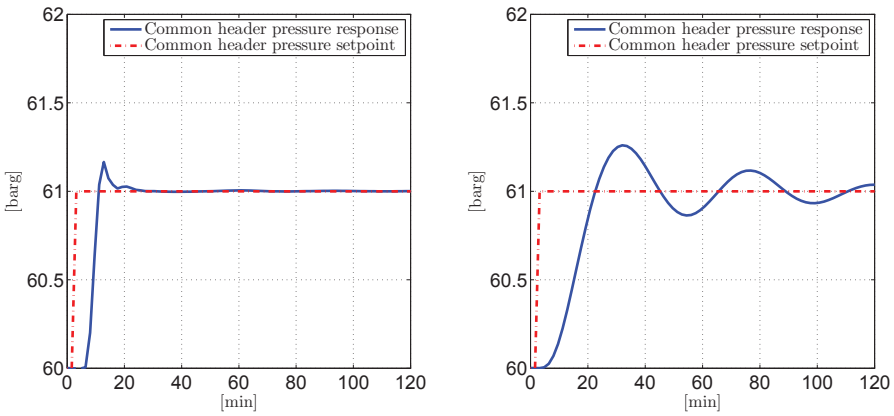

(a) With MPC control. **(b)** Without MPC control.

Figure 7.1: Case I: Common header pressure responses for a setpoint change with and without MPC control.

Table 7.1: Case I: Steam production data.

Boiler	Steam production at the beginning		Steam production at the end	
	MPC	PI	MPC	PI
Åsgard A	84,000 [kg/h]	84,000 [kg/h]	84,000 [kg/h]	84,000 [kg/h]
Åsgard B	84,000 [kg/h]	84,000 [kg/h]	84,000 [kg/h]	84,000 [kg/h]
Moss	79,000 [kg/h]	79,000 [kg/h]	79,000 [kg/h]	79,000 [kg/h]
Sleipner	82,000 [kg/h]	82,000 [kg/h]	82,000 [kg/h]	82,000 [kg/h]
Foster Wheeler A	53,000 [kg/h]	53,000 [kg/h]	53,000 [kg/h]	53,000 [kg/h]
Foster Wheeler B	53,000 [kg/h]	53,000 [kg/h]	53,000 [kg/h]	53,000 [kg/h]
Foster Wheeler C	53,000 [kg/h]	53,000 [kg/h]	53,000 [kg/h]	53,000 [kg/h]
Total steam	488,000[kg/h]	488,000 [kg/h]	488,000 [kg/h]	488,000 [kg/h]

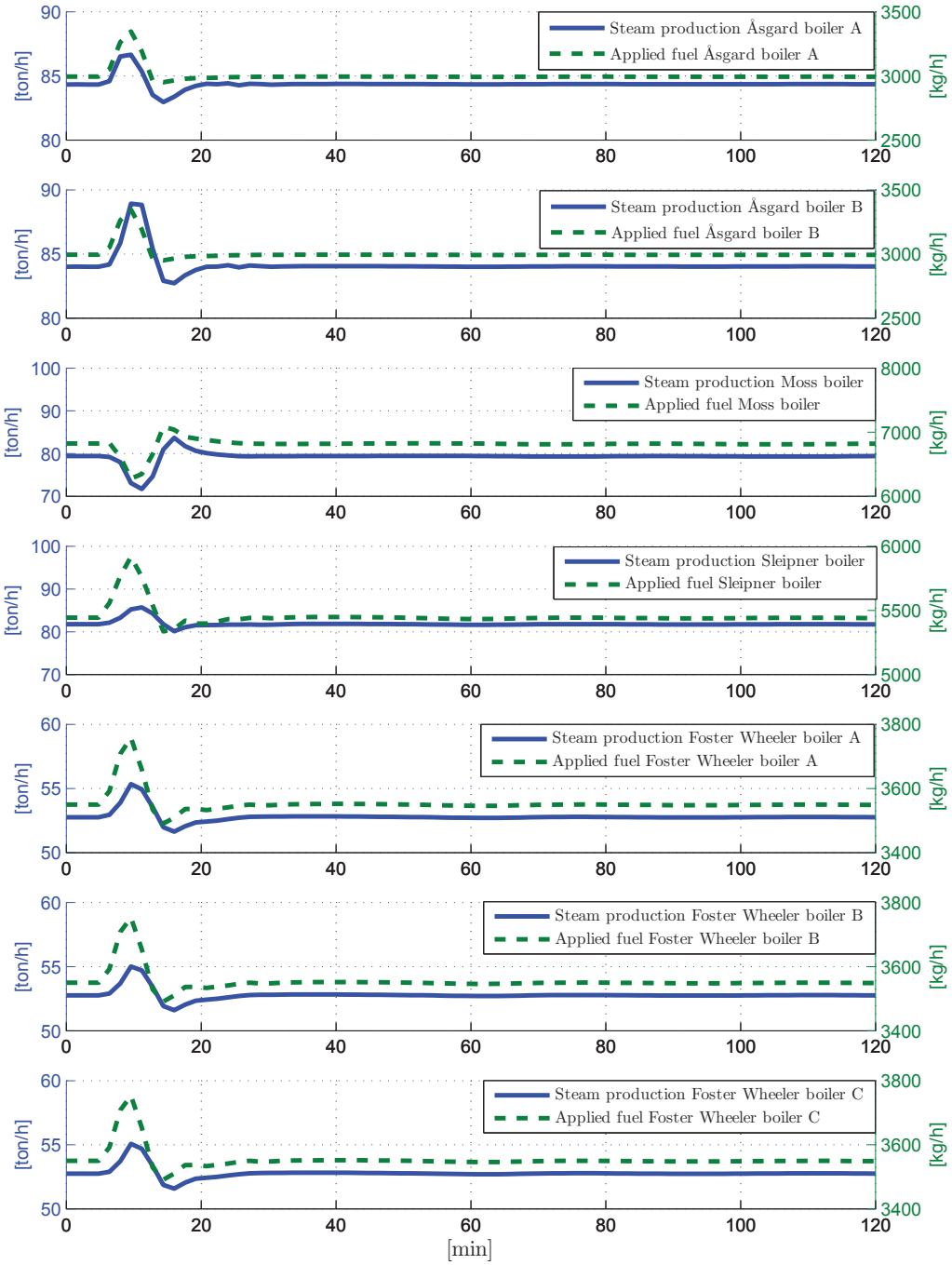

Figure 7.2: Case I: Steam production and applied fuel for all the boilers with MPC control.

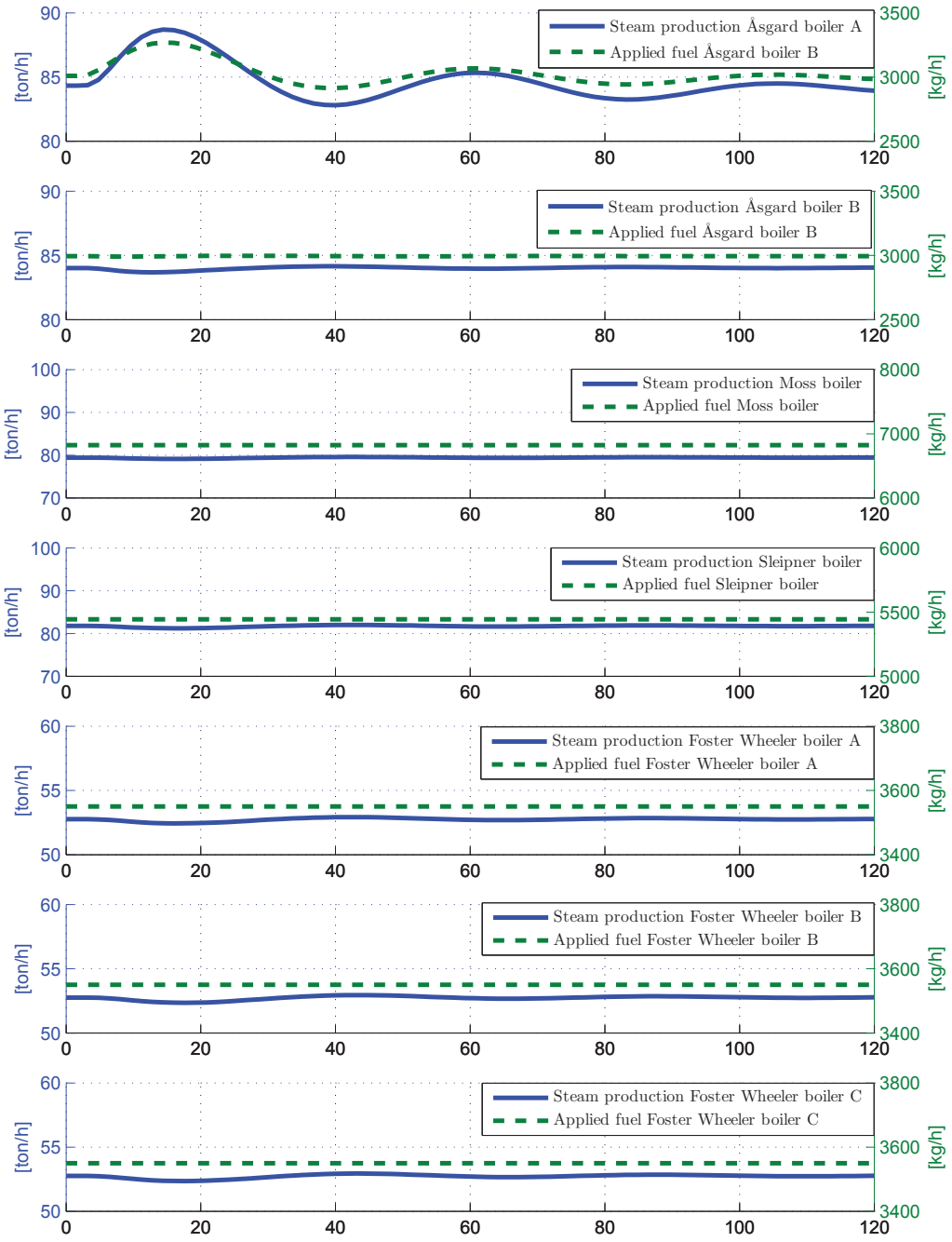

Figure 7.3: Case I: Steam production and applied fuel for all the boilers without MPC control.

7.1.2 Case II: Handling a loss in steam demand

Case II presents the performance of the steam delivery network when a loss in steam demand occurs. The loss is equal to 40,000 $[kg/h]$ and occurs over a period of two minutes. The simulations were carried out from the nominal operating point 1 with an initial common header pressure at 60 $[barg]$, presented in Table B.1 in Appendix B on page 113.

The common header pressure responses for the simulations with and without MPC control are shown in figures 7.4a and 7.4b, respectively. The steam production and applied fuel for each boiler for the simulations with and without MPC control are presented in figures 7.5 and 7.6, respectively. Moreover, all the primary CVs stayed within their respective limits and are therefore not presented.

The case were simulated for a period equal to three hours for both control strategies, and the common header pressure experienced a maximum deviation approximately equal to 1.10 $[bar]$ and 3.20 $[bar]$ and settles after approximately 30 and 130 minutes for the case with and without MPC control, respectively. Steam production data for both control strategies are listed in Table 7.2.

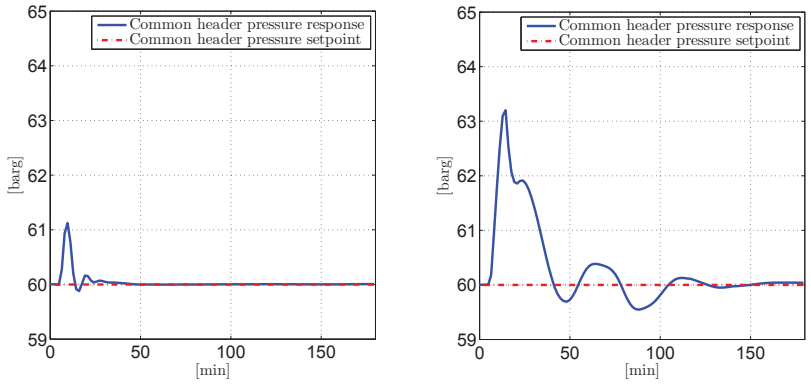

(a) With MPC control. **(b)** Without MPC control.

Figure 7.4: Case II: Common header pressure responses for a loss in steam demand with and without MPC control.

Table 7.2: Case II: Steam production data.

Boiler	Steam production at the beginning		Steam production at the end	
	MPC	PI	MPC	PI
Åsgard A	84,000 $[kg/h]$	84,000 $[kg/h]$	82,000 $[kg/h]$	43,000 $[kg/h]$
Åsgard B	84,000 $[kg/h]$	84,000 $[kg/h]$	82,000 $[kg/h]$	84,000 $[kg/h]$
Moss	79,000 $[kg/h]$	79,000 $[kg/h]$	61,000 $[kg/h]$	79,000 $[kg/h]$
Sleipner	82,000 $[kg/h]$	82,000 $[kg/h]$	76,000 $[kg/h]$	82,000 $[kg/h]$
Foster Wheeler A	53,000 $[kg/h]$	53,000 $[kg/h]$	50,000 $[kg/h]$	53,000 $[kg/h]$
Foster Wheeler B	53,000 $[kg/h]$	53,000 $[kg/h]$	50,000 $[kg/h]$	53,000 $[kg/h]$
Foster Wheeler C	53,000 $[kg/h]$	53,000 $[kg/h]$	50,000 $[kg/h]$	53,000 $[kg/h]$
Total Steam	488,000 $[kg/h]$	488,00 $[kg/h]$	451,00 $[kg/h]$	447,000 $[kg/h]$

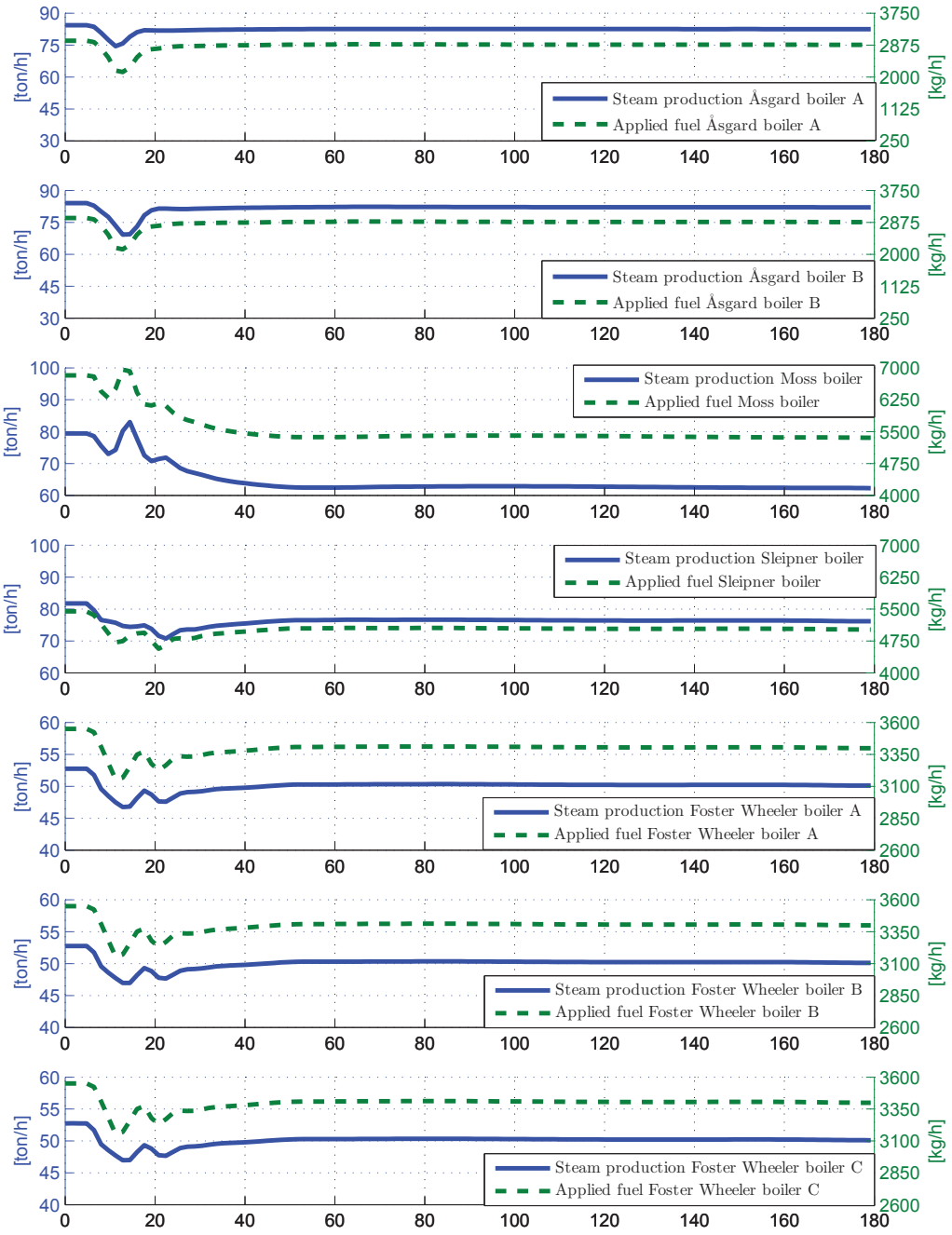

Figure 7.5: Case II: Steam production and applied fuel for all the boilers with MPC control.

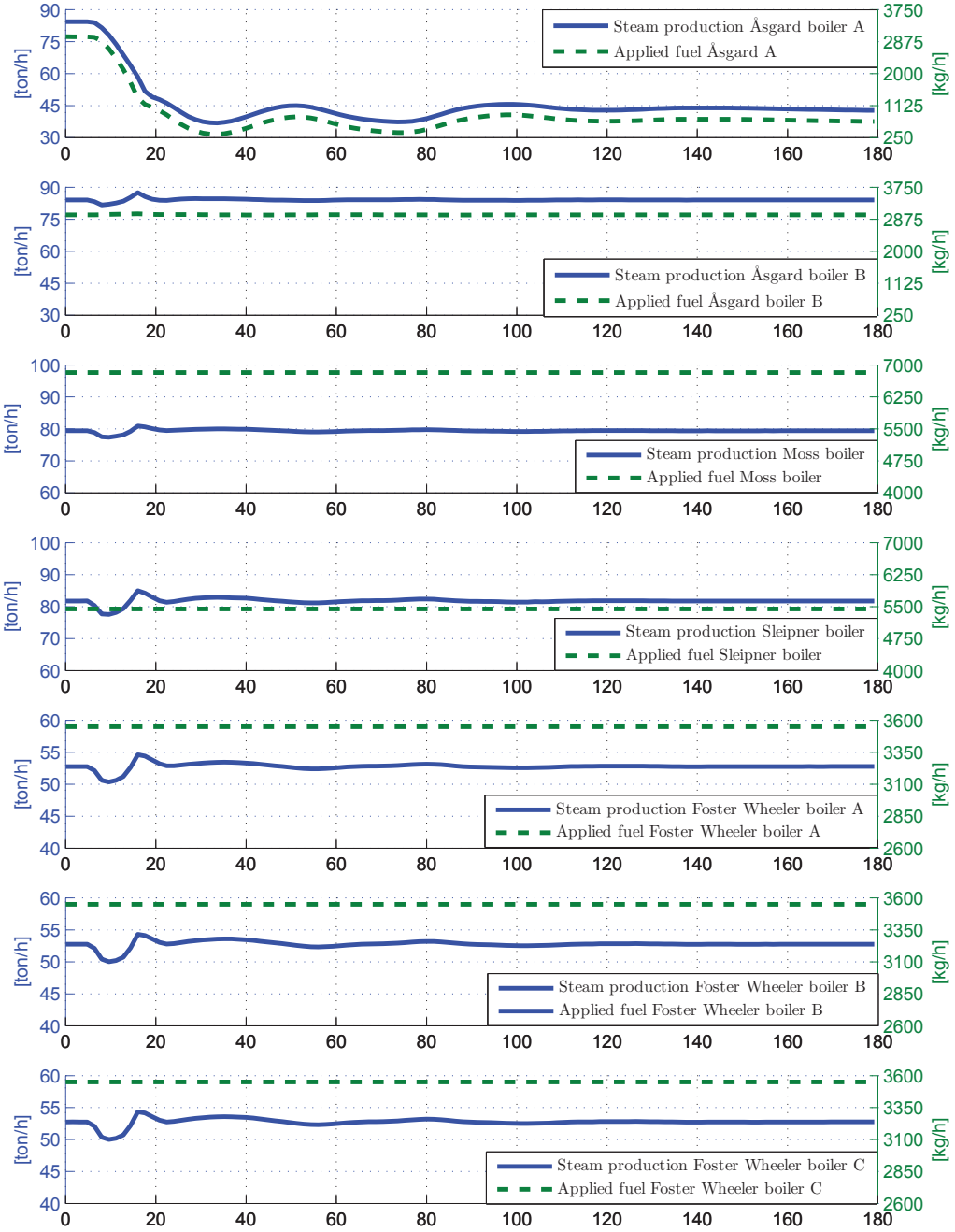

Figure 7.6: Case II: Steam production applied fuel for all the boilers without MPC control.

7.1.3 Case III: Handling a boiler trip

In this final case, the steam delivery network experiences a boiler trip of the Foster Wheeler boiler A. The trip causes a loss in steam production equal to 55,000 $[kg/h]$. The simulations were carried out from the nominal operating point 2 with an initial pressure of 60 $[barg]$, presented in Table B.2 in Appendix B on page 113.

The common header pressure responses for the simulations with and without MPC are presented in figures 7.7a and 7.7b, respectively. The steam production and applied fuel for each boiler for the simulations with and without MPC control are shown in figures 7.8 and 7.9, respectively. The primary CVs for both boilers remained within their hard limits. However, some of the primary CVs for Åsgard boiler A violated their soft constraints and are shown in figures A.1a and A.1b in Appendix B on page 113 for the cases with and without MPC control, respectively.

The simulations were carried out for a period of two hours. The common header pressure dropped to 36.70 $[barg]$ for the PI control strategy, while the MPC control strategy only managed to restore the common header pressure back to 60 $[barg]$ from a maximum deviation of 3.00 $[bar]$ within a time span of 35 minutes. Steam production data for both control strategies are listed in Table 7.3.

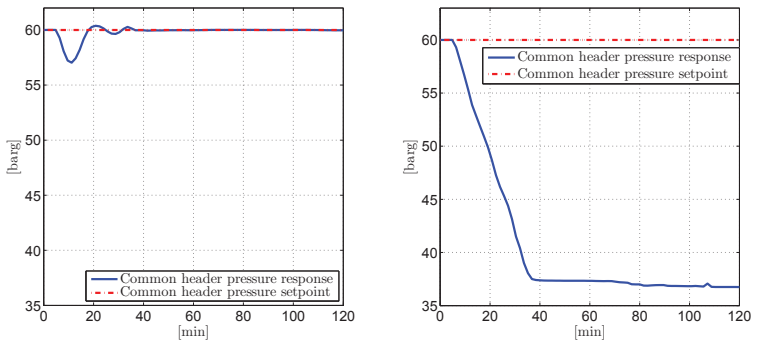

(a) With MPC control. **(b)** Without MPC control.

Figure 7.7: Case III: Common header pressure responses for a boiler trip with and without MPC control.

Table 7.3: Case III: Steam production data.

Boiler	Steam production at the beginning		Steam production at the end	
	MPC	PI	MPC	PI
Åsgard A	73,000 $[kg/h]$	73,000 $[kg/h]$	78,000 $[kg/h]$	100,000 $[kg/h]$
Åsgard B	73,000 $[kg/h]$	73,000 $[kg/h]$	78,000 $[kg/h]$	73,000 $[kg/h]$
Moss	74,000 $[kg/h]$	74,000 $[kg/h]$	85,000 $[kg/h]$	73,000 $[kg/h]$
Sleipner	100,000 $[kg/h]$	100,000 $[kg/h]$	118,000 $[kg/h]$	100,000 $[kg/h]$
Foster Wheeler A	55,000 $[kg/h]$	55,000 $[kg/h]$	0 $[kg/h]$	0 $[kg/h]$
Foster Wheeler B	53,000 $[kg/h]$	53,000 $[kg/h]$	61,000 $[kg/h]$	53,000 $[kg/h]$
Foster Wheeler C	53,000 $[kg/h]$	53,000 $[kg/h]$	61,000 $[kg/h]$	53,000 $[kg/h]$
Total steam	481,000 $[kg/h]$	481,000 $[kg/h]$	481,000 $[kg/h]$	452,000 $[kg/h]$

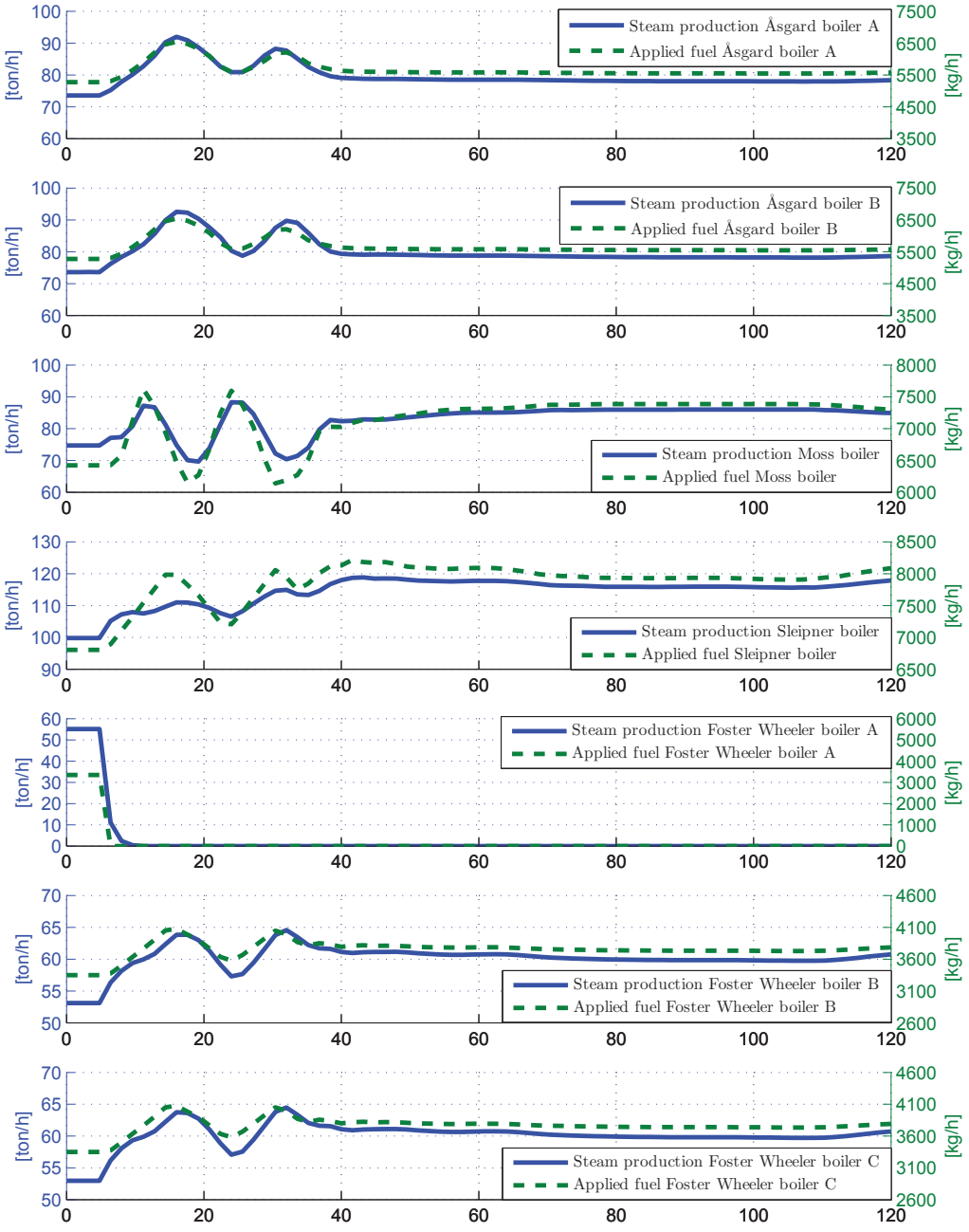

Figure 7.8: Case III: Steam production and applied fuel for all the boilers with MPC control.

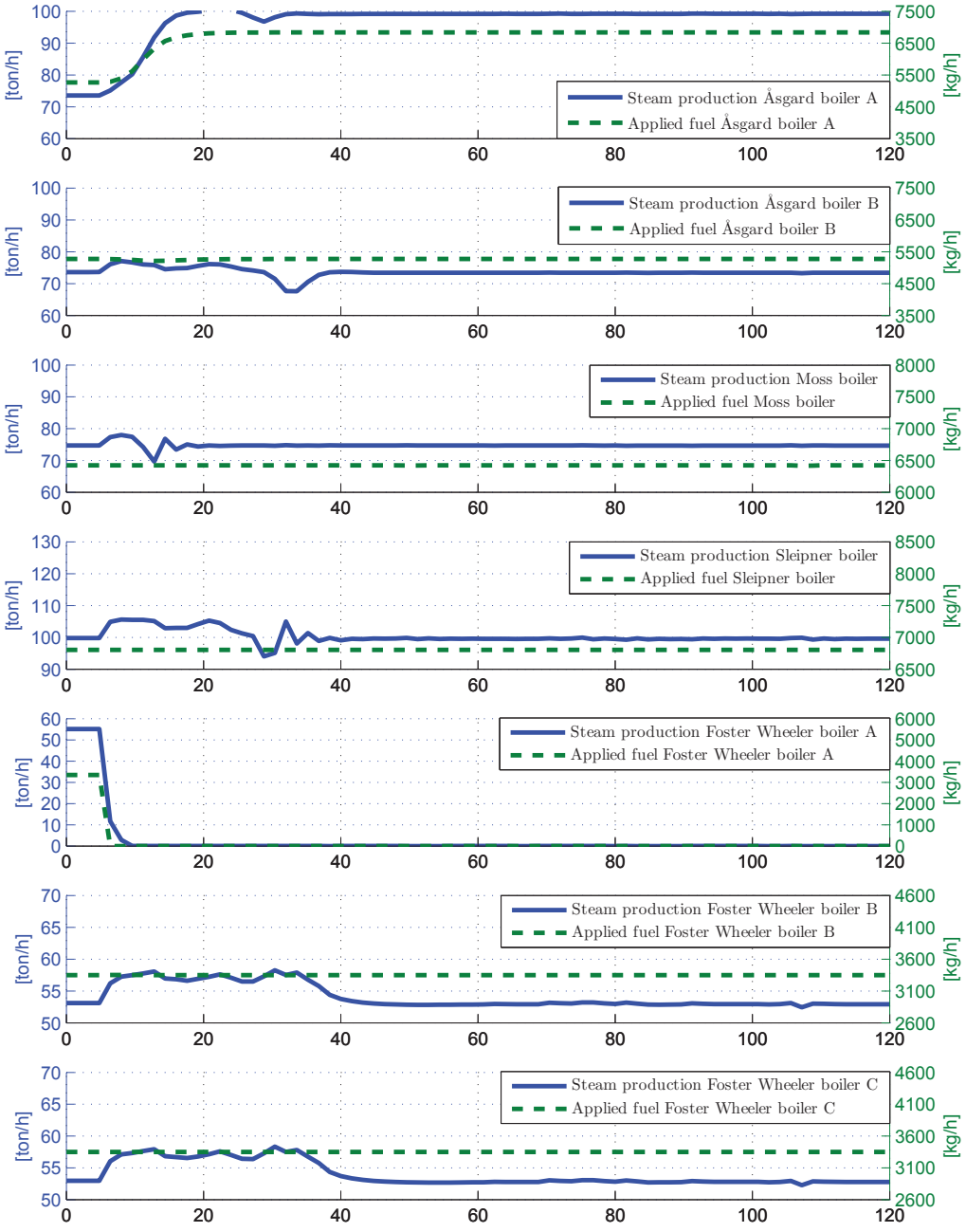

Figure 7.9: Case III: Steam production and applied fuel for all the boilers without MPC control.

7.2 Summary of MPC Performance

The common header pressure depends on the amount of steam within the common header, as explained in the process analysis in Section 5.3. The physical explanation is that the steam within the common header exerts a pressure on the walls enclosing the common header and this pressure constitutes the common header pressure. Hence, the common header pressure increases with the amount of steam within the common header.

In the first case, the common header pressure is increased to reach the new setpoint. The steam consumption remains constant during the whole simulation for both control strategies. Moreover, before the setpoint change occurs, the steam production equals the steam consumption to maintain a constant common header. In order to reach the new increased common header setpoint, the amount of steam within the common header must increase. Therefore, the steam production is increased for a short period of time. When the new common header pressure is reached, each of the control strategies adjusts their steam production to cover the constant steam consumption so that the common header pressure remains constant. In the case with PI control, only the Åsgard boiler A is allowed to adjust its steam production. As seen from Figure 7.3, the steam production increases mostly in the beginning to fill the common header. Following this, the boiler adjusts its steam production to cover the steam consumption and finally settles at the initial steam production. In the case with MPC control, all the boilers are able to adjust their steam production, as shown in Figure 7.2. Hence, all the boilers except of the Moss boiler increase their steam production to fill the common header before they all return to the initial steam production to cover the steam consumption. This response is expected, as the ideal values forces the MPC controller to arrive at the initial steam production for each boiler. Furthermore, this behavior is confirmed since the total amount of steam before and after the setpoint change is equal.

In the second case, the steam production is reduced due to a reduction in steam demand. The steam consumption only changes during the first two minutes where it falls by about 40,000 $[kg/h]$. This reduction results in an increase of steam within the common header and in turn, a rise in common header pressure. In order to restore the common header pressure, the total steam production must first fall below the total steam demand for the steam consumers to utilize the excess of steam within the common header. Then, the steam production must be slightly increased to level the new steam consumption. Again, for the case with PI control, only the Åsgard boiler A is allowed to adjust its steam production, as seen in Figure 7.6. The boiler reduces its steam production sharply in the beginning so that the excess of steam can be drawn from the common header. Then, the steam production is adjusted and slightly increased to cover the new steam consumption. For the case with MPC control, all the boilers are able to adjust their steam production, as shown in Figure 7.5. Thus, all the boilers reduce their steam production to remove the excess of steam within the common header. Then, they all arrive at a new steam production to cover the new steam consumption. The total amount of steam after the loss occurred summarized with the loss equals the total amount of steam before the loss occurred. The ideal values and the move penalties determine

the new steam production for each type of boiler. A small remark is necessary at this point, the number will not match perfectly due to rounding errors and non-existing measurement of the steam consumption.

In the final case, the steam production is increased to cover the loss of a boiler trip. The steam consumption remains constant during the whole simulation for both control strategies. At first, the boilers have to produce enough steam to fill the lack of steam within the common header to reach the setpoint. Then, the steam production must be adjusted to equalize the steam demand. In the case with PI control, the situation is as before, only the Åsgard boiler A is allowed to adjust its steam production, as can be seen from Figure 7.9. The boiler increases its steam production to fill the common header and cover the boiler trip. However, the boiler is limited by its capacity and is not able to fill the common header with enough steam, or cover the steam consumption. As the common header pressure decreases, the pressure difference between the common header and some of the steam consumers become so low that the steam flow between these ceases. These steam consumers will trip and result in lower steam consumption. Hence, the common header pressure stabilizes when enough steam consumers have tripped so that the steam production levels the lowered steam consumption. In the case with MPC control, all the boilers are able to adjust their steam production, as shown in Figure 7.8. The remaining boilers cooperate in covering the lack of steam and to level the steam consumption by increasing their steam production before settling at a new steam production equal to the steam consumption. Again, the ideal values and the move penalty for each type of boiler decide the new steam production. This behavior is verified as the total amount of steam before and after the trip is equal. The primary CVs for the Åsgard boiler A are shown in figures A.1a and A.1b in Appendix B on page 113 for the simulations with and without MPC, respectively. These figures show that the hard limits are respected by both control strategies, but that only the MPC controller are able to respect the soft constraint and produce steam at required temperature (430 $[^{\circ}C]$). Moreover, the PI control strategy destroys its cooling capacity as it reaches saturation, while the MPC controller preserves its cooling capacity. Another noteworthy observation from these figures is that the HP steam temperature is lowered in the intervals where the cooling capacity, the attemperator valve, reaches saturation.

The observant reader might have noticed that the fuel consumption for all but the Åsgard boiler A remains constant for the simulations with PI control. This is due to the PI control structure only allows this boiler to adjust its steam production by changing the combustion process. Another inserting observation for the simulations without MPC control is the fluctuations observed on the boilers with constant steam productions despite of nearly constant fuel consumption. This behavior is easiest explained for Case II using the PI control strategy, shown in figures 7.4b and 7.6 for the common header pressure and steam production, respectively. The sudden increase in common header pressure causes all the boilers but the Åsgard boiler A to experience a short drop in steam production followed by a slightly larger increase. The common header pressure increase results in a larger pressure difference between the steam within the common header and the steam within the

boiler drums. Hence, the pressure of the steam within the drums must be further increased to overcome this pressure difference and given the current combustion, more energy must be applied to the boiler to maintain a constant steam production. The following slightly increase is due to time delays within the boiler and that the small excess of steam, from the period with insufficient energy, is sent from the boilers. A common header pressure drop will cause the boilers to delivery more steam at the current energy supply since the pressure difference between these decreases. Due to time delays within the boilers, some time elapses before the boilers again reach the value of constant combustion for the new common header pressure. This can be observed in figures 7.7b and 7.9 for the common header pressure and the steam production using the PI control strategy, respectively. Note that the steam production increases as long as the common header pressure decreases. The magnitudes of these fluctuations increase with increased pressure difference.

7.3 Optimization Performance

The main objective of this group is to illustrate a possible utilization of the available degrees of freedom, using two different RTO optimization strategies, to reduce both the fuel consumption and the CO_2 emissions. These two RTO optimization strategies are presented in Section 6.3, and are called conservative optimization and strictly economical optimization. The secondary objectives of this group are to illustrate the potential and the challenges that come with optimization.

In case IV, the conservative optimization strategy is illustrated for a steady-state nominal operating point. The following case compares the two optimization strategies for another steady-state nominal operating point. In case VI, the optimization potential for both optimization strategies is illustrated by calculating the fuel and CO_2 savings for a year of real plant data. In case VII, the sensitivity for model errors is illustrated by comparing two simulations with and without model errors. The final case illustrates the robustness against a trip of boiler with the heaviest load, from the optimal operating point calculated by the two optimization strategies.

In all the cases presented, the optimization is performed when the process is at steady-state. Furthermore, for each boiler, the optimized fuel consumption is set as the ideal value to the associated boiler five minutes into the simulations. This is done to better observe the response of a change in ideal value.

It should be mentioned that in the real plant, a boiler shutdown is conducted by continuously decreasing the boilers fuel consumption towards minimum fuel consumption. When the boilers arrive at this fuel consumption, the combustion process is terminated resulting in an abrupt drop in steam consumption. However, in the simulator, a boiler shutdown is performed by continuously decreasing the boilers fuel consumption towards zero. Thus, the abrupt halt is prevented and the intermediate disturbance occurring when performing the boiler shutdown is avoided. Hence, the common header pressure would fluctuate somewhat more in the real plant than in the cases to be presented.

7.3.1 Case IV: Conservative fuel optimization

In this case, the conservative optimization strategy was performed for the steam delivery network at the steady-state nominal operating point 1 with an initial common header pressure of 60 $[barg]$, presented in Table B.1 in Appendix B on page 113. The optimization result is shown in Figure 7.10 and the initial and the optimized fuel consumptions from the optimization are listed in Table 7.4.

The common header pressure response and the total fuel consumption are presented in figures 7.11a and 7.11b, respectively. The fuel consumption for each of the boilers is shown in Figure 7.12.

The simulation was performed for a time period equal to one hour and the optimization result led to a reduction in fuel consumption for the Moss boiler and the Sleipner boiler, while the Foster Wheeler boilers and the Åsgard boilers experienced increased fuel consumption. The maximum setpoint deviation was approximately 0.19 $[barg]$ and the reduction in total fuel consumption was approximately 295 $[kg/h]$.

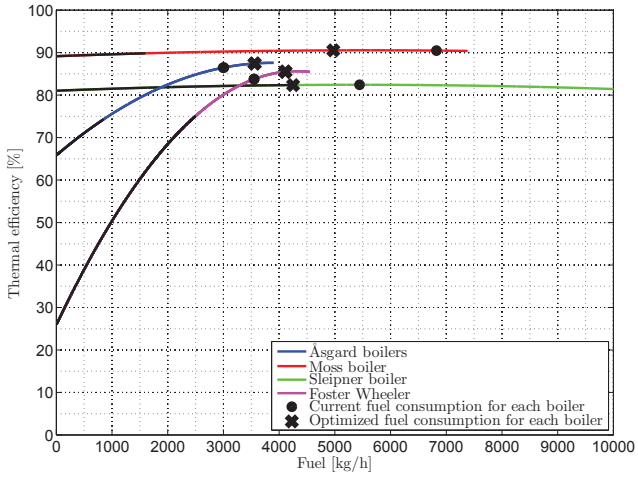

Figure 7.10: Case IV: Optimization result. The colored lines are the allowable operating range of the boilers, while the dark lines are impossible operating areas.

Table 7.4: Case IV: Optimization data.

Boiler	Initial fuel consumption	Optimal fuel consumption
Åsgard A	3008.80 $[kg/h]$	3558.50 $[kg/h]$
Åsgard B	2994.20 $[kg/h]$	3558.50 $[kg/h]$
Moss	6823.80 $[kg/h]$	4972.90 $[kg/h]$
Sleipner	5443.20 $[kg/h]$	4250.00 $[kg/h]$
Foster Wheeler A	3550.00 $[kg/h]$	4111.30 $[kg/h]$
Foster Wheeler B	3550.00 $[kg/h]$	4111.30 $[kg/h]$
Foster Wheeler C	3550.00 $[kg/h]$	4111.30 $[kg/h]$
Total fuel consumption	28,920.0 $[kg/h]$	28,673.8 $[kg/h]$

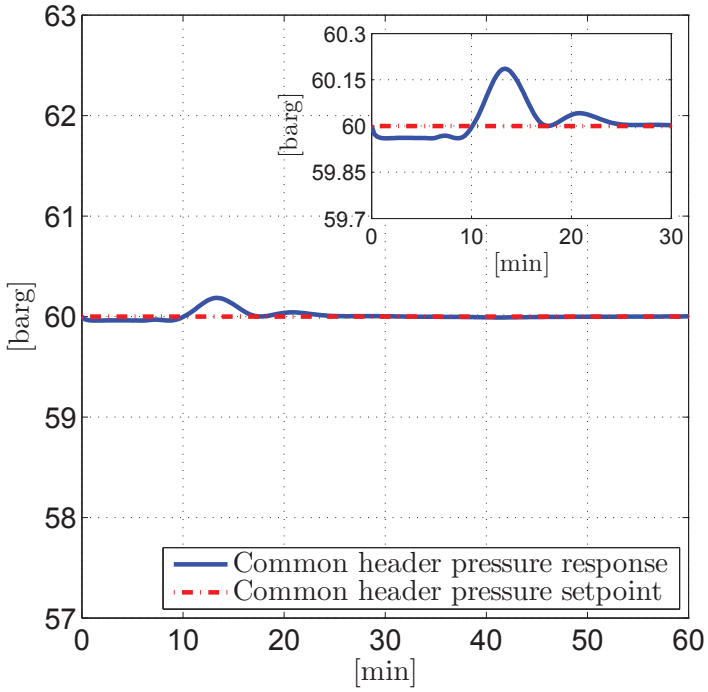

(a) Common header pressure response.

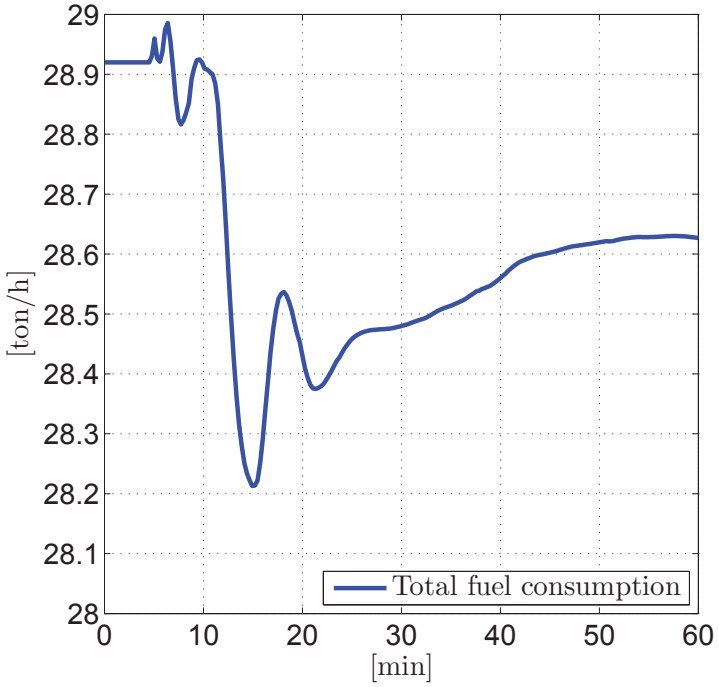

(b) Total fuel consumption response.

Figure 7.11: Case IV: Common header pressure and total fuel consumption responses.

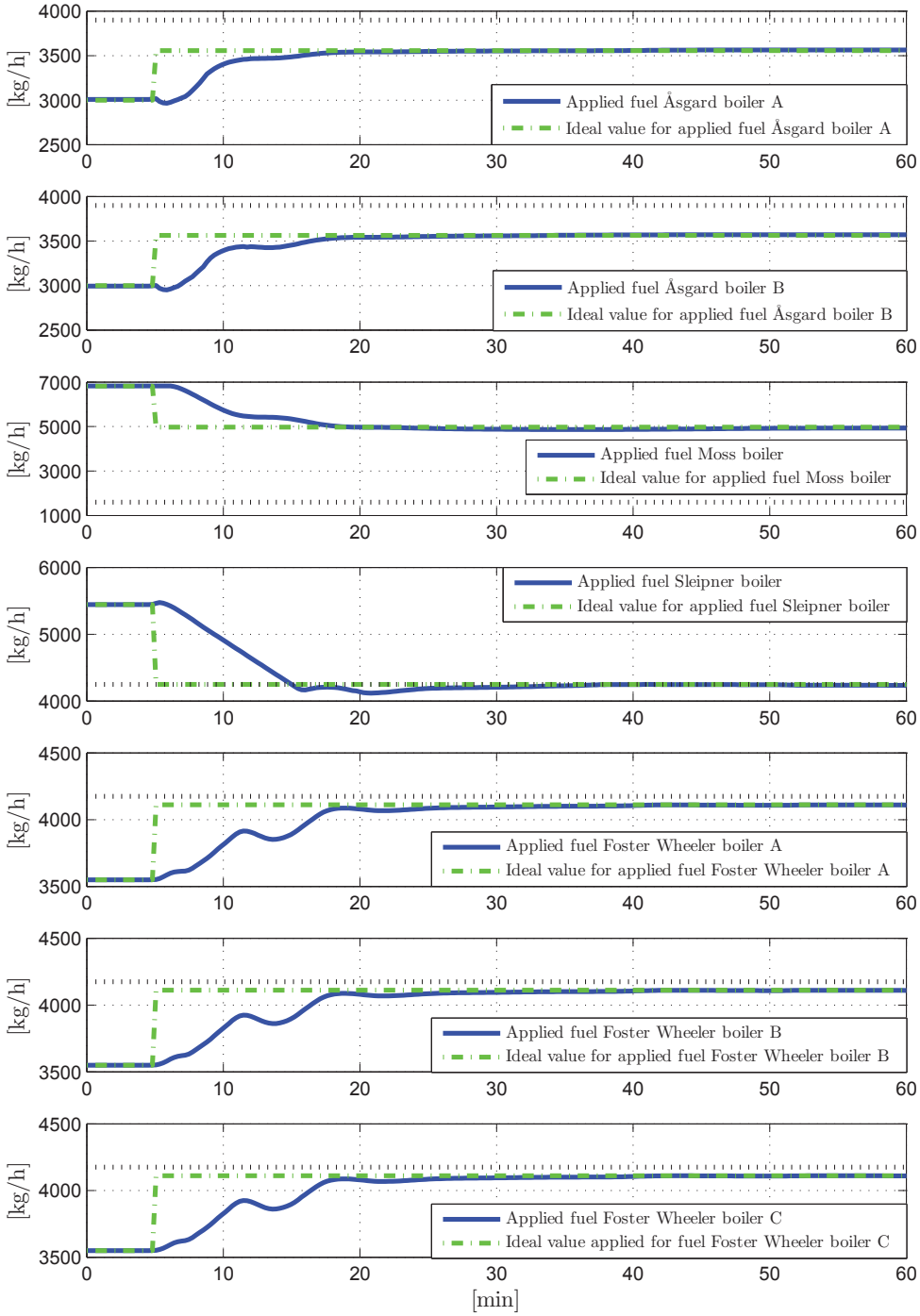

Figure 7.12: Case IV: Fuel consumption for each boiler.

7.3.2 Case V: Strictly economical fuel optimization

In case V, both the conservative and the strictly economical optimization strategies were performed for the steam delivery network at the steady-state nominal operating point 2, listed in Table B.2 in Appendix B on page 113. The optimization results are shown in figures 7.13a and 7.13b and the initial and the optimized fuel consumptions from both optimizations are listed in Table 7.5.

The common header pressure responses are shown in figures 7.14a and 7.14b and the total fuel consumptions are shown in figures 7.14a and 7.15b for the conservative and strictly economical optimization strategies, respectively. The fuel consumption for each boiler is shown in figures 7.16 and 7.17 for the conservative and strictly economical optimization strategies, respectively.

The simulations were performed for a time period equivalent to 70 minutes. The conservative optimization result led to reduction in fuel consumption for the Moss and Sleipner boiler and increased fuel consumption for the remaining boilers. The strictly economical optimization result led to a shutdown of the Sleipner boiler and increased combustion for the active boilers. The maximum setpoint deviations were approximately 0.20 $[bar]$ and 0.18 $[bar]$ and the reduction in fuel consumptions were approximately 452 $[kg/h]$ and 502 $[kg/h]$ for the conservative and strictly economical optimization strategies, respectively.

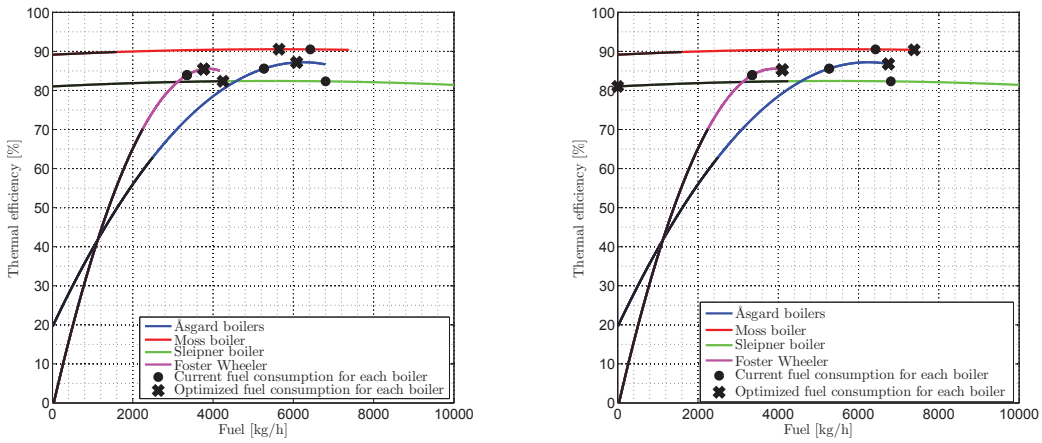

(a) Conservative. **(b)** Strictly economical.

Figure 7.13: Case V: Optimization results for the conservative and strictly economical optimization strategies

Table 7.5: Case V: Optimization data.

Boiler	Conservative optimization		Strictly economical optimization	
	Initial fuel consumption	Optimal fuel consumption	Initial fuel consumption	Optimal fuel consumption
Åsgard A	5265.90 $[kg/h]$	6082.20 $[kg/h]$	5265.90 $[kg/h]$	6744.60 $[kg/h]$
Åsgard B	5272.40 $[kg/h]$	6082.20 $[kg/h]$	5272.40 $[kg/h]$	6744.60 $[kg/h]$
Moss	6422.40 $[kg/h]$	5641.90 $[kg/h]$	7385.00 $[kg/h]$	7385.00 $[kg/h]$
Sleipner	6804.00 $[kg/h]$	4250.00 $[kg/h]$	6804.00 $[kg/h]$	0 $[kg/h]$
Foster Wheeler A	3350.00 $[kg/h]$	3765.20 $[kg/h]$	3350.00 $[kg/h]$	4099.40 $[kg/h]$
Foster Wheeler B	3350.00 $[kg/h]$	3765.20 $[kg/h]$	3350.00 $[kg/h]$	4099.40 $[kg/h]$
Foster Wheeler C	3350.00 $[kg/h]$	3765.20 $[kg/h]$	3350.00 $[kg/h]$	4099.40 $[kg/h]$
Total fuel consumption	33,814.7 $[kg/h]$	33,351.9 $[kg/h]$	33,814.7 $[kg/h]$	33,172.4 $[kg/h]$

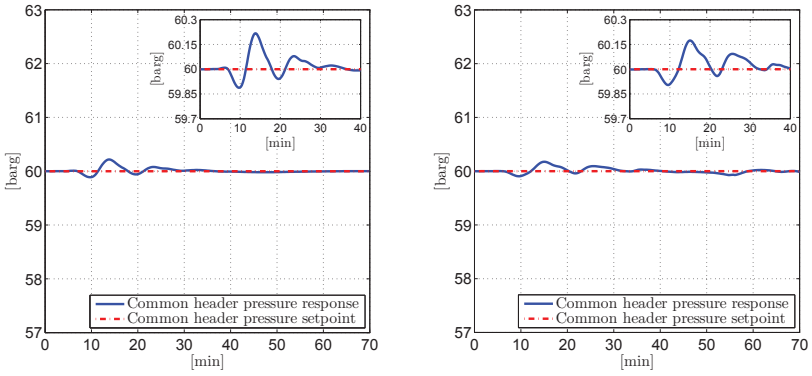

(a) Conservative. **(b)** Strictly economical.

Figure 7.14: Case V: Common header pressures for both optimization strategies.

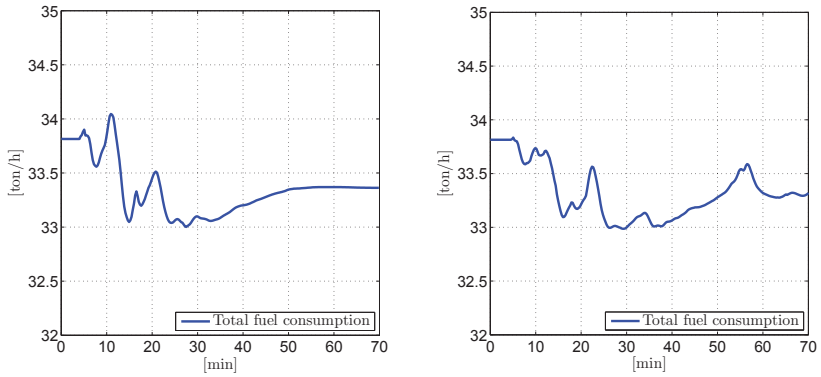

(a) Conservative. **(b)** Strictly economical.

Figure 7.15: Case V: Total fuel consumption for both optimization strategies.

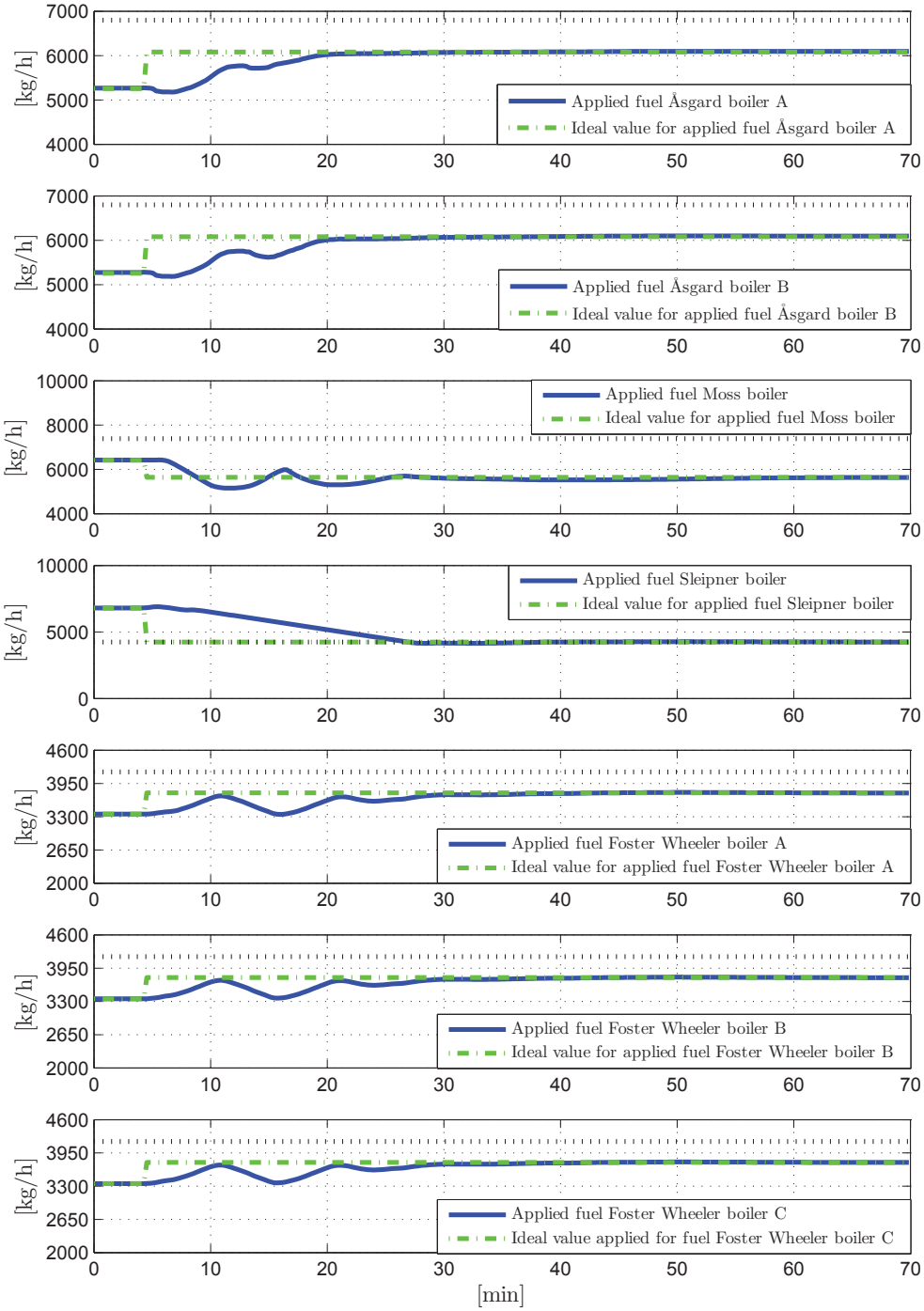

Figure 7.16: Case V: Fuel consumption for each boiler for conservative optimization. The black lines are the closest limit for each of the boilers, respectively.

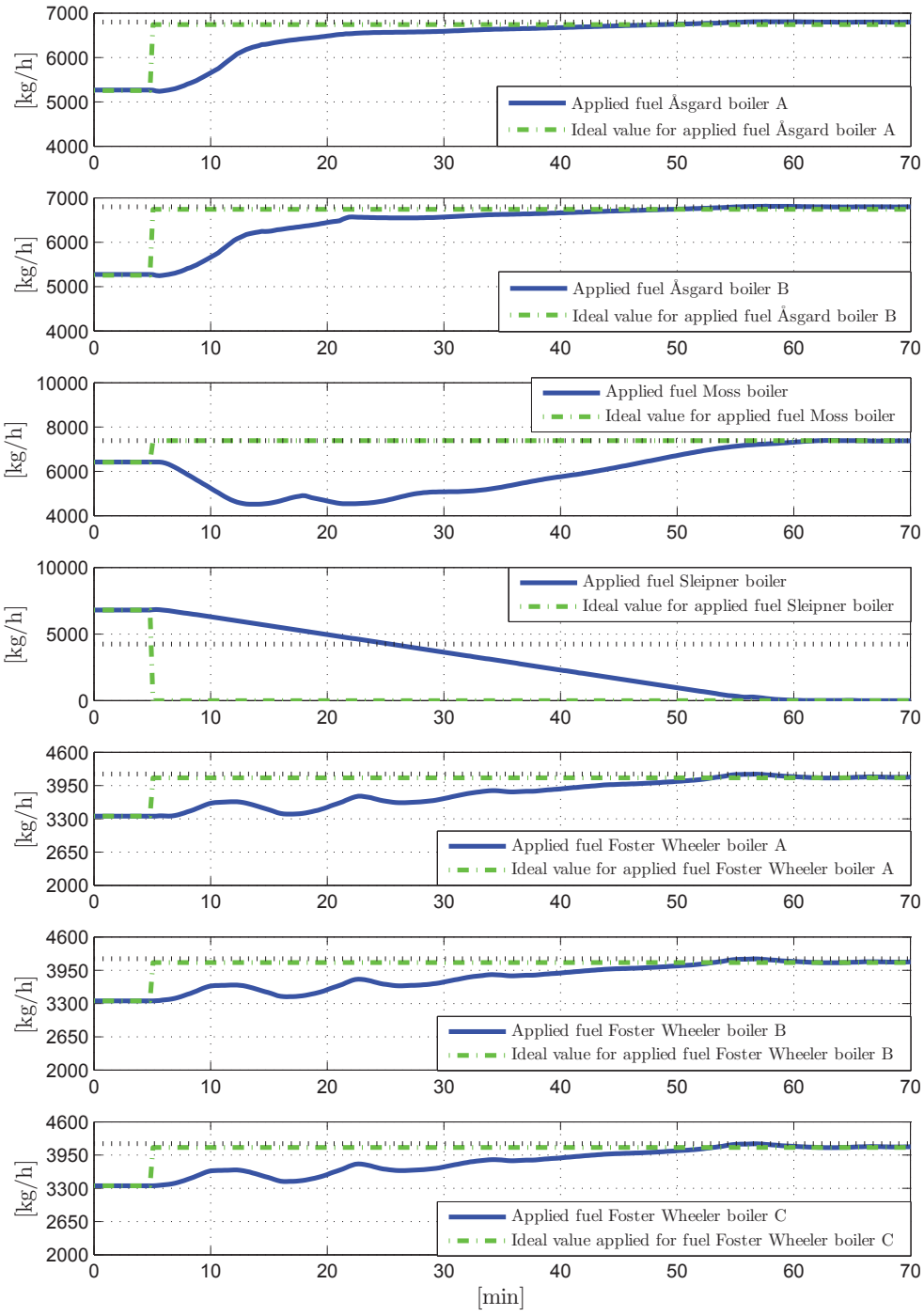

Figure 7.17: Case V: Fuel consumption for each boiler for strictly economical optimization. The black lines are the closest limit for each of the boilers, respectively.

7.3.3 Case VI: Optimization potential

In this case, both the conservative and the strictly economical optimization strategies were performed for a year of real plant data in order to demonstrate the potential of incorporating the RTO optimizer. The optimizations were carried out with a frequency equivalent to four hours and the results are shown in Figure 7.18.

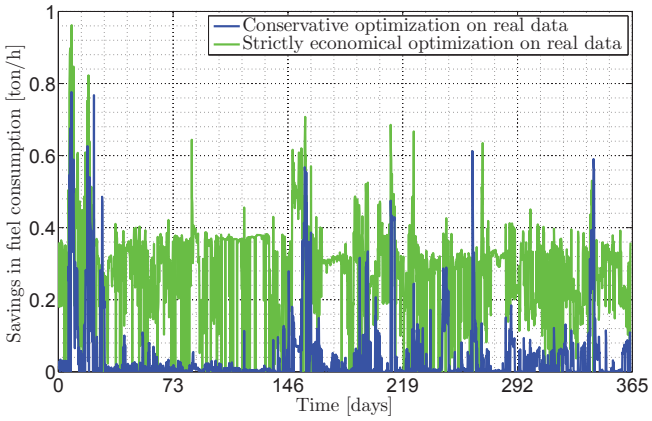

Figure 7.18: Case VI: Potential fuel savings for both optimization strategies.

The total fuel savings are 380,390 $[kg/year]$ and 2,425,700 $[kg/year]$ for the conservative and strictly economical optimization strategies, respectively. Given the total fuel savings and todays gas prices of 2.26 $[\frac{NOK}{Sm^3}]$ (Statoil, 2013.04.30), the fuel savings in $[NOK/year]$ are found using the ideal gas law with standard conditions, introduced in Section 3.1.2, and multiply this with the gas price. The savings in CO_2 emissions are found by extracting the mole fraction of the combustible parts of the fuel and multiplying this with the ratio of the molecular weight of CO_2 to the molecular weight of the combustible parts of the fuel. The composition of the fuel is presented in Table 6.1 and the savings for both optimization strategies are listed in Table 7.6. According to EPA (2008), the average annual CO_2 emission for passenger cars are approximately 4,416 $[kg]$. Thus, the reductions in CO_2 emissions are equivalent to approximately the average annual CO_2 emissions for 468 and 1,857 passenger cars, respectively.

The worst possible disturbance for each of the optimization samples are that the heaviest loaded boiler[1] trips. The average magnitude of the worst possible disturbance is found to be equal to a steam loss of 97,700 $[kg/h]$.

Table 7.6: Case VI: Real optimization data.

Type of optimization	Fuel savings	CO_2 savings
Conservative optimization	1,152,000 $[NOK/year]$	1,186,402 $[kg/year]$
Strictly economical optimization	7,346,200 $[NOK/year]$	8,203,232 $[kg/year]$

[1] A boilers load is the present steam production of that boiler.

7.3.4 Case VII: Optimization sensitivity

In this case, the robustness against model errors for both the optimization methods were examined by introducing errors in the optimization models, that is the thermal efficiency functions. The thermal efficiency of the Åsgard boilers were reduced by 20 %, the Foster Wheeler boilers were increased by 5 % and the Moss boiler was reduced by 5 %. The optimizations were performed for the steam delivery network at the steady-state nominal operating point 2, listed in Table B.2 in Appendix B on page 113. The optimization results with these model errors are shown in figures 7.19a and 7.19b for the conservative and strictly economical optimization strategies, respectively. This optimization, without model errors, were performed in Case V and the results are shown in figures 7.13a and 7.13b on page 77 for the conservative and strictly economical optimization strategies, respectively. The initial and optimized fuel consumption with and without model errors from both optimizations are listed in tables 7.7 and 7.8 for the conservative and strictly economical optimization strategies, respectively.

The common header pressure responses are compared with the equivalent optimization strategies without model errors and are presented in figures 7.20a and 7.20b for the conservative and strictly economical optimization strategies, respectively. A similar comparison is done for the total fuel consumption, which is shown in figures 7.21a and 7.21b for the conservative and strictly economical optimization strategies, respectability. The fuel consumption for each of the boilers is shown in figures 7.22 and 7.23 for the conservative and strictly economical optimization strategies, respectively.

The simulations were conducted for a time period equal to 70 minutes. The conservative optimization result led to a reduction in fuel consumption for the Åsgard boilers and the Sleipner boiler and increased fuel consumption for the remaining boilers. The strictly economical optimization result found a solution which led to a shutdown of Åsgard boiler B, while the remaining boilers experienced increased fuel consumption. The maximum setpoint deviations were approximately 0.10 $[bar]$ and 0.15 $[bar]$ and the fuel savings were approximately 350 $[kg/h]$ and 112 $[kg/h]$ for the conservative and strictly economical optimization strategies with model errors, respectively.

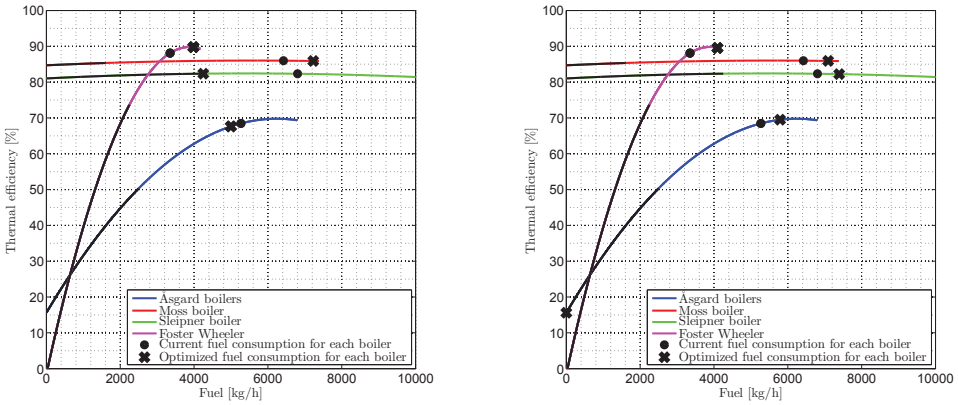

(a) Conservative optimization. **(b)** Strictly economical optimization.

Figure 7.19: Case VII: Optimization results with model errors.

Table 7.7: Case VII: Optimization data using conservative optimization.

Boiler	Initial fuel consumption	Conservative optimization	
		Optimal fuel consumption	Optimal fuel consumption with model errors
Åsgard A	5265.90 $[kg/h]$	6082.20 $[kg/h]$	4999.50 $[kg/h]$
Åsgard B	5272.40 $[kg/h]$	6082.20 $[kg/h]$	4999.50 $[kg/h]$
Moss	6422.40 $[kg/h]$	5641.90 $[kg/h]$	7228.20 $[kg/h]$
Sleipner	6804.00 $[kg/h]$	4250.00 $[kg/h]$	4250.00 $[kg/h]$
Foster Wheeler A	3350.00 $[kg/h]$	3765.20 $[kg/h]$	3982.20 $[kg/h]$
Foster Wheeler B	3350.00 $[kg/h]$	3765.20 $[kg/h]$	3892.20 $[kg/h]$
Foster Wheeler C	3350.00 $[kg/h]$	3765.20 $[kg/h]$	3892.20 $[kg/h]$
Total fuel consumption	33,814.7 $[kg/h]$	33,351.9 $[kg/h]$	33,423.8 $[kg/h]$

Table 7.8: Case VII: Optimization data using strictly economical optimization.

Boiler	Initial fuel consumption	Strictly economical optimization	
		Optimal fuel consumption	Optimal fuel consumption with model errors
Åsgard A	5265.90 $[kg/h]$	6744.60 $[kg/h]$	5790.60 $[kg/h]$
Åsgard B	5272.40 $[kg/h]$	6744.60 $[kg/h]$	0 $[kg/h]$
Moss	6422.40 $[kg/h]$	7385.00 $[kg/h]$	7092.50 $[kg/h]$
Sleipner	6804.00 $[kg/h]$	0 $[kg/h]$	7390.70 $[kg/h]$
Foster Wheeler A	3350.00 $[kg/h]$	4099.40 $[kg/h]$	4094.10 $[kg/h]$
Foster Wheeler B	3350.00 $[kg/h]$	4099.40 $[kg/h]$	4094.10 $[kg/h]$
Foster Wheeler C	3350.00 $[kg/h]$	4099.40 $[kg/h]$	4094.10 $[kg/h]$
Total fuel consumption	33,814.7 $[kg/h]$	33,172. $[kg/h]$	32,556.1 $[kg/h]$

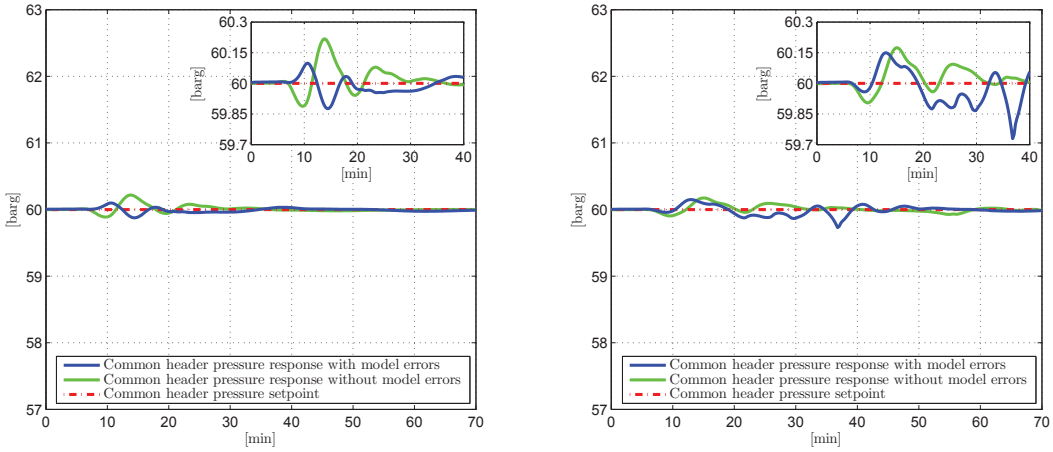

(a) Common header pressure response with conservative optimization.

(b) Common header pressure response with strictly economical optimization.

Figure 7.20: Case VII: Common header pressures for both optimization strategies.

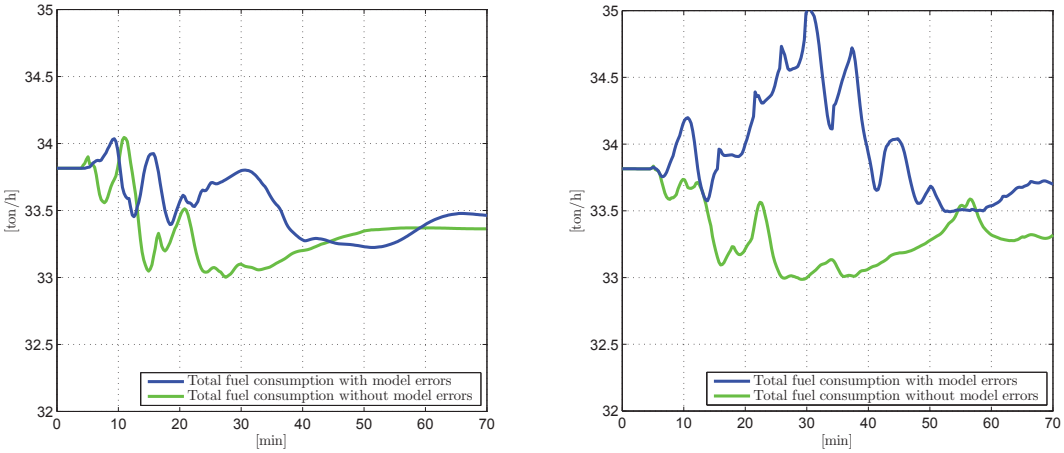

(a) Conservative optimization.

(b) Strictly economical optimization.

Figure 7.21: Case VII: Total fuel consumption for both optimization strategies.

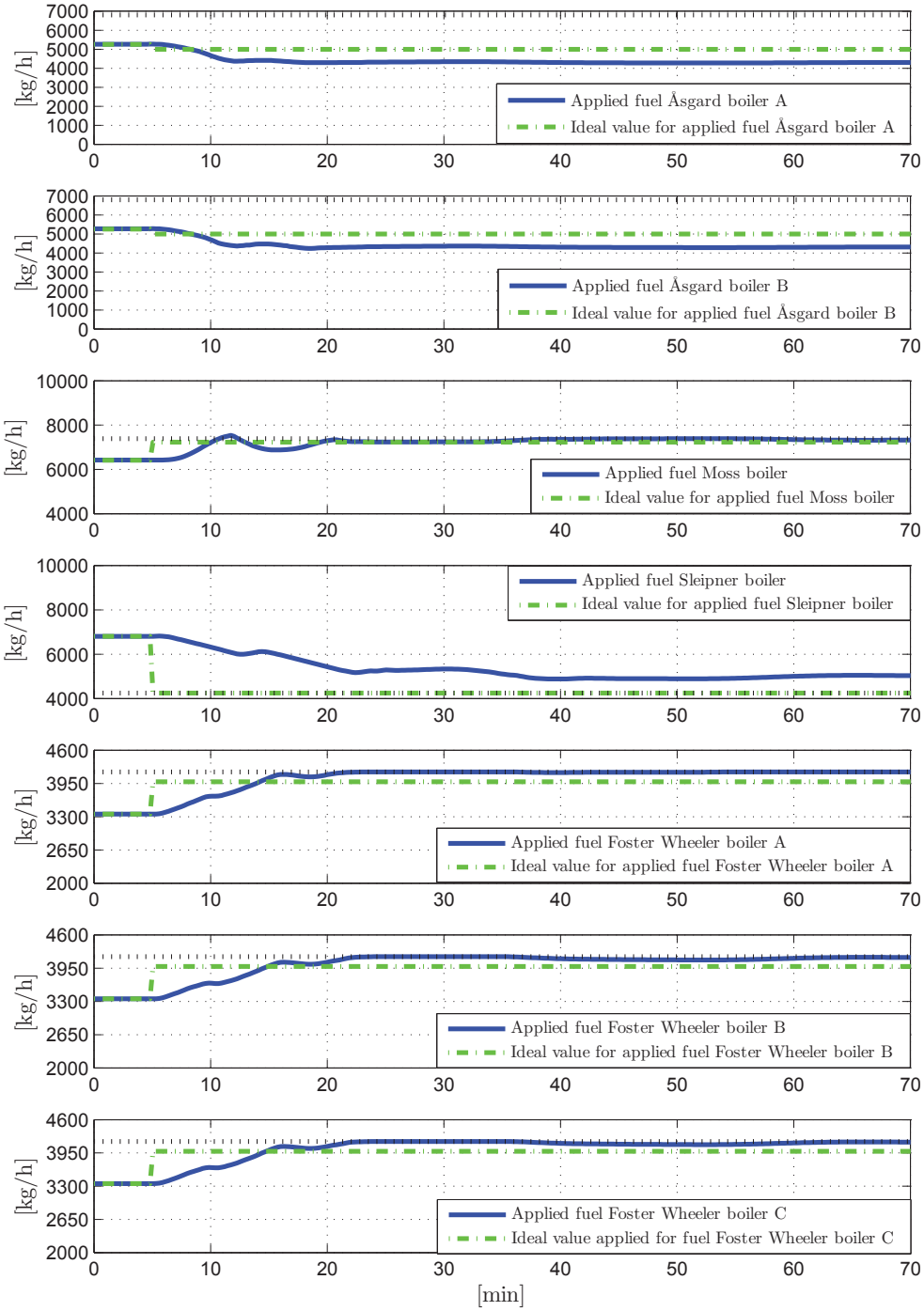

Figure 7.22: Case VII: Fuel consumption for the boilers for the conservative optimization strategy. The black lines are the closest fuel limit for each boiler correspondingly.

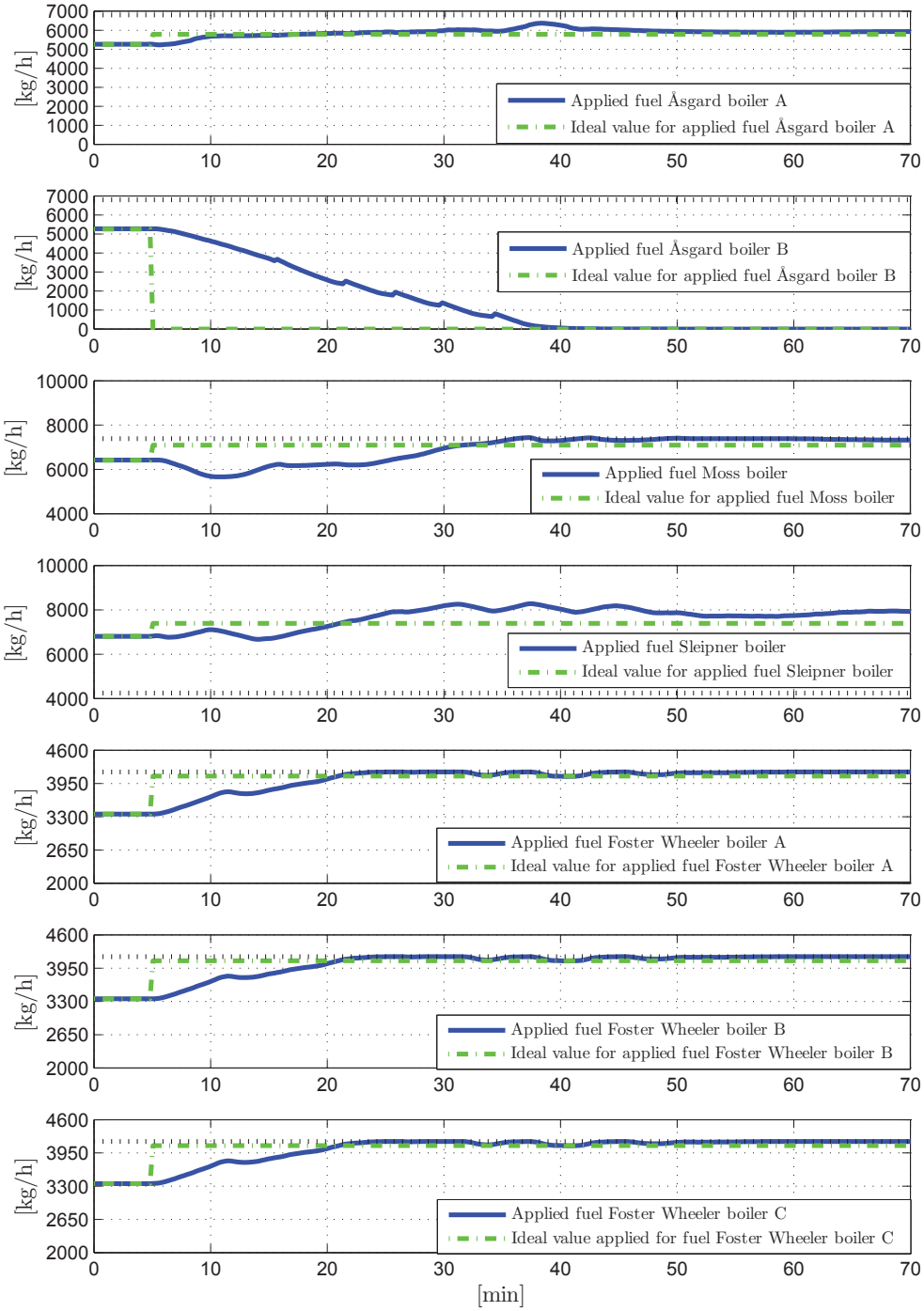

Figure 7.23: Case VII: Fuel consumption for the boilers for the strictly economical optimization strategy. The black lines are the closest fuel limit for each boiler correspondingly.

7.3.5 Case VIII: Optimization robustness

This final case is an extension of Case V. The newly optimized steam production of the steam delivery network experiences a boiler trip after the optimization results for both control strategies are reached. In order to simulate a worst case scenario, the heaviest loaded boiler is chosen to trip[2]. The Åsgard boilers have the largest load and hence, Åsgard boiler A is selected to trip. The trip causes a loss in steam production approximately equivalent to 89,000 $[kg/h]$ and 97,000 $[kg/h]$ for the conservative and strictly economical optimization strategies, respectively.

The common header pressure responses are shown in figures 7.24a and 7.24b and the fuel consumption for each boiler are shown in figures 7.25 and 7.26 for the conservative and strictly economical optimization strategies, respectively. The total fuel consumptions are shown in figures A.2a and A.2b in Appendix A on page 109 for the conservative and strictly economical optimization strategies, respectively.

The simulations were performed for a time period equivalent to 70 minutes. The maximum setpoint deviations were approximately 10 $[bar]$ and 32 $[bar]$ for the conservative and strictly economical optimization strategies, respectively. Since the strictly economical optimization strategy failed in maintaining a constant common header pressure, only the reduction in fuel consumption as the consequence of the boiler trip is calculated for the conservative optimization strategy. The reduction was approximately equal to 241 $[kg/h]$.

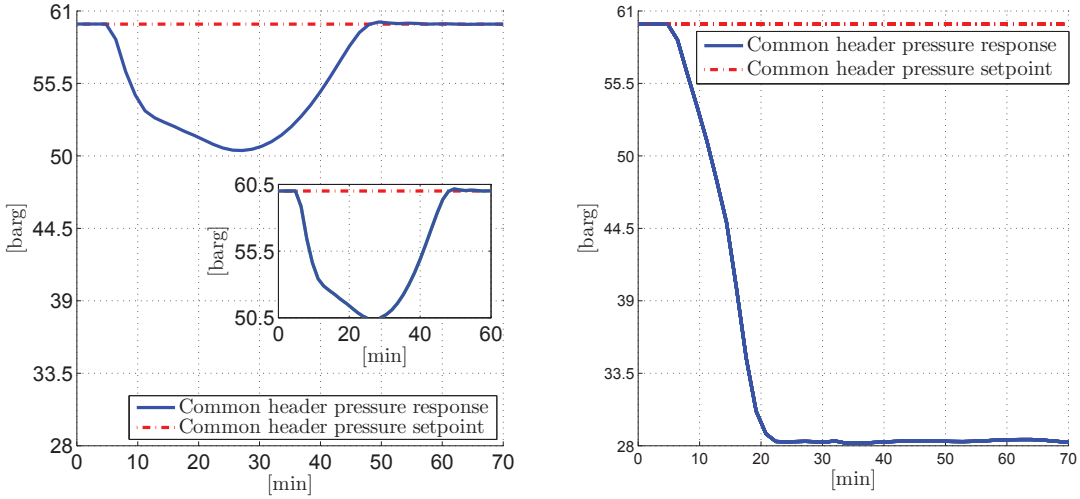

(a) Common header pressure response after conservative optimization.

(b) Common header pressure response after strictly economical optimization.

Figure 7.24: Case VIII: Common header pressures for both optimization strategies.

[2]A boilers load is the present steam production of that boiler.

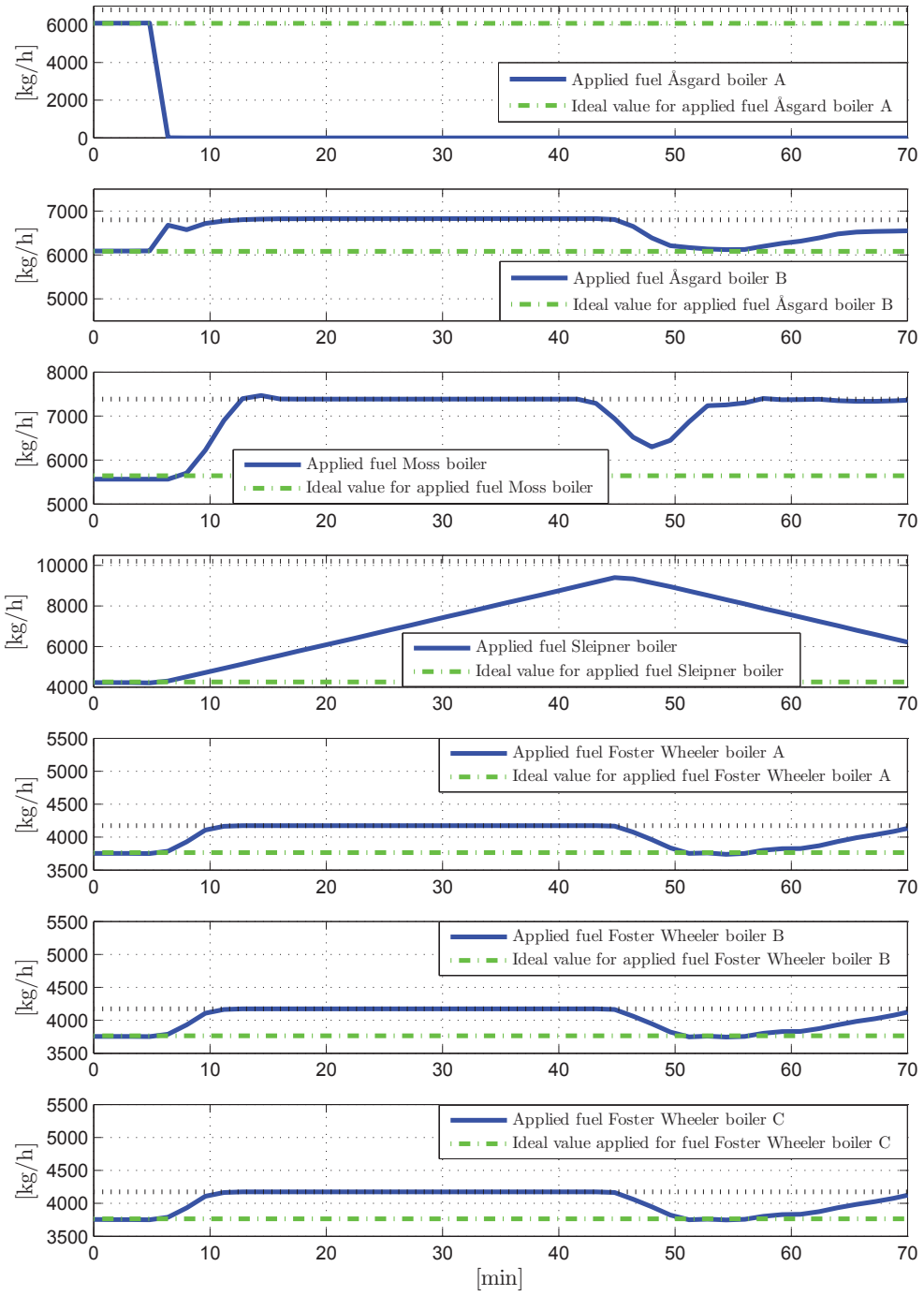

Figure 7.25: Case VIII: Fuel consumption for the boilers for the conservative optimization strategy. The black lines are the closest fuel limit for each boiler correspondingly.

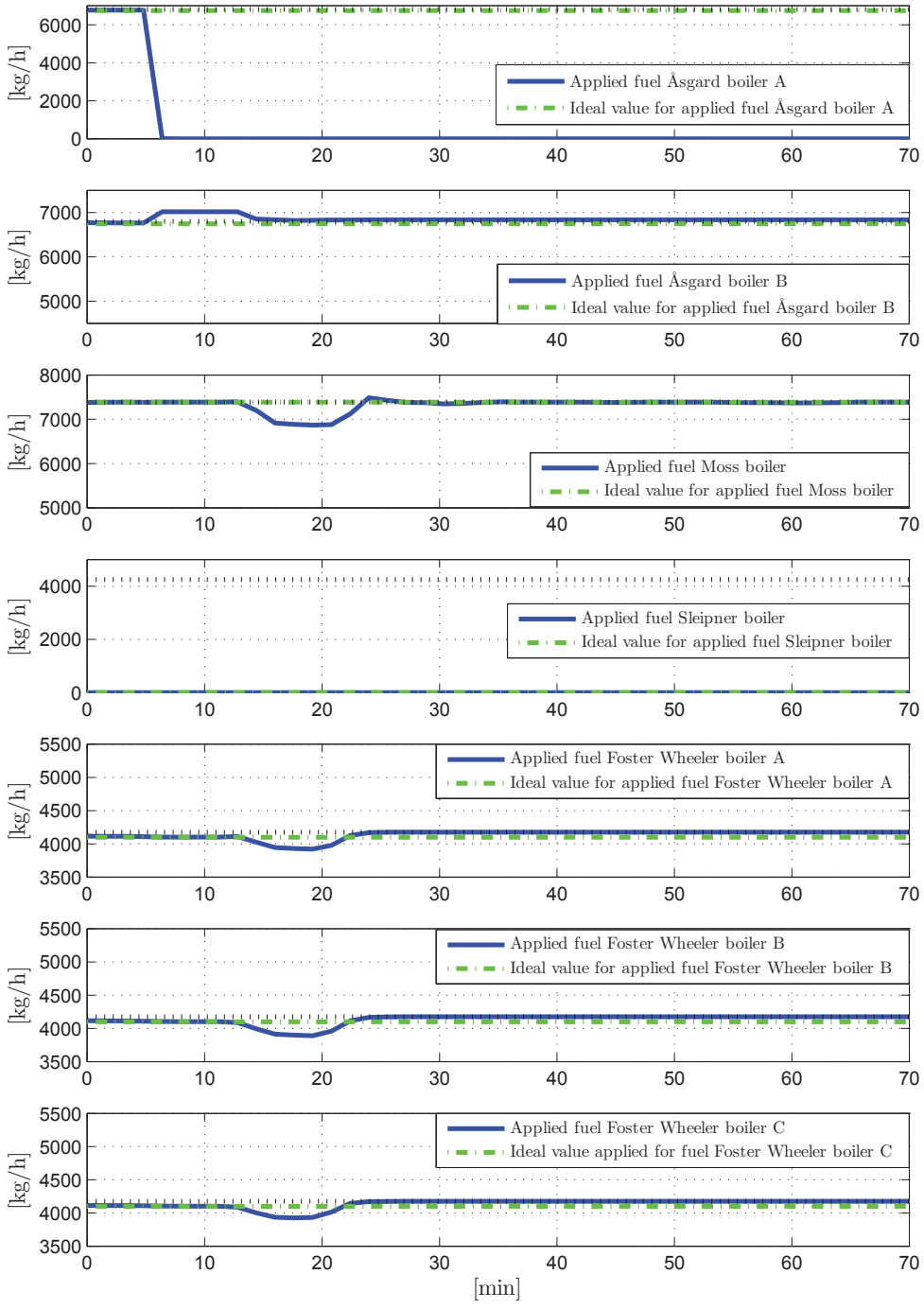

Figure 7.26: Case VIII: Fuel consumption for the boilers for the strictly economical optimization strategy. The black lines are the closest fuel limit for each boiler correspondingly.

7.4 Summary of Optimization Performance

In this group, the optimal fuel consumptions, calculated by the optimization strategies, are passed down to the respective boilers as ideal values. Given these, the boilers change their fuel consumption, so that the steam delivery network is able to produce enough steam to cover the constant steam consumption at the economical optimum. This is done in separate simulations for each of the optimization strategies, respectively. Furthermore, the applied fuel consumptions determine the amount of heat used to evaporate the condensate and thus, the steam production of a boiler.

In Case IV, the conservative optimization strategy is used to optimize the steam production for a constant steam consumption. The result of the conservative optimization strategy, presented in Figure 7.10, finds it optimal to produce steam at maximum efficiency for the Foster Wheeler boilers and Åsgard boilers, and at minimum fuel consumption for the Sleipner boiler, as this boiler has the lowest efficiency. The remaining steam consumption, not covered by the other boilers, is left for the Moss boiler to cover, as this boiler offers the cheapest production of steam without lying in the optimum. This is because the Moss boiler has the highest efficiency regardless of applied fuel consumption. Furthermore, the fuel consumption for each of the boilers, presented in Figure 7.12, shows that all the boilers arrive at their optimal ideal values. The fuel consumption for the Moss and Sleipner boilers decreases continuously towards their ideal values, and as a result of this, the fuel consumption for the remaining boilers increases towards their ideal values to compensate for the reduction in steam production. Because of this behavior, the common header pressure fluctuates around the setpoint, as shown in Figure 7.11a.

In Case V, the two different optimization strategies are used to optimize the steam production for a constant steam consumption in two separate simulations. The result of the conservative optimization strategy, presented in Figure 7.13a, arrives at a solution in which the Foster Wheeler boilers and the Åsgard boilers produce steam at maximum efficiency, and the Sleipner boiler produce steam at minimum fuel consumption, as this boiler has the lowest efficiency. Again, the Moss boiler is used to level the remaining steam consumption, not covered by the other boilers, as this boiler offers the cheapest production of steam without lying at the optimum. This is due to the same reasons as above. Moreover, the fuel consumption for each of the boilers, presented in Figure 7.16, shows that all the boilers reaches their ideal values. The fuel consumption for the Sleipner boiler decreases continuously towards its ideal value, and as the steam production decreases, the fuel consumption for the other boilers moves towards their ideal values to cover this loss. This behavior causes the common header to fluctuate around its setpoint, as shown in Figure 7.14a. The result of the strictly economical optimization strategy, shown in Figure 7.13b, finds it optimal to shut down the boiler with the lowest efficiency, which leads to steam production at maximum fuel consumption, that is at maximum capacity, for the remaining boilers. This is shown in Figure 7.17. The Sleipner boiler is shut down because the required steam production is cheaper produced by only utilizing the other boilers. Furthermore,

the fuel consumption for each of the boilers, presented in Figure 7.17, shows that all the boilers arrive at their optimal ideal values. Again, the fuel consumption for the Sleipner boiler decreases continuously towards zero. Hence, the fuel consumption for the other boilers moves towards their ideal values to level the reduction in steam production. As a consequence of this behavior, the common header pressure fluctuates around its setpoint, as observed in Figure 7.14b.

In Case VI, the optimization potential for the conservative and the strictly economical optimization strategies are calculated using real data. The fuel savings, presented in Figure 7.18, show that the conservative optimization strategy rarely saves more than 100 $[kg/h]$, but that the strictly economical optimization strategy often saves up to 400 $[kg/h]$.

Case VII studies the two optimization strategies sensitivity against model errors in two separate simulations. The result of the conservative optimization strategy, presented in Figure 7.19a, arrives at a solution in which steam is produced at maximum fuel consumption for the Moss boiler and Foster Wheeler boilers, and at minimum fuel consumption for the Sleipner boiler. The reaming steam consumption, not covered by these boilers, is left for the Åsgard boilers to cover. The optimization strategy arrives at this solution because producing steam at higher capacity for the Sleipner boiler would force the Åsgard boilers to produce steam at lower efficiency, which would become too expensive. The fuel consumption for each of the boilers, presented in Figure 7.22, shows that all the boilers, except of the Moss boiler, misses their ideal values. This is as expected since the optimization models of these boilers contain errors. Furthermore, the common header pressure fluctuates as a result of the changes in fuel consumption for each of the boiler, as shown in Figure 7.20a. The result of the strictly economical optimization strategy, shown in Figure 7.19b, finds it optimal to turn off one of the boilers with the lowest efficiency. Hence, the Åsgard boiler B is turned off, while the Åsgard boiler A is selected to produce steam at maximum efficiency due to its low efficiency. The Foster Wheeler boilers and the Moss boiler are set to produce steam at near maximum fuel consumption, while the remaining steam consumption, not covered by the other boilers, is left for the Sleipner boiler to cover. The fuel consumption for each of the boilers, presented in Figure 7.23, shows that all, but the Moss boiler, misses their ideal values. This is as expected due to the errors within these models. Furthermore, the common header pressure fluctuates as a consequence of the changes in fuel consumption for each of the boilers, as shown in Figure 7.20b. Despite of these model errors, both optimization strategies manages to save fuel. However, the savings are somewhat smaller than for the case without model errors, as seen from figures 7.21a and 7.21b for the conservative and strictly economical optimization strategies, respectively.

In the final case, optimization robustness against a boiler trip is studied for the optimal operating point obtained from the conservative and strictly economical optimization strategies in Case V, respectively. In order to examine the worst possible scenario, the heaviest loaded boiler trips, in this case the Åsgard boiler A. The steam loss causes a drop in common header pressure, as seen in figures 7.24a and 7.24b for the conservative and strictly economical optimization strategies re-

spectively. This drop forces the active boilers to increase their combustion above their ideal values, as seen in figures 7.25 and 7.26 for the conservative and strictly economical optimization strategies, respectively. For the conservative optimization strategy, all the boilers but the Sleipner boiler quickly reaches saturation, which leads to a slow recovery of the common header pressure. For the strictly economical optimization strategy, the steam production capacity of the steam delivery network is destroyed as all the boilers reaches saturation. Therefore, the common header pressure drops until enough steam consumers have fallen off and the steam production levels the steam consumption.

The fluctuations in common header pressure and fuel consumption for each of the boilers in Case IV, V and VII deserve an explanation. Since the models applied by the MPC controller are not perfect, the common header pressure experiences some minor fluctuations. In order to maintain a common header pressure, the MPC controller slightly adjusts the fuel consumption for each of the boilers. These changes are observed as the fluctuations in the fuel consumption and are largest for the boilers closest to their ideal values. Moreover, in some of the simulations, the Moss boiler moves away from its ideal value in the beginning of the simulation. This is mainly because the Moss boiler has the lowest penalty for ideal value deviations. Ergo, when there is a lack of degrees of freedom, the Moss boiler will be the first boiler not to consider its ideal value deviation.

The tables presented in Case IV, V and VII shows the result obtained by solving the optimization problem and not the actual immediate fuel savings obtained by implementing the solution into the simulator. The actual immediate fuel savings and the fuel savings indicated by the solution of the optimization problem differ because the thermal efficiency functions are imperfect. However, the difference are small and thus, neglectable.

Chapter 8

Discussion

In this chapter, the results from the previous chapter are discussed. The chapter is divided into two parts. The first part focuses on the comparison between the MPC controller and the PI control structure, while the following part focuses on the performance and issues when using a RTO optimizer.

8.1 MPC Performance Discussion

The main objective of this thesis was to develop an MPC controller for stable and efficient operation of the steam delivery network, while ensuring safe operation. Therefore, the objective of the MPC performance studies was to prove improved stabilization and performance for various disturbances when using an MPC controller. The MPC performance was evaluated by exposing the steam delivery network for three different levels of disturbances, according to their severity:

- small disturbances, e.g. setpoint changes.
- intermediate disturbances, e.g. lost or accumulated steam in the common header.
- large disturbances, e.g. boiler trips.

The general observations, when comparing the simulations with and without MPC control for various disturbances, were significantly faster and tighter response for small and intermediate disturbances. In the case of a large disturbance, only the MPC controller was able to recover from the disturbance.

There are several reasons for the faster and tighter response achieved when using the MPC controller. The main reason is the MPC controller's ability to utilize all the boilers, and level the load over these boilers. The load is leveled according to the boilers rate of change limitations and their ideal value deviation penalty. Another contributing factor is the MPC controller's ability to optimize the future response towards setpoint using the step response models of the boilers. However, it should be pointed out that the large response difference observed would

probably be reduced if the PI controllers, in the PI control structure, were tuned more aggressively.

The PI control structure, currently used at the plant, is not able to handle large disturbances and is therefore continuously supervised by operators. Therefore, in the case of large disturbances, the operators would shut down some of the steam consumers and adjust the steam production on the other boilers. This is an expensive procedure and the hope is that the MPC controller will be able to handle such disturbances without experiencing a too large common header pressure deviation.

8.1.1 Small disturbances

In Case I, the two control strategies were compared for the response of a setpoint change in the common header pressure. Both control strategies managed to increase the common header pressure without breaking any constraints, with a response time[1] of approximately 20 $[min]$ and 95 $[min]$, for the simulations with and without MPC control, respectively. The results show that the MPC controller achieves faster and tighter control than the PI control structure. The PI control structure experienced significant fluctuations around the setpoint, while the MPC controller only experienced a small overshoot before settling. This overshoot is somewhat larger than the maximum overshoot suggested by Skogestad (2002). However, the MPC controller is preferred to be this aggressive, as the setpoint should quickly be reached. Furthermore, the MPC controller achieved load leveling by distributing the load over the boilers, while the PI control structure did not achieve load leveling, as it only changed the load on Åsgard boiler A

8.1.2 Intermediate disturbances

In Case II, the two control strategies were compared for a change in steam consumption. Again, both control strategies managed to restore the common header pressure without breaking any constraints, with a response time of approximately 40 $[min]$ and 120 $[min]$ for the simulations with and without MPC control, respectively. The results clearly show that the MPC controller achieves much faster and tighter control of the common header pressure, as it only experienced a small common header pressure deviation. However, the PI control structure experienced a huge common header pressure deviation for a much longer time than the MPC controller. Again, load leveling was achieved by the MPC controllers, as it distributed the load over the boilers. The PI control structure did not achieve load leveling, as the Åsgard boiler A was the only boiler allowed to change its steam production.

8.1.3 Large disturbances

In Case III, the response of the two control strategies was compared for a boiler trip of the Foster Wheeler boiler A. In this case, only the MPC controller was able

[1] The response time is the time elapsed before the controlled variable settles.

to restore the common header pressure with a response time of approximately 30 $[min]$, while the PI control structure failed to restore the common header pressure. This happened because the MPC controller was able to distribute the required steam increase over all the active boilers, while the PI control structure placed the entire load on the Åsgard boiler A. The steam production capacity of the PI control structure became destroyed, as the required steam capacity exceed that of the Åsgard boiler A. Moreover, the steam loss was noticed faster by the MPC controller due to the feedforward link from the combustion controller for the Foster Wheeler boiler A. Hence, the MPC controller was able to counteract the disturbance faster than the PI control structure.

8.2 RTO Performance Discussion

The secondary objective of this thesis was to achieve economical optimal operation by including a RTO optimizer, on top of the MPC controller, to utilize the available degrees of freedom. Therefore, the purpose of the RTO optimizer studies was to illustrate the possible fuel savings achieved by optimizing the steam production, and to illustrate the issues that arise when utilizing two different optimization strategies. The two studied optimization strategies are named conservative and strictly economical optimization, both previously explained. The RTO performance studies are divided into two subgroups, according to their focus of attention. In the first subgroup, the focus is directed towards the possible fuel savings achieved by optimization, and this group is based on the results from cases IV, V and VI. The second subgroup focus on the robustness issues that arise when using these optimization strategies, and is based on the results from cases VII and VIII.

A general observation, when performing optimization without model errors, is that the optimization strategies always manage to save fuel, and that the boilers always reach their respective ideal values. This suggests that the optimization strategies works and that the optimization models are fairly accurate. However, the robustness of the steam delivery network is observed to decrease with the strictly economical optimization strategy. Furthermore, the thermal efficiency functions of the boilers without cross-limiting combustion control are much more varying than for those boilers with cross-limiting combustion control, as explained in Section 6.2. Therefore, is tempting to think that by introducing the cross-limiting control structure for the boilers without cross-limiting combustion control, the thermal efficiency functions would become less varying and the boilers would produce steam cheaper at lower fuel consumption. However, as explained in Section 2.4.1, the ratio control scheme with and without energy controllers are employed by the boilers with a separate connection to a gas turbine because all the available turbine exhaust gases have to be utilized in order to not waste the energy already applied to the turbine exhaust gases. Hence, the replacement of these control structures is a costly investment, as the turbine exhaust gases will not be fully utilized.

8.2.1 Savings discussions

The immediate fuel savings achieved when performing optimization is illustrated in cases IV and V. In Case IV, the performance and the fuel savings are illustrated for the conservative optimization strategy, and in Case V, the performance and the fuel savings are illustrated for both the conservative and the strictly economical optimization strategies. The conservative optimization strategy achieves a significant fuel saving in both cases, which is only slightly smaller than that achieved when using strictly economical optimization. Moreover, the conservative optimization strategy preserves its steam production capacity by keeping all the boilers active, while the strictly economical optimization strategy reduces its steam production capacity by shutting down a boiler. However, the response time of both optimization strategies gets reduced, as both almost maximizes the steam production of every boiler, expect of the Sleipner boiler which minimizes its steam production. Thus, the Sleipner boiler is left with the bulk of available steam production capacity. Furthermore, for both optimization strategies, the fluctuations around setpoint were smaller than that of a small disturbance and thus, not of any concern. Hence, the additional fuel savings, achieved by strictly economical optimization, are expensively paid for by losing the capacity of the biggest boiler, that is the Sleipner boiler.

In Case VI, the optimization potential of both optimization strategies was studied for a year of real plant data. The results show that the strictly economical optimization strategy achieves on average six times larger fuel savings and CO_2 savings than the conservative optimization strategy. Furthermore, the average worst case disturbance, that is the trip of the heaviest load boiler, is found to be approximately 97,700 $[kg/h]$. This is a large disturbance and the strictly economical optimization strategy would struggle to recover from such a disturbance, if at all. Again, this is the price for the larger fuel savings obtained by the strictly economical optimization strategy. Moreover, it is noteworthy to note that the models obtained for the plant are contaminated by noise, as explained in Section 6.2. Hence, the models are imperfect, and as shown in the subsequent section, there is probably a greater savings potential by perfecting these models.

8.2.2 Robustness discussion

In Case VII, the sensitivity against model errors in the thermal efficiency function are studied for both optimization strategies and compared to the similar Case V without model errors. The results show that the conservative optimization strategy manages to save a significant amount of fuel, but slightly less than that achieved without model errors. However, the strictly economical optimization strategy hardly manages to save any fuel. Again, the steam production capacity is unchanged for the conservative optimization strategy and reduced for the strictly economical optimization strategy. Furthermore, the response time is reduced for both optimization strategies, as they maximize the steam production of every boiler, except of the Sleipner and Åsgard boilers. For the strictly economical optimization strategy, only the Sleipner boiler is able to increase its steam pro-

duction. The fluctuations around setpoint are observed as minor and for of both optimization strategies. Thus, the conservative optimization strategy appears to be superior to the strictly economical optimization strategy in this case.

In Case VII, the optimal operating point calculated by the optimization strategies in Case V, is exposed to a worst case disturbance, that is the trip of the heaviest loaded boiler. The results show that the optimal operating point, calculated by the strictly economical optimization strategy, failed in handling the boiler trip. Despite of the load leveling performed by the MPC controller, the remaining steam production capacity was too small to cover the loss in steam production. Hence, the MPC controller lost control over the common header pressure. However, the optimal operating point, calculated by the conservative optimization strategy, managed to recover from the worst case disturbance. The load leveling performed by the MPC controller resulted in a response time of approximately 50 $[min]$ with still some remaining capacity on the Sleipner boiler. Furthermore, as a consequence of the boiler trip, a large saving in fuel consumption was achieved.

Chapter 9

Conclusions and Further Work

In this last chapter, a conclusion based on the previously presented results and discussions are drawn, followed by some suggestions for future work.

9.1 Conclusions

The main objective of this thesis was to achieve stable and efficient operation of the steam delivery network, while ensuring safe operation. This was achieved and illustrated through development and testing of an MPC controller for the steam delivery network in the D-SPICE simulator. The testing showed significantly improved performance for all types of disturbances, even for the cases where the currently employed PI control structure failed. The setpoint deviations were substantially reduced and the response much faster due to the load leveling and optimized response provided by the MPC controller. Furthermore, the steam production capacity was preserved by the MPC controller due to the load leveling.

The secondary objective of this thesis was to achieve economical optimal steam production by optimizing the fuel consumption, for the a constant steam demand, and utilize the available degrees of freedom to reach optimal operation. This was achieved, and the potential illustrated through development and testing of a RTO optimizer, placed on top of the MPC controller for the steam delivery network in the D-SPICE simulator. The testing showed a significant potential for both fuel and CO_2 savings using two different optimization strategies, that is the conservative and strictly economical optimization strategies. The savings were observed to be slightly larger for the strictly economical optimization strategy. However, only the conservative optimization strategy proved to be robust against model errors and worst case disturbances.

Therefore, the conclusion of this thesis is that an MPC controller clearly improves both the stability and performance of a steam delivery network, while ensuring safe operation. Furthermore, a significant reduction in both fuel consumption

and CO_2 emissions are achievable by introducing a RTO optimizer on top of the MPC controller. The results clearly suggest the implementation of the conservative optimization strategy, as this strategy optimizes the performance without affecting the robustness of the steam delivery network. Moreover, the proposed idea of improving the thermal efficiency for the boilers with a separate connection to a gas turbine turned out not to be an option. The idea was to replace the ratio control scheme with the cross-limiting control scheme for the combustion process, but this would result in waste of the energy brought with the turbine exhaust gases.

The results presented in this thesis prove the accomplishment of the work description for this thesis. As a closing remark, it should be mentioned that the conclusion drawn in this thesis is solely based on the limited testing performed. This limits the validity of this conclusion and further work is therefore necessary in order to verify the conclusion.

9.2 Further Work

The results for this thesis proved to be satisfactory, but there is still a great possibility of future work. As explained, extensively testing is necessary to further verify the conclusion of this thesis. The testing should cover a larger range of operating points, stretching from low to large steam production for each of the respective boilers, to statistically verify the conclusion of this thesis.

Moreover, as explained in Section 6.2, the simulator models does not completely reflect the models of the real plant, and improvement of the simulator models are recommended for a better validation of both the MPC performance and the optimization potential.

Furthermore, there is a potential for improved performance and increased robustness for both the PI control structure and the MPC controller by a more aggressive tuning of the PI controllers in the PI control structure. This is a huge task and is left as a proposition for future work.

Lastly, it is interestingly to note that there might be a larger potential in reduction of both the fuel consumption and the CO_2 emissions for an extended version the conservative optimization strategy. To reach this potential, the conservative optimization strategy must allow for a boiler shutdown in the cases where the steam production capacity of the steam delivery network exceeds the steam loss of a worst case disturbance. This would require an additional constraint in the RTO optimization problem, and additional testing. Hence, the study of this potential is recommended for further work.

Bibliography

K.J Åström and R.D Bell. Drum-boiler dynamics. *Automatica*, 36(1):363–378, 2000.

Jens G. Balchen and Kenneth I. Mumme. *Process Control: Structures and applications*. Van Nostrand Reinhold Company Inc, 115 Fifth Avenue, New York, NY, USA, 1988.

Jens G. Balchen, Trond Andresen, and Bjarne A. Foss. *Reguleringsteknikk*. Tapir, Trondheim, Norway, 1999.

James J. Downs and Sigurd Skogestad. An industrial and academic perspective on plantwide control. *Annual Reviews in Control*, 1(1):99–110, 2011.

EPA. Average annual emissions and fuel consumption for gasoline-fueled passenger cars and light trucks. Technical report, United States Environmental Protection Agency, 2008.

D-SPICE User Guide. Fantoft, Sandvika, Norway.

Eduardo D. Glandt, Michael T. Kelin, and Thomas F. Edgar. *Optimization of Chemical Processes*. McGraw-Hill, 1221 Avenue of the Americas, New Yrok, NY, USA, 2001.

Svein Olav Hauger. Model predictive control. *NTNU presentation*, pages 1–76, 2012.

Vladimir Havlena and Jiri Findejs. Application of model predictive control to advanced combustion control. *Control Engineering Practice*, 13(1):671–680, 2005.

B.W. Hogg and N.M. El-Rabaie. Multivariable generalized predictive control of a boiler system. *IEEE Transactions on Energy Conversion*, 6(2):282–288, 1991.

Lars Imsland. *Introduction to Model Predictive Control*. NTNU, Trondheim, Norway, 2002.

Torstein Thode Kristoffersen. *Model Predicitve Control of a Steam Delivery Network*. NTNU, Trondheim, Norway, 2012.

S. Lu and B.W. Hogg. Predictive co-ordinated control for power plant steam pressure and power output. *Control Engineering Practice*, 5(1):79–84, 1997.

J. M. Maciejowski. *Predictive Control with Constraints*. Pearson Education Limited, Edinburgh, England, 2002.

Yrjö Majanne. Model predictive pressure control of steam networks. *Control Engineering Practice*, 13(1):1499–1505, 2005.

Michael J. Moran and Howard N. Shapiro. *Fundamentals of Engineering Thermodynamics*. John Wiley & Sons, 111 River Street, Hoboken, NJ, USA, 2010.

Manfred Morari and Jay H. Lee. Model predictive control: past, present and future. *Computers and Chemical Engineering*, 23(1):667–682, 1998.

Jorge Nocedal and Stephen J. Wright. *Numerical Optimization*. Springer, 233 Springer Street, New Yrok, NY, USA, 2003.

Bruce E. Poling, John M. Prausnitz, and John P. O'Connell. *The Properties of Gases and Liquids*. McGraw-Hill, New York, USA, 2001.

J.G. Proakis and D.G. Manolakis. *Digital signal processing: principles algorithms and applications*. Pearson Education, Edinburgh, England, 2007.

S. Joe Qin and Thomas A. Bagwell. A survey of industrial model predictive control technology. *Control Engineering Practice*, 11(1):733–764, 2003.

Regjeringen. Om innenlands bruk av naturgass mv., 2003. URL `http://www.regjeringen.no/nb/dep/oed/dok/regpubl/stmeld/20022003/Stmeld-nr-9-2002-2003-/4/1/1.html?id=328202`.

Sigurd Skogestad. Simple analytic rules for model reduction and pid controller tuning. *Journal of Process Control*, 13(1):291–309, 2002.

Sigurd Skogestad. Control structure design of complete chemical plants. *Computers and Chemical Engineering*, 28(1):219–234, 2004.

Sigurd Skogestad. *Prosessteknikk*. Tapir, Trondheim, Norway, 2009.

Carlos A. Smith and Armando B. Corripio. *Principles and Practice of Automatic Process Control*. John Wiley & Sons, River Street, Hoboken, NJ, USA, 2006.

Statoil. Kårstø processing plant, 2007. URL `http://www.statoil.com/en/OurOperations/TerminalsRefining/ProcessComplexKarsto/Pages/default.aspx`.

Statoil. Gas prices, 2013.04.30. URL `http://entry.statoil.com`.

Stig Strand and Jan Richard Sagli. *MPC in Statoil - Advantages with in-house technology*. Statoil R&D, Process Control, Trondheim, Norway, 2003.

A. Tyssø. Modelling and parameter estimation of a ship boiler. *Automatica*, 17(1): 157–166, 1981.

Hugh D. Young and Roger A. Freedman. *University Physics*. Pearson Education Inc, 1301 Sansome St., San Fransisco, CA 94111, USA, 2008.

Nomenclature

Controller variables and parameters

d**:** Disturbance variable

u**:** Input variable/Manipulated variable

h**:** Output response coefficients

y**:** Output variable

N**:** Prediction horizon

Physical variables

E**:** Energy

h**:** Enthalpy

Q**:** Heat

U**:** Internal energy

KE**:** Kinetic energy

m**:** Mass

M**:** Molar mass

n**:** Number of moles

PE**:** Potential energy

p**:** Pressure

T**:** Temperature

V**:** Volume

W**:** Work

Chemical substances

C**:** Carbon

CO**:** Carbon monoxide

CO_2**:** Carbon dioxide

H**:** Hydrogen

H_2O**:** Hydrogen oxide (water $\leq 100°C \leq$ vapor)

N_2**:** Nitrogen

NO**:** Nitrogen monoxide

NO_2**:** Nitrogen dioxide

O_2**:** Oxygen

SO_2**:** Sulfur dioxide

Abbreviations

AA: Ambient Air

ABD: Allowable Breaking Distance

AVO: Attemperator Valve Opening

CHP: Common Header Pressure

CP: Combustion Pressure

CV: Controlled Variable

D-SPICE: Dynamic Simulator for Process Instrumentation and Control Engineering

DV: Disturbance Variable

EC: Energy Controller

FFC: Fuel Flow Controller

FIR: Finite Impulse Response

HP: High Pressure

HPC: Header Pressure Controller

HPST: High Pressure Steam Temperature

IP: Intermediate Pressure

IV: Ideal Value

LP: Low Pressure

LPG: Liquid Petroleum Gas

MIMO: Multiple-Input-Multiple-Output

MINLP: Mixed Integer Non-Linear Programming

MPC: Model Predictive Control

MV: Manipulated Variable

NGL: Natural Gas Liquids

NLP: Non-Linear Programming

PI: Proportional Integral

RTO: Real Time Optimization

SEPTIC: Statoil Estimation and Prediction Tool for Identification and Control

SISO: Single-Input-Single-Output

SP: Set Point

TEG Turbine Gas Exhaust

QP : Quadratic Problem

Appendix A

Additional Plots

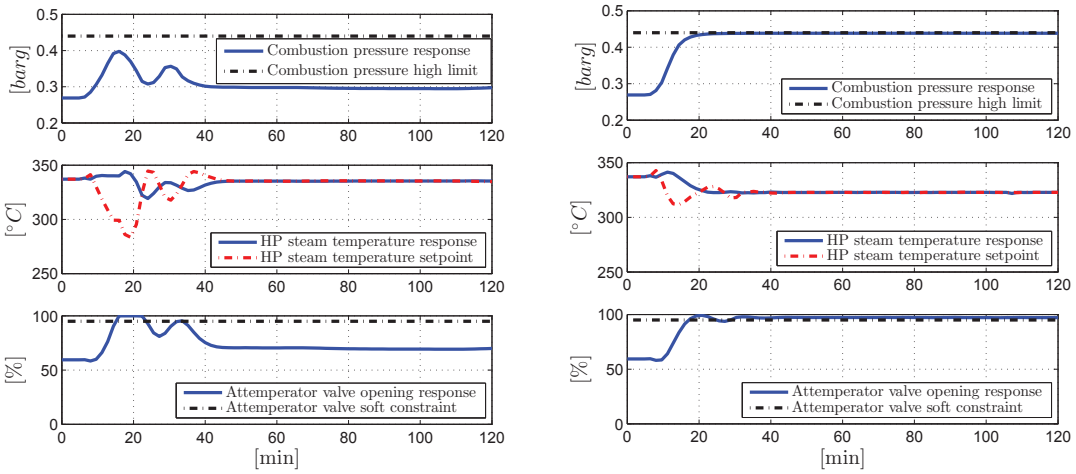

(a) The primary CVs responses with MPC control.

(b) The primary CVs responses with PI control.

Figure A.1: Case III: The primary CVs responses with and without MPC control.

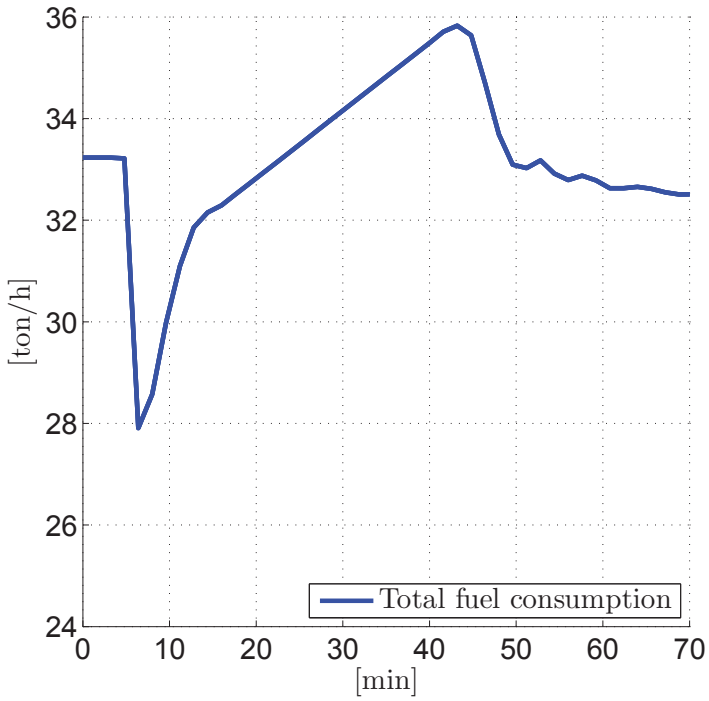

(a) Conservative optimization.

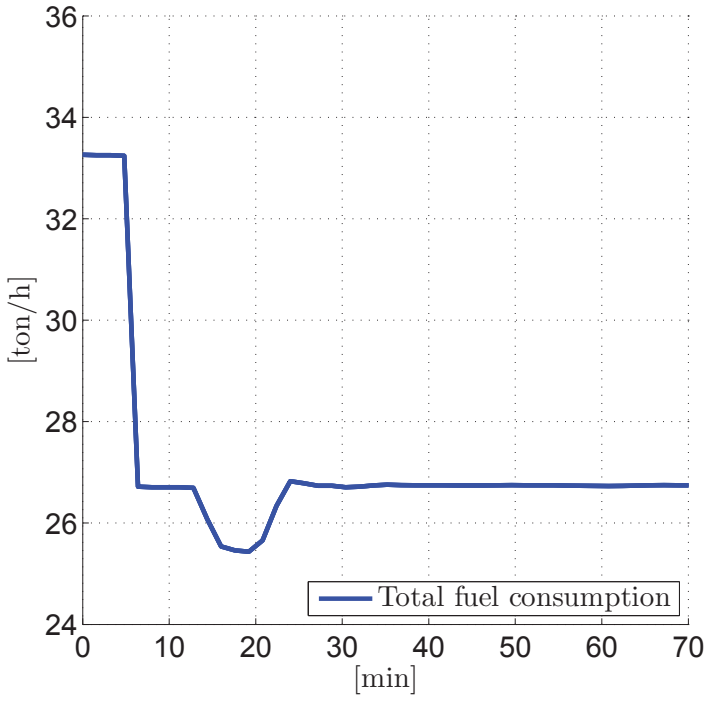

(b) Strictly economical optimization.

Figure A.2: Case VIII: Total fuel consumption for both optimization strategies.

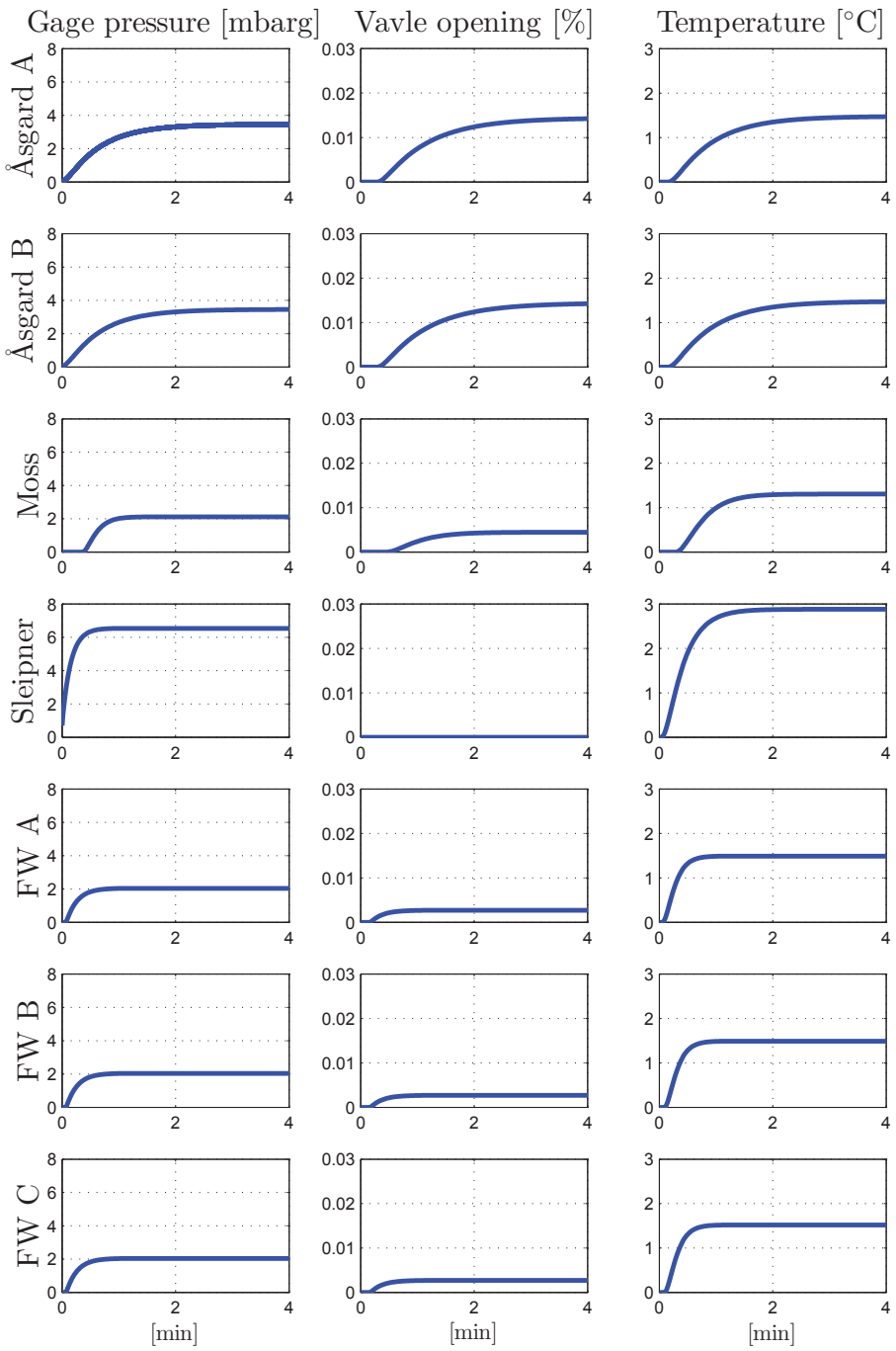

Figure A.3: Step response models of the CVs for all the boilers in SF mode.

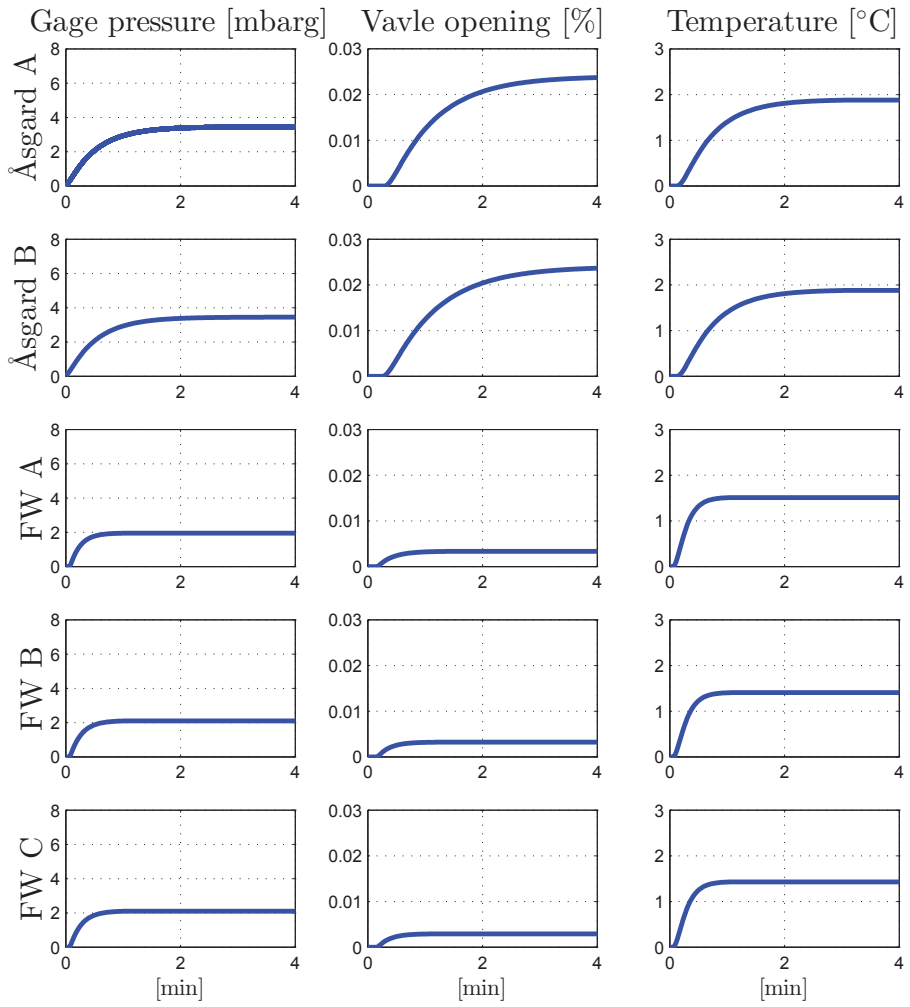

Figure A.4: Step response models of the CVs for all the boilers in TEG mode.

Appendix B

Additional Tables

Table B.1: Nominal operating point 1.

Boiler	Common header pressure	Controller value	Steam production	Operating mode
Åsgard A	60.0 $[barg]$	138.67 $[GJ/h]$	84332.50 $[kg/h]$	TEG
Åsgard B	60.0 $[barg]$	138.00 $[GJ/h]$	84011.00 $[kg/h]$	TEG
Moss	60.0 $[barg]$	85.00 $[bar]$	110291.30 $[kg/h]$	AA
Sleipner	60.0 $[barg]$	32.00 $[bar]$	81761.80 $[kg/h]$	AA
Foster Wheeler A	60.0 $[barg]$	3550.00 $[kg/h]$	52759.40 $[kg/h]$	AA
Foster Wheeler B	60.0 $[barg]$	3550.00 $[kg/h]$	52757.20 $[kg/h]$	AA
Foster Wheeler C	60.0 $[barg]$	3550.00 $[kg/h]$	52751.60 $[kg/h]$	AA

Table B.2: Nominal operating point 2.

Boiler	Common header pressure	Controller value	Steam production	Operating mode
Åsgard A	60.0 $[barg]$	242.69 $[GJ/h]$	76195.50 $[kg/h]$	AA
Åsgard B	60.0 $[barg]$	243.00 $[GJ/h]$	76266.90 $[kg/h]$	AA
Moss	60.0 $[barg]$	80.00 $[barg]$	103756.70 $[kg/h]$	AA
Sleipner	60.0 $[barg]$	40.00 $[barg]$	99807.00 $[kg/h]$	AA
Foster Wheeler A	60.0 $[barg]$	3350.00 $[kg/h]$	55074.50 $[kg/h]$	TEG
Foster Wheeler B	60.0 $[barg]$	3350.00 $[kg/h]$	53098.10 $[kg/h]$	TEG
Foster Wheeler C	60.0 $[barg]$	3350.00 $[kg/h]$	52961.00 $[kg/h]$	TEG

Table B.3: Quadratic thermal efficiency coefficients for the plant.

Boiler(s)	The quadratic equation coefficients β_0	β_1	β_2
AA mode			
Åsgard A/B	$-1.3047 \cdot 10^{-6}$	0.0144	60.1735
Moss	$-1.3363 \cdot 10^{-6}$	0.0138	55.7932
Sleipner	$-2.9244 \cdot 10^{-7}$	0.0034	80.8141
Foster Wheeler A/B/C	$-3.1996 \cdot 10^{-6}$	0.0260	36.9209
TEG mode			
Åsgard A/B	$-5.6150 \cdot 10^{-5}$	0.0253	60.1735
Moss	–	–	–
Sleipner	–	–	–
Foster Wheeler A/B/C	$-1.0907 \cdot 10^{-5}$	0.0472	29.9488

Table B.4: Quadratic thermal efficiency coefficients for the simulator.

Boiler(s)	The quadratic equation coefficients β_0	β_1	β_2
AA mode			
Åsgard A/B	$-1.7388 \cdot 10^{-6}$	0.0217	19.5175
Moss	$-4.4623 \cdot 10^{-8}$	0.0005	89.1509
Sleipner	$-4.7560 \cdot 10^{-8}$	0.0005	81.0275
Foster Wheeler A/B/C	$-3.2199 \cdot 10^{-6}$	0.0277	25.9028
TEG mode			
Åsgard A/B	$-1.4408 \cdot 10^{-6}$	0.0112	65.8275
Moss	–	–	–
Sleipner	–	–	–
Foster Wheeler A/B/C	$-5.7710 \cdot 10^{-6}$	0.0448	-1.4048

Appendix C

Article

The article enclosed in this this is a proposal for a conference article, written after suggestion from the supervisor of this thesis, Professor Lars Imsland. The article provides a brief presentation of the thesis, where only the main results and findings are included.

Optimal and Robust Production of High Pressure Steam ⋆

Torstein Thode Kristoffersen * **Dagfinn Snarheim** **
Lars Imsland *** **Marius Støre Govatsmark** ****

* *Norwegian University of Science and Technology, Trondheim, Norway (e-mail: torstein.t.k@gmail.com).*
** *Statoil Kårstø, Tysværvåg, Norway (e-mail: dsna@statoil.com).*
*** *Norwegian University of Science and Technology, Trondheim, Norway (e-mail: lars.imsland@itk.ntnu.no).*
**** *Statoil Kårstø, Tysværvåg, Norway (e-mail: mariusg@statoil.com).*

Abstract: Steam delivery networks are large energy-consuming processes and an important part in many processing plants. Often, there is a potential for improved operation and reduction in energy consumption by application of advanced control algorithms and real time optimization. In this article, such a solution is investigated by implementing a model predictive controller to control the common header pressure of the steam delivery network. Furthermore, the energy consumption is reduced by incorporating a real time optimizer on top of the model predictive controller providing optimal operating points for the boilers. The potential reduction in energy consumption is examined using data for a real plant, and the application of the model predictive controller with the overlying real time optimization algorithm is examined using a rigorous process simulator.

1. INTRODUCTION

Steam delivery networks are large energy-consuming processes used to generate and deliver steam to various industrial processes like steam turbines, steam-powered pumps and distillation columns. These networks are typically exposed to large disturbances and quickly changing loads, for example boiler trips and start-ups of various steam consumers. This can lead to reduced steam production capacity, which is costly due to reduced feed processing and possible equipment damages. Thus, there is an incentive for improved control and reduction of the energy requirement of a steam delivery network.

Typically, steam delivery networks are controlled by several single-loop PI controllers with little or no coordination [Hogg and El-Rabaie , 1991]. To improve stability and gain more efficient control, Majanne [2005] emphasizes the need for load leveling and stabilization of the common header pressure. Furthermore, the increased cost of energy and the increased global competition in both product quality and pricing forces the process industry to optimize various processes in order to reduce cost to remain competitive [Glandt et al. , 2001]. According to Downs and Skogestad [2011], economical optimization is typically conducted for processes at steady state by a separate overlying optimization. This overlying optimization finds the optimal steady state operating point by solving an optimization problem with respect to an economical objective function.

The dynamics of the steam delivery network has been devoted some interest, but this is mainly restricted to the control of a single boiler. The boiler dynamics have been extensively studied in for instance Tyssø [1981] and Åstrøm and Bell [2000]. This knowledge has enabled Havlena and Findejs [2005], Lu and Hogg [1997] and Majanne [2005] to study the control of a steam delivery network using advanced control algorithms, including using model predictive control. However, to our knowledge, there exists no published material on economically optimal production of high pressure steam. Therefore, the objective of this article is to illustrate improved control of a steam delivery network using a model predictive controller, and further minimize the fuel consumption of the active boilers by incorporating an optimizer on top of the model predictive controller.

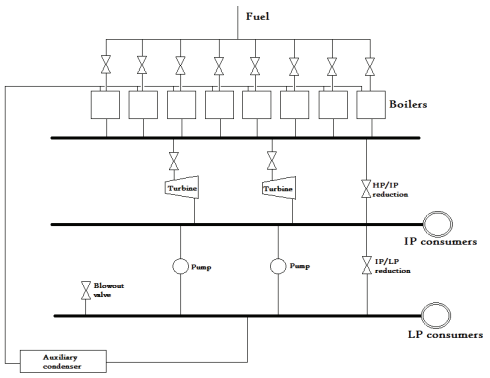

Fig. 1. A simplified steam delivery network.

2. BACKGROUND

The steam delivery network under study is the Kårstø gas processing plant north of Stavanger, illustrated in Figure

⋆ This article is based on the master thesis Kristoffersen [2013] submitted at the Norwegian University of Science and Technology. Thanks to Håvard Håkon Raaen for proof reading.

1. The plant is owned by Gassled, operated by Gasco, while Statoil is the technical service provider (TSP). The network consists of eight parallel operating boilers, all feeding high pressure (HP) steam into the common header. The objective of these boilers is to produce enough steam to cover the steam consumption at the plant to maintain a common header pressure of 60 *barg*.

The steam delivery network consists of three different headers; the high pressure (HP), the intermediate pressure (IP) and the low pressure (LP) common header, shown as the thick dark lines in decreasing order in Figure 1. The HP and IP common headers are connected through steam turbines, that drive compressors used to cool propane and ethane, and export natural gas to Europe. The IP and LP common headers are connected through steam-powered pumps. The steam from the IP common header is returned to the boilers after exploiting the remaining heat potential in various heat exchangers. This heat is, for example used as heat source in distillate columns to separate the light component from the heavier components.

In order to achieve stable and efficient operation, these three common headers need to be controlled. This means that the pressure fall from a higher header to a lower header must happen without large fluctuations, that is, the pressure fall from the HP header to the IP header and the pressure fall from the IP header to the LP header. The HP common header is controlled by the steam generation of the boilers, while the IP and LP common headers are controlled by the turbines and pumps, respectively. Compared to the boilers, both the turbines and the pumps have much wider control range and much faster control response. In practice, this means that the turbines and pumps have to be constrained to prevent disturbances in the LP and HP headers to propagate into the HP common header. According to Majanne [2005], this is accomplished by overriding parallel operating controllers actuating the turbines and pumps. These controllers are assumed to provide fast and robust stabilization of the IP and LP common header for the reminder of this article. Thus, this article will focus on the control of the HP common header, while simultaneously minimizing the energy usage. This is achieved using a model predictive controller with an overlying real time optimizer, both introduced in the next subsections.

Furthermore, five of the boilers are connected to separate gas turbines enabling utilization of turbine gas exhaust (TEG) in addition to ambient air (AA) in the combustion process. The TEG provides additional energy, meaning that the oxygen source needs less heating to reach desired temperature. Hence, less fuel is needed. This changes the dynamics of the boiler, and two models, one for AA mode and one for TEG mode, are required to fully describe the boiler dynamics.

2.1 Model Predictive Control

The Model Predictive Control (MPC) method is an advanced controller which has gained a lot of attention due to its success in the chemical industries [Qin and Bagwell , 2003]. According to Maciejowski [2002], the main reasons for the controllers success is that

- it handles multivariable control problems naturally,
- it can take actuator limitations into account,
- it allows operation closer to constraints, which frequently leads to more profitable operation.

The MPC principle is that the control algorithm uses a multivariable process model to predict the future behavior of the process. At each time instant, the controller solves a mathematical optimization problem to obtain an optimal input sequence with respect to constraints on both the Manipulated Variables (MV) and the Controlled Variables (CV). Only the first element in the optimal input sequence is applied to the process and the procedure is repeated at the next time instant. This is because the models employed may be inaccurate and the available measurements often are affected by noise. In the optimization problem, the objective function weights the MVs and CVs according to their importance. Typically, the MVs are limited by hard constraints, while the CVs are restricted by soft constraints. In this article, the Statoil Estimation and Prediction Tool for Identification and Control (SEPTIC) is the MPC controller used to control the steam delivery network [Strand and Sagli , 2003].

2.2 Real Time Optimization

Once the equipment and the controllers are installed, plant engineers strive to enhance the various processes in order to minimize cost and increase product quality. Typically, this is achieved by formulation of an economic optimization problem, which is minimized on an hourly or daily basis, depending on the time scale of the process. This optimization problem consists of an economical objective function which typically involves the cost of raw materials and the value of products. The constraints typically includes operating conditions and limits on product impurities. The optimization problem is either minimized manually by plant engineers, or on-line using a Real Time Optimization (RTO) optimizer. Finally, the solution is passed down as setpoints and/or ideal values to the respective variables in the MPC controller [Glandt et al. , 2001].

3. MPC AND RTO DEVELOPMENT

According to Majanne [2005], the steam delivery network control problem is to design an overall controller that ensures stable and efficient operation of the steam delivery network. Stable operation is guaranteed by tight control of the common header pressure, while efficient control is achieved through load leveling, that is by distributing the required change in steam production over the active boilers to increase the response time. Another objective of this article is to incorporate a RTO optimizer on top of the MPC controller to achieve optimal steam production.

3.1 MPC controller design

Stable and safe operation of a boiler is achieved through tight control of the common header pressure, while ensuring that the critical variables are kept within prescribed limits. A typical MPC configuration for a boiler is derived from the work by Hogg and El-Rabaie [1991], Lu and Hogg [1997], Havlena and Findejs [2005] and Majanne [2005], and is presented in Table 1. A primary objective

Table 1. A typical MPC configuration.

Variable	Description	Type of control	Constraints
CV	Combustion pressure		hard
CV	HP steam temperature		hard
CV	Attemperator valve opening		soft
CV	Header pressure	set-point	soft
MV	Combustion controller	ideal value	hard

of the MPC controller is to guarantee safe operation, that is guaranteeing that explosions and meltdowns are prevented. This is guaranteed by security mechanisms in the regulatory layer, but the MPC controller must also guarantee this so that it does not control the boiler towards instability. In earlier works, researchers have identified good measurements of critical variables which needs control to prevent these undesired events. The combustion pressure provides a good measurement of the combustion process and is controlled to prevent explosions. Meltdown is prevented by control of the HP steam temperature. Furthermore, the MPC controller needs to be aware of its cooling capacity to control the HP steam temperature. Therefore, the attemperator valve opening is chosen as a CV. A secondary objective of the MPC controller is to ensure tight and stable operation, which is guaranteed by setpoint control of the boiler's header pressure. Furthermore, the steam production of a boiler is decided by the energy supplied to the boiler and therefore depends on the combustion process. The combustion is controlled by several PI controllers connected in such a way that there always is an excess of oxygen in the combustion process. Typically, the setpoint of the fuel flow is decided by an external source, for examples operators or an MPC controller, while the setpoint point of the air flow is set by the fuel flow multiplied by the desired air to fuel ratio. Hence, the only degree of freedom is the setpoint to the fuel flow controller and therefore this is MV for the boiler. The constraints are chosen according to specific physical properties of these variables and the severity of a constraint violation.

Efficient operation, that is load leveling, is achieved by combining all the MPC controllers for the boilers into a single MPC controller for the steam delivery network. This is achieved by merging all the header pressure into a single header pressure, that is, the common header pressure. Now, this controller has the desired ability of distributing the load over all the active boilers according to their rate of change limitations and penalty for ideal value deviation.

Step response models for the variables are used as models for the MPC controller. These are derived by performing a step on each of the MVs and record the response on the respective CVs. These responses are modeled as first order transfer functions.

3.2 RTO optimizer design

At steady state, a single boiler can be used to control the common header pressure, while the other boilers produce a constant amount of steam. That is, there is a surplus of unused degrees of freedom. Hence, these available degrees of freedom can be used to economically optimize the production of HP steam by incorporating a RTO optimizer on top of the MPC controller.

Since steam delivery network are closed systems and no products are extracted, the only cost is the energy used to heat the condensate. Hence, the economical objective function is given as

$$f = \sum_{i=0}^{n} u_i, \tag{1}$$

where n and u_i are the number of boilers and the fuel consumption for boiler i, respectively. Furthermore, the optimization is only conducted at steady state, that is at constant common header pressure. Therefore, an operational constraint is derived from the mass rate balance for the common header,

$$0 = \dot{m}_{in} - \dot{m}_{out}, \tag{2}$$

where $\dot{m}_{in}$ and $\dot{m}_{out}$ are the steam in and out of the common header, respectively. The steam into the common header is the total amount of steam produced by the boilers and is derived from the thermal efficiency functions for each of the boilers. The thermal efficiency are functions of the applied fuel consumption. Thus, the steam into the common header is given as

$$\dot{m}_{in} = \frac{k}{\Delta h}(\boldsymbol{\eta}^T \mathbf{u}), \qquad \boldsymbol{\eta} = \boldsymbol{\eta}(\mathbf{u}) \tag{3}$$

where k, Δh, $\boldsymbol{\eta}$ and $\mathbf{u}$ are the lower heating value of the fuel, the enthalpy of evaporation, the thermal efficiency and the applied fuel, respectively [1]. The optimization is conducted at steady state, meaning that the steam consumption is constant. Initially, before the optimal steam production is calculated, the steam out of the common header equals the steam into the common header, hence

$$\dot{m}_{out} = \frac{k}{\Delta h}(\boldsymbol{\eta}^T \mathbf{u}_0), \tag{4}$$

where $\mathbf{u}_0$ is the initial fuel consumption. These equation are further extended to include both operating modes, that is AA and TEG mode. This is achieved by introducing a binary vector $\mathbf{H}$, in which 0 and 1 represent AA and TEG mode, respectively. Then, by utilization of the Hadamard product [2] and insertion into equation (2), the operational constraint yields after some simple restructuring

$$\frac{k}{\Delta h}\left(((\mathbf{1}-\mathbf{H}) \circ \boldsymbol{\eta}_{AA})^T + (\mathbf{H} \circ \boldsymbol{\eta}_{TEG})^T\right)(\mathbf{u}-\mathbf{u}_0) = 0, \tag{5}$$

where $\boldsymbol{\eta}_{AA}$ and $\boldsymbol{\eta}_{TEG}$ are the thermal efficiency functions in AA and TEG mode respectively, and $\mathbf{1}$ is a vector consisting of only ones. Furthermore, the optimization needs to account of the range of actuation for each of the boiler. This range is expressed as a concave quadratic function, as shown in Figure 2 for one type of boiler. The function only allows for a solution in which the boiler is either off or in the range between minimum and maximum fuel consumption. The allowable operation points are displayed as blue lines, while the dark lines are unallowable operating areas. Hence, the range of actuation is expressed as

[1] The bold characters symbolize column vectors.

[2] The Hadamard product is an element-wise multiplication of two matrices, symbolized by $\circ$.

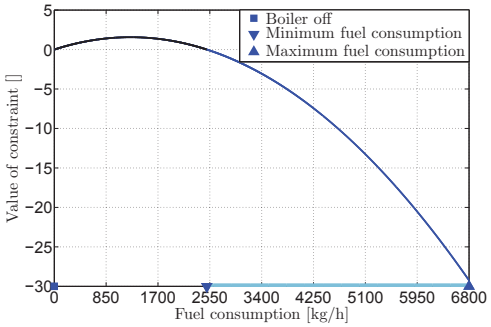

Fig. 2. Range of actuation.

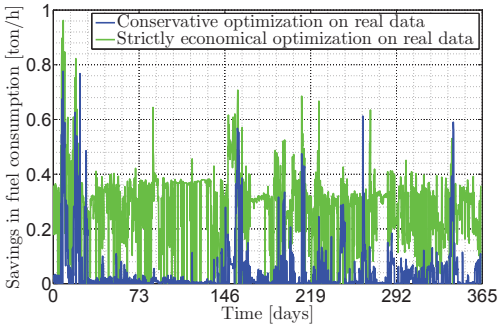

Fig. 3. Potential fuel saving over an entire year.

$$-\mathbf{u} \circ \mathbf{u} + \mathbf{B}\mathbf{u} \leq 0, \tag{6}$$

where $\mathbf{B}$ is a vector consisting of the point of minimum fuel consumption for each of the boilers. The extended version is given as

$$-\mathbf{u} \circ \mathbf{u} + ((\mathbf{1} - \mathbf{H}) \circ \mathbf{B}_{AA} + \mathbf{H} - \mathbf{B}_{TEG}) \circ \mathbf{u} \leq 0, \tag{7}$$

where $\mathbf{B}_{AA}$ and $\mathbf{B}_{TEG}$ are the minimum fuel consumption in AA and TEG mode, respectively. The interested reader is referred to Kristoffersen [2013] for a more thorough derivation.

Thus, the optimization problem optimizes the steam production for constant steam production and is summarized as

$$\min_{u} \quad f = \sum_{i=0}^{n} u_i, \tag{8}$$

$$s.t. \quad (5), \tag{9}$$

$$(7). \tag{10}$$

Two different optimization strategies are examined. The first optimization strategy, called conservative optimization, does not allow for a boiler shutdown, while the second optimization strategy, named strictly economical optimization, allows for a boiler shutdown. The optimal solution of these optimization strategies are passed down to the respective boilers as ideal values.

For the conservative optimization strategy, the additional points of no fuel consumption are of no interest. Thus, the feasible region is convex, shown by the light blue line in Figure 2, and the problem is a Non–Linear Programming (NLP) problem. The optimization problem is implemented in the MATLAB and solved using the *fmincon*-function for non-linear constrained optimization. However, for the strictly economical optimization strategy, boiler shutdown is an alternative, meaning the feasible region is non-convex (disjoint, see Figure 2), and the problem is naturally formulated as a Mixed Integer Non-Linear Programming (MINLP) problem. The solution approach taken in this case is to solve a sequence of NLPs for all the relevant combinations of active and disabled boilers, and choosing the best solution of these. Each of the resulting NLPs is solved using the *fmincon* as above. It is possible to solve this MINLP more efficiently, but this has not been investigated. Since the number of integer variables is small, the overall complexity is in any case limited.

4. CASE STUDY

A dynamic model of the Kårstø gas processing plant is available in the D-SPICE simulator. This high performance simulator is briefly described in Kongsberg [2007] and is used in this study to verify the MPC controller and the RTO optimizer.

The RTO optimizer utilizes thermal efficiency functions derived for each of the boilers and their different operating modes. These thermal efficiency are derived by performing a thermal efficiency analysis on given data sets for both the simulator and the real plant. In order to get an mathematical representation of the data, *linear regression* was used to obtain an empirical quadratic function representing the thermal efficiency. This analysis is conducted in Kristoffersen [2013].

4.1 RTO optimizer potential

In order to illustrate the potential reduction in fuel consumption and CO_2 emissions, both RTO optimization strategies are performed for a year of real plant data with an optimization frequency of four hours. The achieved fuel savings for both optimization strategies are shown in Figure 3.

The two optimization strategies achieved a total fuel saving of approximately 380,390 $kg/year$ and 2,425,700 $kg/year$, which led to reduction in CO_2 emissions of approximately 1,186,402 $kg/year$ and 8,203,232 $kg/year$ for the conservative and strictly economical optimization strategies, respectively. According to EPA [2008], the average annual CO_2 emissions per passenger car in the United States is approximately 4,416 $kg/year$. Thus, the reduction in CO_2 emissions is equivalent to the emissions of 468 and 1,857 passenger cars, respectively.

4.2 Illustration of MPC performance

The response of a boiler trip was compared for two simulations with and without MPC control. The result is shown in Figure 4, where the first plot shows the common header pressure response and the following plots shows the steam production for each of the boilers, respectively. The solid and dashed lines represent the simulations with and without MPC control, respectively.

The results show that only the MPC controller was able to restore the common header pressure due to the load

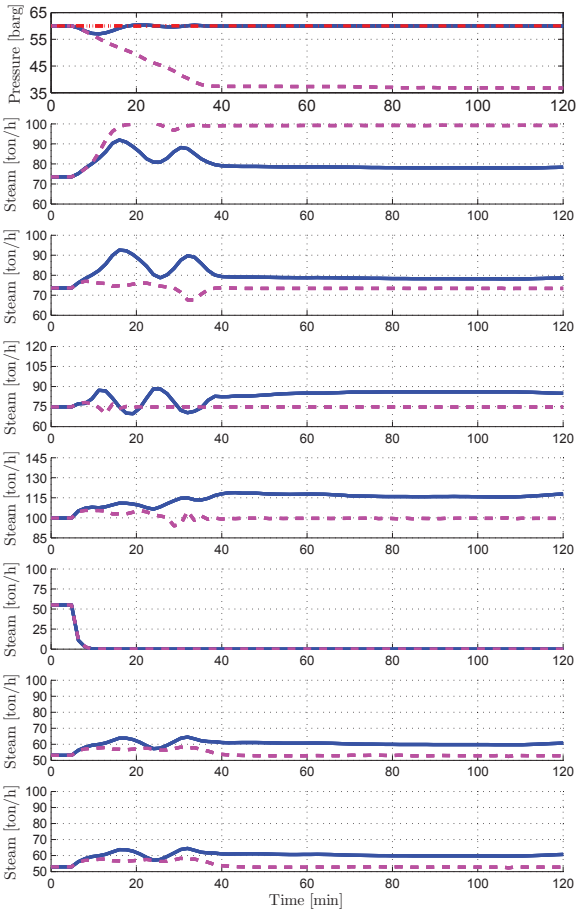

Fig. 4. The response of a boiler trip.

leveling. The controller distributes the required load over each of the boilers, while the PI controllers places the entire load increase on the first boiler. The common header pressure stabilizes as the steam production equals the steam consumption. For the case without MPC control, as the common header drops, HP steam consumers trips as the pressure difference becomes negative. Therefore, when enough steam consumers have tripped, the common header pressure stabilizes. In reality, operators would aid the PI controllers so that the common header pressure would be restored. This is further discussed in Kristoffersen [2013].

4.3 Illustration of RTO performance

The performance of the two optimization strategies were compared for optimization of a steady state operating point in the simulator. The results of the optimization strategies are shown in Figure 5

The conservative optimization strategy arrives at a solution in which steam is produced at maximum efficiency for the two types of boiler with the next highest maximum efficiency, and at minimum efficiency for the boiler with the lowest efficiency. The remaining steam production is covered by the boiler with the highest maximum efficiency,

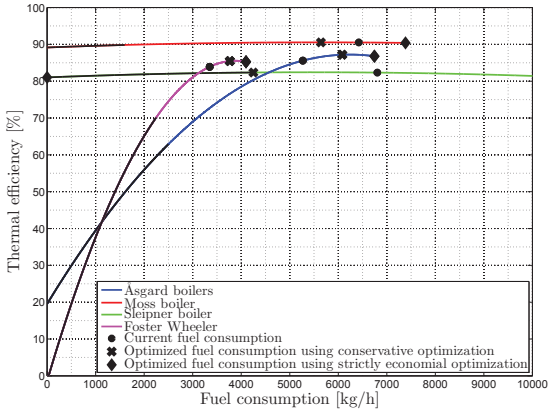

Fig. 5. Optimization result for steady state optimization.

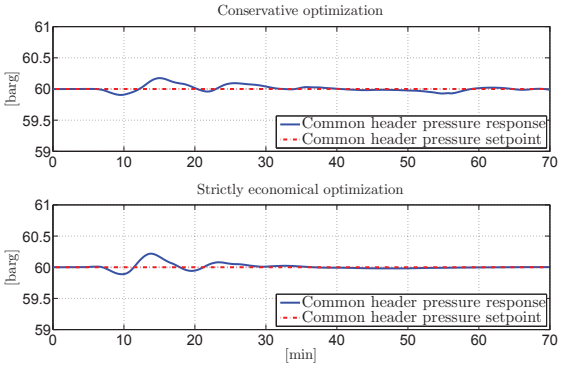

Fig. 6. Common header pressure responses for both optimization strategies.

as the efficiency of this boiler is nearly constant. The strictly economical optimization strategy finds it optimal to produce steam at maximum fuel consumption for the two boilers with the highest efficiency at maximum fuel consumption, while the boiler with the lowest maximum efficiency is shut down. The remaining steam consumption is covered by the boiler with the next lowest maximum efficiency, which happens to be almost at the point of maximum fuel consumption.

When these operating points are implemented through the MPC, the common header pressure fluctuates as a consequence of the changes in steam production towards optimal operation. This applies for both optimization strategies and are shown in Figure 6. This reduction is due to the imperfect models employed by the MPC controller. These fluctuations are so small that they are of no concern. The immediate reduction in fuel consumption, achieved by optimizing the steam production for this initial operating point, was approximately 452 kg/h and 502 kg/h for the conservative and strictly economical optimization strategies, respectively. A more detailed presentation and discussion can be found in Kristoffersen [2013].

4.4 RTO robustness against model errors

Robustness against model errors were examined by introducing errors in the optimization models. The optimization was performed for the same operating point as above

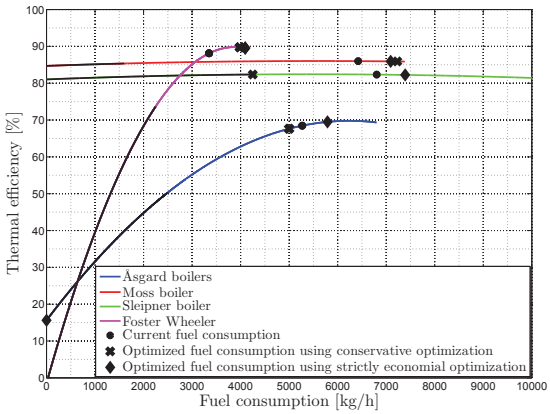

Fig. 7. Optimization result for steady state optimization when including model errors.

and the optimization results from the two optimization strategies are shown in Figure 7.

The errors introduced were a reduction of 5% of the type of boiler with the highest maximum efficiency, a reduction of 15% of the type of boilers with the next highest maximum efficiency and an increase of 5% of the type of boilers with the next lowest maximum efficiency.

The conservative optimization strategy arrives at a solution in which steam is produced at maximum fuel consumption for the two types of boilers with the highest maximum efficiency, and at minimum fuel consumption for the type of boilers with the next lowest maximum efficiency. The remaining steam consumption is covered by the type of boilers with lowest maximum efficiency, because lowering the fuel consumption of these boilers would become too expensive. The strictly economical optimization strategy finds it optimal to shut down one of the two boilers with the lowest maximum efficiency and let the other produce steam at maximum efficiency. Furthermore, the two types of boilers with the highest maximum efficiency is set to produce steam at maximum fuel consumption, and the remaining steam consumption is covered by the type of boiler with the next lowest maximum efficiency.

The common header pressure experiences only minor fluctuations, as a consequence of changes towards optimal steam production. This applies for both optimization strategies and is shown in Figure 8. The common header pressure fluctuates due to the same reasons as above and are too small to be of any concern. Despite of the model errors, both optimization strategies manages to reduce the fuel consumption. The conservative optimization strategy achieved a fuel reduction of approximately 350 kg/h, only 100 kg/h less than the optimization without model errors. However, the strictly economical optimization strategy achieved a reduction of approximately 112 kg/h in fuel consumption, 390 kg/h less than without the equivalent optimization strategy without model errors. Hence, both strategies provide robustness against model errors, but the conservative optimization strategy is superior to the strictly economical optimization strategy. Moreover, due to the model errors, the boilers experienced a bias from their optimal ideal values.

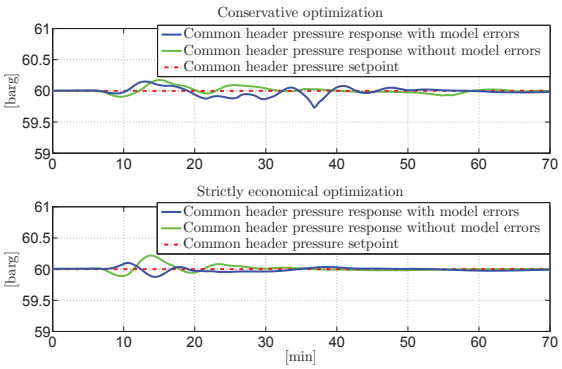

Fig. 8. Common header pressure responses for both optimization strategies with model errors.

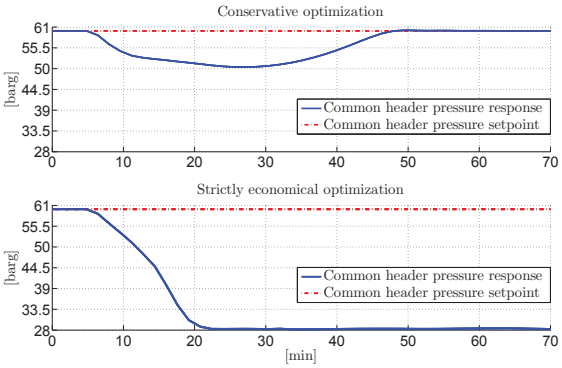

Fig. 9. Common header pressure responses for both optimization strategies following a worst case disturbance.

4.5 RTO robustness against worst case disturbances

The robustness against a worst case disturbance was examined for the optimal solution provided by the optimization strategies in the previous section. A worst case disturbance is a boiler trip of the heaviest loaded boiler. The common header pressure from such a disturbance is shown in Figure 9 for both optimization strategies.

The results clearly show that only the conservative optimization strategy manages to restore the common header pressure, while the strictly economical optimization strategy fails completely. This is because the steam production capacity of the steam delivery network, using the strictly economical optimization strategy, has become less than the steam loss caused by the worst case disturbance due to the shut down of the boiler with the lowest maximum efficiency. However, the conservative optimization strategy preserves the steam production capacity of the steam delivery network, as no boiler is shut down. Hence, it manages to restore the common header pressure and is the only optimization strategy robust against a worst case disturbance. For additional plots and discussion, the reader is referred to Kristoffersen [2013].

5. CONCLUSION

The results of this article clearly illustrates improved performance when using an MPC controller compared to the traditional PI controllers. Furthermore, the results indicate a significant possible reduction in both fuel consump-

tion and CO_2 emissions by incorporating a RTO optimizer using the conservative optimization strategy. The strictly economical optimization strategy is not recommended as this proved to have reduced robustness against both model errors and worst case disturbances. However, the yearly reduction in fuel consumption is significantly smaller using the conservative optimization strategy. Therefore, larger reductions might be possible by extending the conservative optimization strategy to allow for a boiler shutdown, given that the steam production capacity is large enough to cover a worst case disturbance.

REFERENCES

K.J Åstrøm and R.D. Bell. Drum-boiler dynamics. *Automatica*, 36:363–378. 2000.

J.J. Downs and S. Skogestad. An Industrial and Academic Perspective on Plantwide Control. *Annual Reviews in Control*, 1:99–110. 2011.

United States Environmental Protection Agency. Average Annual Emissions and Fuel Consumption for Gasoline-Fueled Passenger Cars. *Technical Report*, 2008.

Kongsberg, Fantoft. *D-SPICE User Guide*, 2007.

E.D. Glandt, M.T Kelin and T.F. Edgar. *Optimization of Chemical Processes*. McGraw Hill, 1221 Avenue of Americas, New York, NY, USA. 2001.

V. Havlena and J. Findejs. Application of Model Predictive Control to Advanced Combustion Control. *Control Engineering Practice*, 13:671–680. 2005.

B. W. Hogg and N.M. El-Rabaie. Multivariable Generalized Predictive Control of a Boiler System. *IEEE Transactions on Energy Conversion*, 6:282–288, 1991.

T.T Kristoffersen. Master Thesis: *Optimal and Stable Production of High Pressure Steam. Norwegian University of Science and Technology*, 2013.

S. Lu and B.W. Hogg. Predictive Co-ordinated Control for a Power Plant Steam Pressure and Power Output. *Control Engineering Practice*, 5:79–84, 1997.

J.M. Maciejowski. *Predictive Control with Constraint*. Pearson Education Limited, Edinburgh, England, 2002.

Y. Majanne. Model Predictive Pressure Control of Steam Networks. *Control Engineering Practice*, 13:1499–1505. 2005.

S. Strand and J.R. Sagli. MPC in Statoil - Advantages with In-House Technology. *Adechem*, 1:1–7. 2003.

S.J. Qin and T.A. Bagwell. A Survey of Industrial Model Predictive Control Technology. *Control Engineering Practice*, 11:733–764. 2003.

A. Tyssø. Modeling and Parameter Estimation of a Ship Boiler. *Automatica*, 17:157–166. 1981.